Crystal Nucleation and Polymorph Control

Self-association, Template Nucleation, Liquid-Liquid phase Separation

Proefschrift

ter verkrijging van de graad van doctor
aan de Technische Universiteit Delft,
op gezag van de Rector Magnificus prof. ir. K.C.A.M. Luyben,
voorzitter van het College voor Promoties,
in het openbaar te verdedigen op vrijdag 14 november 2014 om 10:00 uur

door

Samir Ashok Kulkarni
Master of Science in Applied Chemistry
Muenster University of Applied Sciences, Germany
geboren te Aurangabad, India

Dit proefschrift is goedgekeurd door de promotoren:

Prof. dr. ir. A. I. Stankiewicz

Prof. dr. ir. J. H. ter Horst

Samenstelling promotiecommissie:

Rector Magnificus	Voorzitter.
Prof. dr.ir. A. I. Stankiewicz	Technische Universiteit Delft, promotor.
Prof. dr. ir. J. H. ter Horst	University of Strathclyde UK, TU Delft, promotor.
Dr. H. L. M. Meekes	Radboud University Nijmegen, NL.
Prof. dr. S. Veesler	Aix-Marseille University, France.
Prof. dr. S. L. M. Schroeder	The University of Leeds, UK.
Prof. dr. ir. A. de Haan	Technische Universiteit Delft, NL.
Prof. dr. R. M. Kellogg	University of Groningen, NL.
Prof. Dr. Ir. T. J.H. Vlugt	Technische Universiteit Delft, NL.

Printed in the Netherlands by Ipskamp Drukkers.

Dedicated to my beloved parents and family

SUMMARY

Crystallization is an essential step in many processes in chemical industries, ranging from bulk chemicals to special products. It is a separation and purification technique that results in a solid particulate product, which is generally preferred in the pharmaceutical industry. The crystal product quality is determined by the specific crystal form (polymorph) crystallized, and by the crystal size, morphology and purity. It depends heavily on the process conditions under which crystal nucleation occurs. During the crystal nucleation event, parameters that are essential for the product quality, in particular the polymorph formed, are not very well established. The nucleation event is still poorly understood and is therefore difficult to control and optimize.

Crystal nucleation sets the initial crystal size distribution at the start of unseeded batch crystallization processes and is the first and most important step in this process (**Chapter 1**). A fundamental understanding of crystal nucleation is needed for the rigorous control and prediction of the crystalline product quality of any crystallization processes on industrial scale. Also the lead compounds in pharmaceutical industry become more and more complex. As a result crystallization research becomes increasingly fundamental while model compounds have shifted from bulk chemicals to high added-value chemicals. A fundamental understanding of molecular processes during crystallization is becoming increasingly important not in the least when applied on an industrial scale.

In this thesis we improve the knowledge and understanding of crystal nucleation of organic compounds from solution. The research starts with comparing two newly developed methods to measure heterogeneous nucleation kinetics by determining crystal nucleation rates in stirred solutions (**Chapter 2**). Both methods make use of the stochastic nature of crystal nucleation by determining and analysing the variation in nucleation kinetic measurements. The values of the kinetic parameter *(A)* obtained in the present thesis are low

compared to the theoretical values. This could be due to both a lower than expected attachment frequency of building units to the nucleus and a lower than expected concentration of active nucleation sites (heterogeneous particles) in the solution.

It was further identified that the single nucleus mechanism, in which all crystals in the suspension originate from the same parent single crystal, might occur more generally than is currently recognized, even in larger volumes. In this thesis we used concomitant polymorphism as a tool to validate this single nucleus mechanism (**Chapter 3**). The single nucleus mechanism has important implications for the control of industrial crystallization processes of polymorphic compounds. In terms of crystal size distribution, control can be obtained by controlling the secondary rather than the primary nucleation event for which completely different control procedures are needed. In terms of polymorphism, the control can be achieved by controlling the primary nucleation event that leads to the single crystal, which in turn defines the crystal form of the secondary nuclei.

One of the major challenges the pharmaceutical industry is faced in production, where often during cooling crystallization the product separates not as crystals but as a viscous liquid. This phenomenon is referred to as oiling out or liquid-liquid phase separation (LLPS). The effect of LLPS on the crystallization of 4-hydroxyacetophenon (4HAP) in water, water-ethanol mixtures and ethyl acetate solutions were shown in **Chapter 4**. For HAP, the LLPS is a stable region above the saturation temperature of 52 °C, 36 °C and 30 °C of 4HAP in water, water-ethanol (90-10 wt%) and water-ethanol (80-20 wt%) mixtures, respectively. Cooling crystallization experiments always resulted into mixtures of polymorphic fractions if the LLPS preceded 4HAP crystallization. The results suggest that the crystallization behavior is strongly influenced by the presence of this LLPS. Due to the LLPS the nucleation may proceed on the droplet surface and the single nucleus

mechanism does not hold anymore. The crystallization within the LLPS region seems to lead to agglomeration of the particles.

One of the causes for the low kinetic parameter *A* of the nucleation rate equation was identified in **Chapter 3** to be the building units that attach to the nucleus and thus determine the attachment frequency. The effect of these solution-building units or associates in solution was investigated in **Chapter 5**. The model compound used was isonicotinamide, which has an amide group that can form both homosynthons and heterosynthons by self-association. We show that, in a controlled and reproducible way, specific solvents lead to specific polymorphic forms of isonicotinamide. We argue on the basis of Raman and FTIR spectroscopy that the hydrogen bonding (self-association) in solution kinetically drives the nucleation towards a specific form. The self-association in solution reflects the crystal structure of the obtained polymorph. The method based on self-association of molecules in solution may help in reproducible production of polymorphs.

In **chapter 6** we propose a polymorph screening method based on the identification of crystal building units using Raman, FTIR and NMR techniques. We demonstrated this new approach by relating the structural outcome of the crystallization process of Isonicotinamide (INA), Nicotinamide (NA), Picolinamide (PA), Carbamazepine (CBZ) and Diprophylline (DPL) to the association and self-association processes in solutions, which are largely influenced by the hydrogen bonding capacity of the solvent. The screening method based on the identification of crystal building units may help to discover new polymorphs. The self-association method offers the ability to identify solvents or solvent mixtures that promote or avoid the presence of specific building units and in this way control the building unit towards polymorphs having specific structural features.

As identified in chapter 3, another cause for the low kinetic factor in nucleation is the heterogeneous particle. Nothing is known about the actual concentration and functionality of these heterogeneous particles while they tremendously affect nucleation behavior. We therefore investigated the interplay

between self-associates in solution and well-defined heterogeneous template surface by studying the crystallization behavior of isonicotinamide (INA) and 2,6-dihydroxy benzoic acid (DHB) (**Chapter 7**). Well-defined templates were prepared by making Self-Assembled Monolayers (SAM) onto a gold surface. The self-association of INA and DHB were investigated using spectroscopic techniques. Raman spectroscopy of the crystal-template surface after template crystallization suggests that molecular interactions between INA or DHB associates and the SAM are responsible for the formation of specific polymorphs. XRPD helped in the identification of the crystal orientation on the template surface further verifying the importance of solute interactions with the functionalized template surface. The systematic analysis of the association processes in solutions and the interplay with well-defined templates is beneficial in the development of polymorph discovery and preparation methods as well as control over crystallization processes.

Industrially, the thesis results may not only help to discover new polymorphs but can also help in reproducible industrial production of polymorphs. On Industrial scale seeding approaches using only a single crystal can lead to the avoidance of primary nucleation and thus control over the polymorph obtained. The combination of well-defined template surfaces and the self-association method can be used as a screening method in the early drug discovery and development phase but also define robust conditions for industrial crystallization of polymorphs. This will not only help to discover and reproducibly prepare polymorphs, but a more comprehensive screening can be performed at reduced cost. Industries can implement the results to improve crystal product qualities and can also discover and optimize the quality of new crystal products by incorporating the methods in the development process.

Scientifically, this thesis opened the route towards a thorough study of heterogeneous nucleation of polymorphic compounds taking into account self-association, template effects and relative stability of polymorphs. Such a study would result in an accurate molecular interpretation of crystal nucleation and

would finally enable the validation of heterogeneous nucleation theories. As analytical techniques become more and more powerful, finding new and better ways to powerful insights in the crystal nucleation research become easier. Utilization of these principles and tools not only allow studying crystal nucleation, but also allows the understanding of nucleation processes to a new level. Molecular simulations are still needed to bridge the gap between solution chemistry and crystal nucleation rate analysis to come to a molecular interpretation of crystal nucleation of organic compounds. The new experimental approaches described in this thesis will boost the existing methods for polymorph prediction and in particular for predicting the conditions for polymorph formation.

Summary/ Samenvatting

SAMENVATTING

Kristallisatie is een essentiële stap in veel processen in de chemische industrie, variërend van bulk chemicaliën tot speciale producten. Het is een scheidings- en zuiveringstechniek die resulteert in een product van vaste deeltjes, wat doorgaans ook gewenst is in de farmaceutische industrie. De productkwaliteit van het kristal wordt bepaald door de specifieke kristalvorm (polymorf), en door de kristalgrootte, morfologie en zuiverheid. Het hangt grotendeels af van de procescondities waaronder kristalnucleatie plaatsvindt. Parameters die tijdens de kristalnucleatie essentieel zijn voor de productkwaliteit, en dan voornamelijk de polymorf die gevormd wordt, zijn nog niet goed begrepen. Nucleatie zelf wordt nog steeds niet goed begrepen en is daarom moeilijk te controleren en optimaliseren.

Kristalnucleatie stelt de initiële kristalgrootteverdeling aan het begin van niet-geëntte batch kristallisatieprocessen vast en is dus de eerste en daarmee de belangrijkste stap in dit proces (**Hoofdstuk 1**). Een fundamenteel begrip van kristalnucleatie is nodig voor zowel een goede controle als een goede voorspelling van de kristallijne productkwaliteit van elk industrieel kristallisatieproces. Daarnaast worden de nieuwe medicijnen in de farmaceutische industrie steeds complexer. Als gevolg is kristallisatieonderzoek fundamenteler van aard geworden, terwijl de modelstoffen verschuiven van bulk chemicaliën naar chemicaliën zoals medicijnen die een hoge toegevoegde waarde hebben. Een fundamenteel begrip van de moleculaire processen die plaatsvinden tijdens kristallisatie wordt daardoor steeds belangrijker, zeker ook op industriële schaal.

In dit proefschrift verbeteren we de kennis en het begrip van kristalnucleatie van organische stoffen uit de oplossing. Het onderzoek start met de vergelijking van twee nieuw ontwikkelde methodes om heterogene nucleatiekinetiek te meten, door de kristalnucleatiesnelheden in geroerde oplossingen te bepalen (**Hoofdstuk 2**). Beide methodes maken gebruik van het stochastische gedrag van kristalnucleatie door het bepalen en analyseren van de variatie in metingen van de nucleatiekinetiek. De in dit proefschrift verkregen

waardes van de kinetische parameter (A) zijn laag in vergelijking met de theoretische waardes. Dit kan komen door zowel een lager dan verwachte aanhechtingsfrequentie van bouweenheden aan de nucleus, als door een lager dan verwachte concentratie van actieve nucleatieplaatsen (heterogene deeltjes) in de oplossing.

Verder is er aangetoond dat het single-nucleus mechanisme, waarin alle kristallen in de suspensie ontstaan uit hetzelfde moederkristal, vaker voorkomt dan momenteel erkend wordt, zelfs in grotere volumes. In dit proefschrift hebben we polymorfisme gebruikt om dit single-nucleus mechanisme te valideren (**Hoofdstuk 3**). Het single-nucleus mechanisme heeft belangrijke implicaties voor de controle van industriële kristallisatieprocessen van polymorfe stoffen. In het kader van kristalgrootteverdeling kan controle worden verkregen door de secundaire, in plaats van de primaire nucleatie the controleren, waarvoor compleet andere controleprocedures nodig zijn. In het kader van polymorfisme kan deze controle worden bereikt door de primaire nucleatie van het moederkristal te controleren, wat op zijn beurt de kristalvorm van de secundaire nucleï bepaalt.

Een van de grote uitdagingen in de farmaceutische industrie doet zich voor in de productie, waar tijdens koelkristallisatie vaak niet de gewenste kristallen worden gevormd, maar een geconcentreerde viskeuze vloeistof. Dit fenomeen wordt ook wel 'oiling out' of 'vloeistof-vloeistof fasescheiding' (VVFS) genoemd. Wij demonstreren het effect van VVFS op de kristallisatie van hydroxyacetofenon (HAP) in water, water-ethanol mengsels en ethylacetaat (**Hoofdstuk 4**). Voor HAP is de VVFS een stabiel gebied boven de verzadigingstemperatuur van respectievelijk 52 °C, 36 °C en 30 °C van HAP in water, water-ethanol (90-10 wt%) en water-ethanol (80-20 wt%) mengsels. Koelkristallisatie-experimenten resulteerden steeds in mengsels van polymorfe fracties als VVFS voorafging aan HAP kristallisatie. Dit wijst erop dat het kristallisatiegedrag sterk beïnvloed wordt

door de aanwezigheid van deze VVFS. Vanwege de VVFS kan de nucleatie op het druppeloppervlak plaatsvinden, waardoor het single-nucleus mechanisme niet meer werkt. De kristallisatie binnen het VVFS-gebied lijkt te leiden to agglomeratie van de deeltjes.

Een van de mogelijke oorzaken in **Hoofdstuk 3** van de lage kinetische parameter A van de nucleatiesnelheidsvergelijking was de lage aanhechtingsfrequentie. Het effect van de oplossingsbouweenheden of molecuul-associaties in oplossing is onderzocht in **Hoofdstuk 5**. De modelstof voor dit onderzoek was isonicotinamide, dat een amidegroep heeft die zowel homosynthons als heterosynthons kan vormen door middel van zelf-associatie. Wij laten op een gecontroleerde en reproduceerbare manier zien dat specifieke oplosmiddelen leiden tot specifieke polymorfen van isonicotinamide. Wij stellen op basis van Raman en FTIR spectroscopie dat de waterstofbinding (zelf-associatie) in oplossing de nucleatie kinetisch naar een specifieke vorm stuurt. De zelf-associatie in oplossing reflecteert de kristalstructuur van de verkregen polymorf. De methode gebaseerd op deze zelf-associatie van moleculen in oplossing kan helpen bij de reproduceerbare productie van polymorfen.

In **Hoofdstuk 6** stellen we een polymorfscreeningsmethode voor die gebaseerd is op de identificatie van kristalbouweenheden en gebruik maakt van Raman, FTIR en NMR technieken. We hebben deze nieuwe benadering gedemonstreerd door de resulterende kristalstructuren van het kristallisatieproces van isonicotinamide (INA), nicotinamide (NA), picolinamide (PA), carbamazepine (CBZ) en diprophylline (DPL) te relateren aan de associatie- en zelf-associatieprocessen in oplossingen, die grotendeels beïnvloed worden door de waterstofbindingscapaciteit van het oplosmiddel. De screeningsmethode gebaseerd op de identificatie van kristalbouweenheden kan helpen om nieuwe polymorfen te ontdekken. De zelf-associatiemethode biedt de mogelijkheid om oplosmiddelen of mengsels van oplosmiddelen te identificeren die de aanwezigheid van specifieke bouweenheden kunnen promoten of juist voorkomen

en daarmee de bouweenheid kunnen sturen richting polymorfen met specifieke structuureigenschappen.

Zoals in **Hoofdstuk 3** is geïdentificeerd, zijn heterogene deeltjes een andere oorzaak van de lage waarde voor de kinetische factor A in nucleatie. Er is niets bekend over de werkelijke concentratie en functionaliteit van deze heterogene deeltjes, terwijl ze een enorm effect hebben op het nucleatiegedrag. Daarom hebben wij de wisselwerking onderzocht tussen zelf-associaties in oplossing en goed gedefinieerde heterogene oppervlakken, door het kristallisatiegedrag van isonicotinamide (INA) en 2,4-dihydroxy benzoëzuur (DHB) te bestuderen (**Hoofdstuk 7**). Goed gedefinieerde oppervlakken zijn geprepareerd door Self-Assembled Monolayers (SAM) te maken op een goudoppervlak. De zelf-associatie van INA en DHB in de oplossing zijn onderzocht met behulp van spectroscopische technieken. Raman spectroscopie van het grensvlak tussen kristal en SAM-oppervlak na kristallisatie suggereert dat moleculaire interacties tussen INA of DHB associaties en de SAM verantwoordelijk zijn voor de vorming van specifieke polymorfen. XRPD heeft geholpen bij de identificatie van de kristaloriëntatie op het heterogene oppervlak en daarmee bij de verdere verificatie van het belang van de interacties van de opgeloste stof met het gefunctionaliseerde oppervlak. De systematische analyse van de associatieprocessen in oplossingen en de wisselwerking met goed gedefinieerde oppervlakken is bevorderlijk voor zowel de ontwikkeling van polymorfontdekkings- en preparatiemethodes, als voor controle over kristallisatieprocessen.

Industrieel kan dit proefschrift niet alleen helpen om nieuwe polymorfen te ontdekken, maar het kan ook helpen bij de reproduceerbare productie ervan. Op industriële schaal kan de aanpak met het enten van slechts een enkel kristal leiden tot het ontwijken van primaire nucleatie en dus tot controle over de verkregen polymorf. De combinatie van goed gedefinieerde oppervlakken en de zelf-associatiemethode kan worden gebruikt als een screeningsmethode in de vroege stadia van medicijnontdekking en ontwikkeling, maar het kan ook robuuste

condities voor industriële kristallisatie van polymorfen definiëren. Dit zal niet alleen helpen om polymorfen te ontdekken en reproduceerbaar te prepareren, maar ook om de kosten te reduceren van een begrijpelijk screeningsproces. Industrieën kunnen de resultaten implementeren om de kwaliteit van bestaande kristalproducten te verbeteren en om de kwaliteit van nieuwe kristalproducten ontdekken en optimaliseren door de methodes in het ontwikkelingsproces in te voeren.

Wetenschappelijk heeft dit proefschrift de deur geopend naar een grondige studie van heterogene nucleatie van polymorfe stoffen, daarbij rekening houdend met zelf-associatie, oppervlakte-effecten en de relatieve stabiliteit van polymorfen. Een dergelijke studie zou resulteren in een accurate moleculaire interpretatie van kristalnucleatie en zou uiteindelijk de validatie mogelijk maken van heterogene nucleatietheorieën. Met het sterker worden van de analytische technieken wordt het vinden van nieuwe en betere manieren om belangrijke inzichten te krijgen in het kristalnucleatieonderzoek gemakkelijker. Gebruik van deze principes en gereedschappen maakt niet alleen het bestuderen van kristalnucleatie mogelijk, het tilt ook het begrip van nucleatieprocessen naar een nieuw niveau. Moleculaire simulaties zijn nog steeds nodig om het gat te dichten tussen oplossingschemie en kristalnucleatiesnelheidsanalyse, om zo tot een moleculaire interpretatie te komen van kristalnucleatie van organische stoffen. De nieuwe experimentele aanpakken die in dit proefschrift zijn beschreven zullen de bestaande methodes voor polymorfvoorspelling een boost geven, en dan met name voor het voorspellen van de condities voor polymorfvorming.

Table of content

CHAPTER 1

Introduction

Chapter 1

1. Introduction

Crystallization is an essential step in many processes in chemical industries, ranging from bulk chemicals to special products. It is a separation and purification technique that results in a solid particulate product, which is generally preferred in the pharmaceutical industry. The crystal product quality is determined by the specific crystal form (polymorph) crystallized, and by the crystal size, morphology and purity. It depends heavily on the process conditions under which crystal nucleation occurs. During the crystal nucleation event, parameters that are essential for the product quality, in particular the polymorph formed, are already established. The nucleation event is, however, still poorly understood and is therefore difficult to control and optimize.

Crystal product quality aspects like particle size distribution, crystal shape and purity, are strongly related to the process conditions during industrial crystallization.[1] Crystal nucleation is the start of a phase transition during which nuclei of the crystalline phase are formed and eventually growing out to macroscopically large crystals.[2, 3] Crystal nucleation sets the initial crystal size distribution at the start of unseeded batch crystallization processes and is thus the first and most important step in this process. A fundamental understanding of crystal nucleation is needed for the rigorous control and prediction of the crystalline product quality of any crystallization processes on industrial scale.[4]

The lead compounds in pharmaceutical industry become more and more complex. As a result crystallization research becomes increasingly fundamental while model compounds have shifted from bulk chemicals to high added-value chemicals. A fundamental understanding of molecular processes during crystallization is becoming increasingly important not in the least when applied on an industrial scale.

In the pharmaceutical industry the formation of unwanted polymorphic forms is a major problem. The crystal product quality is

intimately related to the actual polymorph. In crystallization processes the nucleation stage is understood to determine which polymorph is formed. The importance of polymorph control is illustrated by the pharmaceutical Ritonavir.[5] Ritonavir prevents viral replication and thus prevents HIV to develop into AIDS. The pharmaceutical company Abbott put the crystalline drug on the market in 1996. Two years after market introduction the product failed its set specifications. It turned out that the chemical compound Ritonavir suddenly crystallized as a different, crystalline compound, a previously unknown and more stable polymorph.[5] The solubility of this new polymorph was much lower and upon administering Ritonavir the effective concentration in the body could not be reached. Abbott was forced to withdraw Ritonavir from the market. It took a full year of thorough investigations to reintroduce a suitable pharmaceutical product based on Ritonavir. Apart from the implications for the patients, the costs for Abbott extended many hundreds of millions of dollars.[5] More recently in 2008, Neupro (transdermal rotigotine) patches were recalled because of the crystallization in the patches after formation of a new polymorph that resembled snowflake-like crystals.[6] In 2010, a popular blood thinner Coumadin (warfarin sodium 2-propanol solvate) was withdrawn due to the variation in the 2-propanol levels, which affect the crystallinity of warfarin sodium.[7]

We will use a systematic approach based on scientific principles, with mutual feedback of the experimental techniques. This will lead to a detailed understanding of the relation between crystal nucleation and polymorph discovery and control on the one hand and experimental nucleation conditions and template choice on the other hand.

1.1. Crystal Nucleation

The crystal product quality in crystallization is largely determined by the kinetics of two successive steps: Crystal Nucleation and Growth.[2] Crystal Nucleation is the start of a phase transition to a solid during which crystal

nuclei are made which eventually grow out to macroscopically large crystals (**Figure 1.1**).[2] Within the classical nucleation theory it is assumed that nucleation is a stochastic process in which pre-nucleus sized clusters are unstable and can dissolve until they grow to a certain size also known as critical size of nucleus (**Figure 1.1**).[2, 8]

Nucleation of crystals occurs either homogeneously or heterogeneously. Homogeneous nucleation occurs from a pure solution or melts while heterogeneous nucleation occurs onto foreign particles like dust particles or the crystallizer wall. Heterogeneous nucleation is energetically more favourable and as foreign particles are always present in practice, heterogeneous nucleation is the dominant nucleation mechanism.

The primary heterogeneous nucleation rate J is the number of nuclei produced per unit of volume and time. It determines the number of crystals during a crystallization process and thus the crystal size distribution. The essential parameters for J in classical nucleation theory are highlighted in **equation 1.1**.[2]

$$J = z^* f^* C_0 \, exp\left[-\frac{4}{27} \frac{c v_0^2 \, \xi^3 \gamma^3}{k^3 T^3 ln^2 S}\right] \qquad \text{eq. (1.1)}$$

Where C_0 is the concentration of nucleation sites, ξ is the activity factor and γ is the interfacial energy.

The supersaturation ratio S is the system's relative deviation from equilibrium. The nucleation rate is highly non-linear with respect to the supersaturation: slightly larger supersaturations lead to large increases in the nucleation rate. The interfacial energy γ between nucleus and solution describes the energy increase due to the crystal surface formed. A large interfacial energy corresponds to small nucleation rates. The activity factor ξ covers the reduction of the interfacial energy for nucleation on a heterogeneous particle or substrate. In case of polymorphism a metastable form with a relatively low interfacial energy can have a higher nucleation rate

than the stable form. This phenomenon is responsible for Ostwald's rule of stages stating that metastable polymorphs are formed first, possibly followed by a transition to the stable polymorph. The concentration C_0 of nucleation sites determines the concentration of heterogeneous particles. A problem of heterogeneous nucleation is the ill-defined character of the heterogeneous particles in the solution which in effect makes two of the four parameters, C_0 and ξ, difficult to quantify.[2, 9]
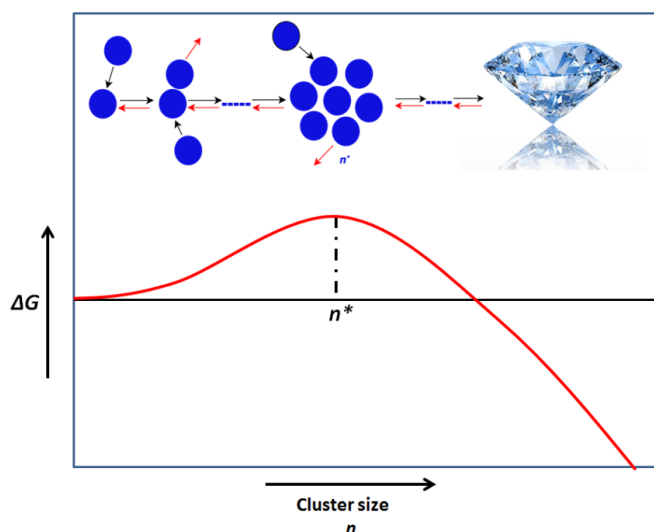
Figure 1.1: Free energy change during nucleation (Mullin 2001).[1]

The nucleation rates of microscopic phases were calculated using classical nucleation theory (CNT) by neglecting size dependence and temperature dependence of the surface energy. This assumption fails for nuclei containing 20-50 molecules, which are small enough that the centre is not in the thermodynamic limit and the interface is sharply curved, changing its free energy.[10] Even though the nucleation theory has made progress, the understanding of nucleation phenomenon is far from complete. New approaches are necessary in order to identify possible new directions for further improvement of nucleation theory. So it is very important to find techniques to accurately measure nucleation rates.

1.2. Polymorphism

Polymorphism can be defined as the ability of a single chemical compound to form more than one crystal structure.[11] Polymorphism of active pharmaceutical ingredients is the subject of intense interest in both science and industry.[12, 13] On the one hand, this is because crystalline product quality aspects such as drug efficacy, bioavailability and safety are affected by the polymorphic form present. On the other hand, polymorphs have economic and intellectual property implications.
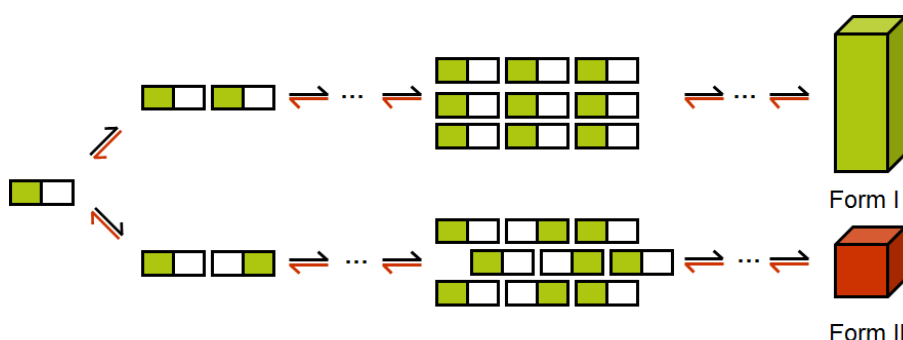
Figure 1.2: The two structural models of cluster formation during crystal nucleation of different polymorphs from supersaturated solutions. Top and the bottom pictures show the building units attach differently to form different types of crystals (form I and form II).

According to Brienstein et al,[14] polymorphism of pharmaceutical crystal has two different categories. One is packing polymorphism or orientational polymorphism, in which the packing and bonding arrangement of the relatively rigid molecules are significantly different in different three-dimensional structures. The second is conformational polymorphism, in which flexible molecules can bend into different conformations and then assembled into different three-dimensional structures.[14] The hydrogen atom plays an important role in conformational polymorphism which helps to build molecular shape in fluid and they are identical to that to be found in crystal structure.[15] Intermolecular interactions, torsional degree of freedom and

crystal forces might play an important role in conformational polymorphism.[15] It is believed that the differences in the nature of the intermolecular interactions (like hydrogen bonds, Van der Waals forces, π- π stacking, electrostatic forces, etc) results in the structural difference in different polymorphs (**Figure 1.2**).[16-18] Therefore, a full understanding of the nucleation, crystal growth and phase transformation in the crystallization sequence is crucial for the control of the polymorphic form.

1.3. Thesis outline

The Aim of the thesis was to improve the knowledge and understanding of crystal nucleation of organic compounds from solution. The research starts with two newly developed methods to measure nucleation kinetics and these two recently developed methods were compared by determining crystal nucleation rates in stirred solutions. Both methods make use of the stochastic nature of crystal nucleation by determining and analysing the variation in nucleation kinetic measurements (Chapter 1). It was also identified that the single nucleus mechanism, in which all crystals in the suspension originate from the same parent single crystal, might occur more generally than is currently recognized, even in larger volumes. This has important implications for the control of industrial crystallization processes of polymorphic compounds. We used polymorphism as a tool to validate this single nucleus mechanism (Chapter 2).

Sometimes, during cooling crystallization, the product separates not as crystals but as a liquid. This phenomenon is called as oiling out or liquid-liquid phase separation (LLPS). LLPS can only offer two different compositional environments but has no stand on the nucleation mechanism, which can be either classical or non-classical nucleation.[19] The LLPS can occur prior to crystallization, which can hinder the primary and secondary nucleation. For some systems the LLPS region was a metastable region below the saturation temperature where the nucleation starts. Due to this metastable region the

nucleation proceed with different mechanism and the single nucleus mechanism does not hold anymore. The in-situ analysis of LLPS during crystallization of 4-hydroxyacetophenone (HAP) from solution has been reported. The underlying reasons for this phenomenon are discussed and its impacts on the nucleation mechanisms are highlighted (Chapter 3).

In solution different intermolecular interactions between like (solute) and unlike (solvent) molecule occurs and due to different solute-solute interactions, different associates or building units are formed. The associates or building units will be function of the solvent used, temperature and composition in solution. The dominant building unit in a solution is determined by the interactions between the species present, i.e., the relative molecular association strengths. We show that, in a controlled and reproducible way, specific solvents lead to specific polymorphic forms of organic compounds. The self-association in solution controls the polymorph nucleation by controlling the building unit attaching to the nucleus (Chapter 4 and Chapter 5). Other than building units, the relative stability of polymorph, heterogeneous particles in solution are important in order to nucleate and grow stable as well as metastable polymorphs. In solution the metastable form can transform to stable form. The heterogeneous particles can reduce the energy barrier of the metastable form in order to nucleate the metastable polymorph rather than stable form.

It is also known that templates or organized substrates can be used to facilitate the formation of specific types of polymorphs. Self-assembled monolayers (SAMs) have been used to control crystallization. The interplay between template interaction and solution association is still not well understood. We show the interplay between self-associates and templates. We chose SAMs with strong hydrogen bond acceptor and donor surface groups to favour specific molecular interactions between the solute and surface to enable the crystallization of polymorphs structurally related or unrelated to the

associates in solution. The solution crystallization and template-induced nucleation may provide an understanding of polymorph nucleation from solution and also the underlying surface chemistry that controls nucleation and growth (Chapter 6).

1.4. Project organization

The project was divided into three important work packages. These work packages are discussed below, after the relevant nucleation parameters have been defined. Understanding of nucleation will be achieved by performing accurate nucleation measurements. Three work packages are defined in each separate area, which is defined to connect our new level of understanding to methods for product quality optimization. The first area was to develop a technique to accurately determine relevant nucleation kinetics of organic compounds from solution. The second area was to find accurate nucleation rate measurement method for polymorphic systems. In the third part the heterogeneous nucleation using well-defined nanoparticles or template molecules as heterogeneous particles was investigated.

During the course of my PhD we also investigated the role of the solvent in polymorph formation. In many cases, the effect of a different solvent leading to another polymorph can be interpreted as being due to a difference in solubility or supersaturation. Nevertheless, there are situations for which the solvent determines which polymorph is formed, possibly due to a change in the interaction between the solvent and a specific crystal surface or interfacial energy. Such an effect of the solvent are also investigated as forth work package. In the fifth part we investigated the underlying reasons for liquid-liquid phase separation phenomenon and discussed its impacts on the nucleation mechanisms.

1.5. References

(1) Mullin, J. W., Crystallization. 4th ed.; Butterworth-Heinemann: London, 2001.

(2) Kashchiev, D., Nucleation: Basic Theory with Application. ed.; Butterworth-Heinemann: Oxford, 2000.

(3) Bernardes, C. E. S.; da Piedade, M. E. M., Crystallization of 4-Hydroxyacetophenone from Water: Control of Polymorphism via Phase Diagram Studies. Crystal Growth & Design 2012, 12, (6), 2932-2941.

(4) Kramer, H. J. M.; Jansens, P. J., Tools for Design and Control of Industrial Crystallizers – State of Art and Future Needs. Chemical Engineering & Technology 2003, 26, (3), 247-255.

(5) Bauer, J.; Spanton, S.; Henry, R.; Quick, J.; Dziki, W.; Porter, W.; Morris, J., Ritonavir: an extraordinary example of conformational polymorphism. Pharmaceutical research 2001, 18, (6), 859-66.

(6) Chen, J. J.; Swope, D. M.; Dashtipour, K.; Lyons, K. E., Transdermal rotigotine: a clinically innovative dopamine-receptor agonist for the management of Parkinson's disease. Pharmacotherapy 2009, 29, (12), 1452-67.

(7) Gao, D.; Maurin, M. B., Physical chemical stability of warfarin sodium. AAPS pharmSci 2001, 3, (1), E3.

(8) Horst, J. H. t.; Kashchiev, D., Determining the nucleation rate from the dimer growth probability. The Journal of Chemical Physics 2005, 123, (11), 114507.

(9) ter Horst, J. H.; Kashchiev, D., Determining the nucleation rate from the dimer growth probability. The Journal of Chemical Physics 2005, 123, (11), -.

(10) Erdemir, D.; Lee, A. Y.; Myerson, A. S., Nucleation of Crystals from Solution: Classical and Two-Step Models. Accounts of Chemical Research 2009, 42, (5), 621-629.

(11) Bernstein, J., Polymorphism in Molecular Crystals. ed.; Clarendon Press: Oxford, 2002.

(12) Chadwick, K.; Myerson, A.; Trout, B., Polymorphic control by heterogeneous nucleation - A new method for selecting crystalline substrates. CrystEngComm 2011, 13, (22), 6625-6627.

(13) Bernstein, J.; Davey, R. J.; Henck, J.-O., Concomitant Polymorphs. Angewandte Chemie International Edition 1999, 38, (23), 3440-3461.

(14) Bernstein, J.; Hagler, A. T., Conformational polymorphism. The influence of crystal structure on molecular conformation. Journal of the American Chemical Society 1978, 100, (3), 673-681.

(15) Cruz-Cabeza, A. J.; Bernstein, J., Conformational Polymorphism. Chemical Reviews 2013, 114, (4), 2170-2191.

(16) Datta, S.; Grant, D. J. W., Crystal structures of drugs: advances in determination, prediction and engineering. Nat Rev Drug Discov 2004, 3, (1), 42-57.

(17) Scheiner, S., Hydrogen Bonding: A Theoretical Perspective. Oxford Univ. Press, Oxford 1997.

(18) Desiraju, G. R., Hydrogen Bridges in Crystal Engineering: Interactions without Borders. Accounts of Chemical Research 2002, 35, (7), 565-573.

(19)   Davey, R. J.; Schroeder, S. L. M.; ter Horst, J. H., Nucleation of Organic Crystals – A Molecular Perspective. Angewandte Chemie International Edition 2012.

CHAPTER 2

Crystal Nucleation Kinetics using Induction Times and Metastable Zone Widths

This Chapter is published as

Samir A. Kulkarni, Somnath S. Kadam, Hugo Meekes, Andrzej I. Stankiewicz, Joop H. ter Horst, Crystal Growth and Design, DOI: 10.1021/cg400139t.

Abstract

We compare two recently developed methods to determine crystal nucleation rates in stirred solutions by using Isonicotinamide (INA) in ethanol as an example. The two developed methods make use of the stochastic nature of crystal nucleation, which is reflected in induction time and metastable zone width variations measured in sufficiently small volumes. These methods give easy experimental access to the nucleation rate parameters in solution under industrially realistic crystallization conditions. While the metastable zone width method is less labour intensive, the induction time method has higher accuracy and is easier to analyze.

2.1. Introduction

Crystal product quality aspects like particle size distribution, crystal shape and purity, are strongly related to the process conditions during industrial crystallization.[1] Crystal nucleation is the start of a phase transition during which nuclei of the crystalline phase are formed, eventually growing out to macroscopically large crystals. [2, 3] Crystal nucleation sets the initial crystal size distribution at the start of unseeded batch crystallization processes and is thus the first and most important step in this process. Accurate nucleation kinetics under industrially relevant conditions, however, are difficult to obtain.[4]

We have recently reported on two newly developed methods to measure nucleation kinetics. [5, 6] Both methods make use of the stochastic nature of crystal nucleation by determining and analyzing the variation in nucleation kinetics measurements. The first method is based on the variations in induction time measurements under equal supersaturation conditions.[6] The induction time is defined as the time period between the moments a constant supersaturation is created and crystals are detected.[7] A set of induction times under equal supersaturation and temperature results in the crystal nucleation rate.

The second method is based on the variations in metastable zone widths (MSZW).[5, 8] The MSZW is defined as the temperature difference between the saturation temperature and the temperature at which crystals are detected upon applying a constant cooling rate.[5] A set of MSZW at a specific cooling rate and concentration results in the nucleation rate parameters.

The objective of this study is to compare both methods by measuring the crystal nucleation rate of isonicotinamide (INA) from ethanol.[9] While a number of supersaturations are used to measure nucleation rates with the induction time method, different cooling rates are used to measure the nucleation rate parameters with the MSZW method. The determined nucleation rates as well as both measuring methods are discussed.

2.2. Experimental Section

INA, with a purity of ≥99%, was obtained from Sigma Aldrich. Ethanol (≥99.5%, Fluka) was used as solvent. Solubility, induction time and metastable zone width measurements were carried out in a 1.5 mL multiple reactor set up (Crystal16, Avantium, Amsterdam). Because of a small constant temperature difference between the actual temperature in the well and the set temperature of the well, a recalibration of the Crystal16 set temperature was performed. We used GNUPLOT, a public domain script-driven engine for data visualization and curve fitting.

2.2.1. Solubility measurements

The saturation temperature of INA was measured in ethanol at different concentrations by adding a known amount of INA and 1 mL of solvent respectively to a 1.5 mL glass vial. The vials were then placed in the Crystal16 and the heating rate and cooling rate were set to 0.3 °C/min. The samples were stirred with a controlled stirring speed of 700 rpm using magnetic stirring bars. The samples were heated with a heating rate of 0.3 °C/min from 5 °C to 60 °C. The temperature at which the suspension turned into a clear solution was recorded and assumed to be the saturation temperature. After a waiting time of 30 minutes at 60°C the clear solution was cooled to 5 °C with a cooling rate of 0.3 °C/min to recrystallize the INA. Then the same temperature profile was repeated three times for each sample. A fit of the Van't Hoff equation to the data facilitated the interpolation of the solubility as well as the determination of the prevailing supersaturation ratio $S=x/x^*$ in a certain solution composition.

The supersaturation ratios used during the induction time measurement were S= 1.28, 1.36, 1.40, 1.44, and 1.48 and the concentration

used during the metastable zone width measurement was 102 mg/mL for different cooling rates.

2.2.2. Induction time measurements

For all measurements at one supersaturation ratio, a 100 mL solution was prepared by dissolving INA in the solvent. A hot bottle-top dispenser platform was used to avoid crystallization during sample preparation and to dispense 1 mL of clear solution into each vial. We thus avoided concentration fluctuations between the vials. Before the induction time measurements started, the samples were stirred above their saturation temperature for at least 30 min to make sure that the crystals, possibly formed in the vials upon sample storage, were dissolved. The stirring speed was controlled at 700 rpm. The clear solution was quickly cooled down to 25 °C with a rate of 5 °C/min. We investigated higher cooling rates (10 °C/min and 15 °C/min), but with higher cooling rates the temperature difference between the cooling coil and sample interior was considerable. When using lower cooling rates it takes more time for the supersaturated sample to reach the final temperature and the probability for nucleation during cooling becomes too high. The cooling temperature 5 °C/min was optimum for our calculations. The moment the solution reached a temperature of 25 °C was taken as time zero, after which a constant temperature of 25 °C was maintained. At some point in time, the transmission decreased due to the presence of crystals. The difference between the time at which the transmission started to decrease and time zero was taken as the induction time. Induction times up to 5 h were measured. For the induction time measurement the temperature was chosen in such a way that crystallization does not occur during cooling but later. Then, the sample was reheated with a rate of 0.3 °C/min and maintained above the saturation temperature to dissolve the crystals and to obtain a clear solution again. Then a subsequent induction time measurement was started. This cool-hold-heat cycle was repeated several times to obtain a total of 144 induction time measurements for each supersaturation ratio. **Figure 2.1** shows two

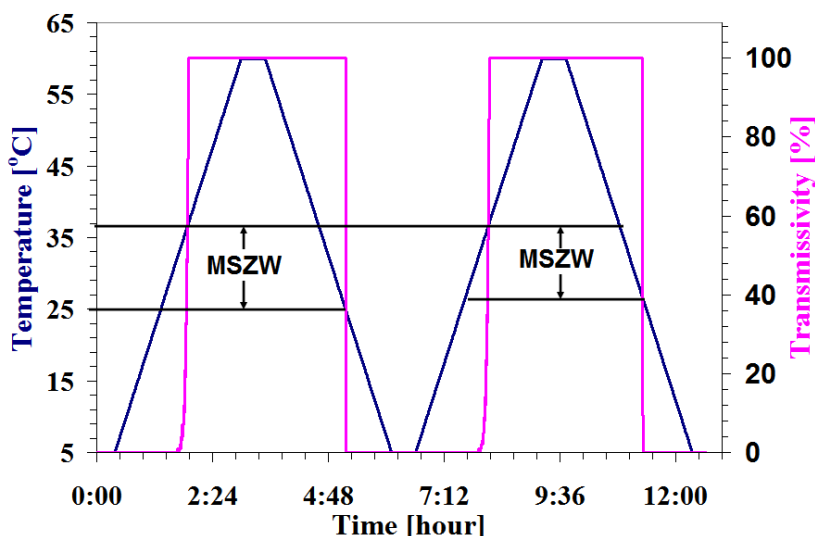subsequent induction time measurements of the same sample. The solubility of INA at 25 °C is 71 mg/mL.
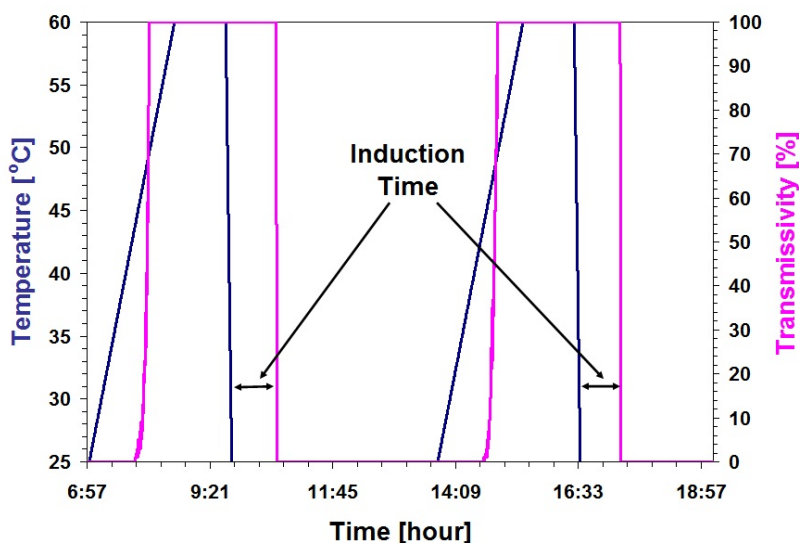
Figure 2.1: Two subsequent induction time measurements of the same sample of INA in ethanol at a supersaturation ratio of 1.44 (102 mg/mL) at 25 °C. Similar Induction time measurements were carried out for 5 different supersaturation ratios S= 1.26, 1.30, 1.36, 1.40 and 1.28 at 25 °C. The measured induction times are 2191 and 2826 seconds.

Similar induction time experiments were carried out after filtering the INA solution with a 0.45 μm filter and also by using vials of which the interior glass wall was silanized with Sigmacote silanizing agent (Sigma, Steinheim, Germany), according to the manufacturer's instructions. A hot filtration platform was used to avoid crystallization during filtration.

2.2.3. Metastable zone width measurements

The same sample preparation method as that for the induction time measurements was used for the MSZW measurements. Only the cool-hold-heat cycle, as shown in **Figure 2.2**, was chosen differently. Sets of up to 150 MSZW

were measured with five different cooling rates. We also performed the MSZW experiments with the filtered INA solution (0.45 μm filter) as well as with the silanized vials.

Figure 2.2: Two subsequent MSZW measurements of the same sample of INA in ethanol at a concentration of 102 mg/mL with a cooling rate of 0.4 °C/min. Similar MSZW measurements were carried out for 5 different Cooling rates. The measured MSZW are 12 and 10 °C.

2.3. Results and discussion

Although INA is a polymorphic compound [10-12] multiple crystallization experiments under various conditions showed that only INA form II crystallized from ethanol.[9] In situ Raman spectroscopy in the early stages of the crystallization did not indicate the presence of any other polymorphic form than form II. The transformation of other forms into the stable form II was further measured to be in the order of 24 hours. This made us confidant that form II is the initially crystallizing form and that the determined nucleation rates are those of form II. The experimentally determined solubility curve of INA form II in ethanol is shown in **Figure 2.3**.
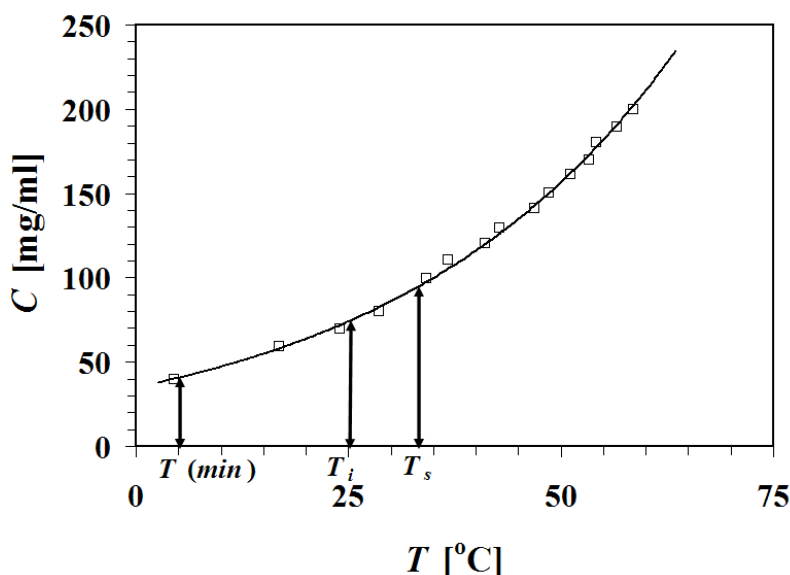
Figure 2.3: Temperature dependent solubility of INA in ethanol. The solid squares represent the average value of several saturation temperature measurements of a single sample where the error bar is smaller than the symbol. The line is a fit of the Van't Hoff equation to the experimental data. The temperature at which induction time measurements were carried out is indicated by T_i, the saturation temperature of the samples for the MSZW measurement is indicated by T_s and T(min) is the temperature for the lowest MSZ limit measured in the MSZW measurements. At temperature 25 °C the solubility of INA in ethanol is 71 mg/mL.

2.3.1. Induction time measurements

Figure 2.4 show the measured induction times for INA in ethanol at a temperature of 25 °C using a concentration of 102 mg/mL. This combination of temperature and mole fraction (x) results in a supersaturation ratio of $S=x/xeq*=1.44$. For a supersaturation of S=1.44 the smallest measured induction time was 114 s while the largest was as large as 3 h. We avoided induction times smaller than about 120s since then there is a larger chance that crystals formed during cooling rather than during constant T. The sample

mean is $(2.6 \pm 0.5) \times 10^3$ and the data were estimated based on the 95% confidence interval. While we had good control over the temperature, volume and concentration of the solution samples, we thus measured a large variation in induction times for these equally supersaturated samples. This was not due to concentration differences since the induction time of a single sample in subsequent measurements shows a similar variation in induction times. Such a variation was also measured for other systems in other studies.[6, 8] We attribute this variation to the stochastic nature of nucleation and it thus contains valuable information on the crystal nucleation rate. In different experiments the time instances of formation of the nuclei are variable and thus the detection of the presence of crystals and hence the measured induction time shows large variations.

For *M* isolated experiments, we define the probability *P(t)* to measure an induction time between time zero and t as:

$$P(t) = \frac{M^+(t)}{M}$$

(2.1)

where *M⁺(t)* is the number of experiments in which crystals are detected at time *t*. Using eq. (2.1) the measured induction times can thus be translated into a cumulative probability distribution *P(t)*. The experimental probability distributions of the induction time at different supersaturation ratios S=1.26, 1.30, 1.36, 1.40, 1.44 and 1.48 are shown in **Figure 2.5**. The experimentally determined probability distribution *P(t)* can be described by the cumulative probability distribution function [6]:

$$P(t) = 1 - \exp(-JV(t - t_g))$$

(2.2)

where *J* is the nucleation rate, *V* is the volume and t_g is the growth time, accounting for the delay in detection due to, among others, growth. Fitting eq. (2.2) to the experimental probability distribution leads to a value for the nucleation rate *J* and the growth time t_g at the used supersaturation. The

crystal nucleation rates obtained for INA in ethanol at the supersaturation ratios S=1.26, 1.30, 1.36, 1.40, 1.44 and 1.48 are 22 ±1, 64 ±1, 268 ±1, 450 ±2, 710 ±2 and $(1.15\pm0.02)\times10^3$ m^{-3} s^{-1}, respectively.

Classically, the crystal nucleation rate is often expressed as [2]

$$J(S) = AS \exp\left(-\frac{B}{\ln^2 S}\right)$$

(2.3)

Where *A* and *B* are respectively the kinetic and thermodynamic nucleation rate parameter and *S* is the supersaturation ratio. With aid of the obtained nucleation rates at different supersaturations the parameters *A* and *B* could then be determined using a plot of *ln(J/S)* against *ln^{-2}S* (**Figure 2.6**). The determined parameters *A* and *B* for INA in 1 mL stirred solution are 6.6×10^3 ± 1.1 m^{-3} s^{-1} and 0.323 ± 0.008, respectively (**Table 2.1**).
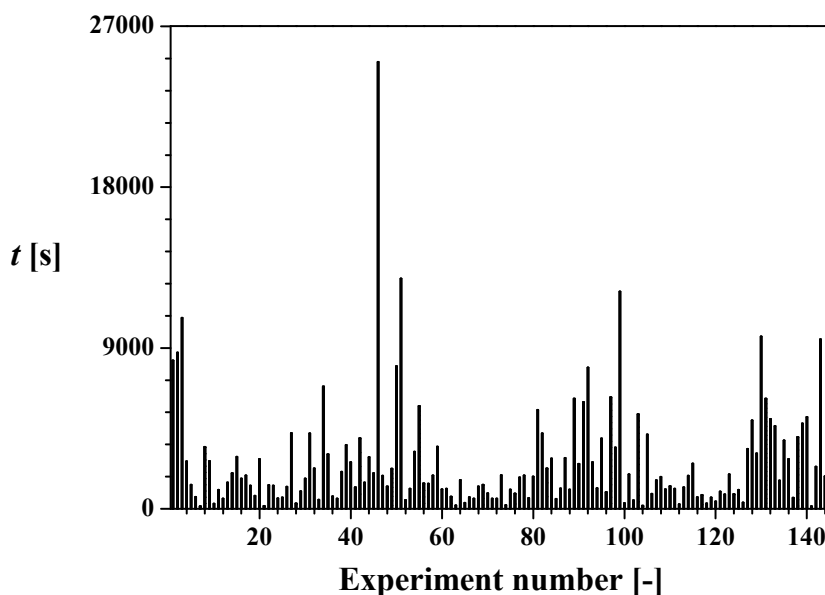
Figure 2.4: The induction time in 144 measurements for INA in ethanol at a supersaturation ratio S = 1.44 (102 mg/mL) and temperature T=25 °C.
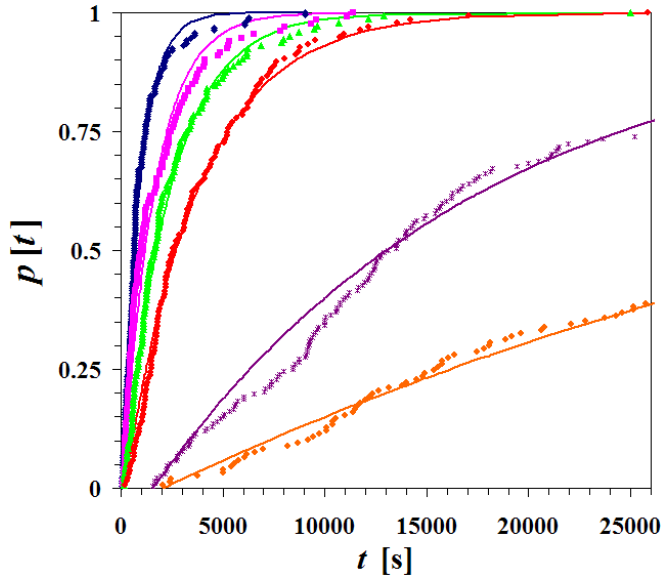
Figure 2.5: Experimentally determined probability distributions $P(t)$ of induction times for INA at 5 different supersaturation ratios S= 1.26 (orange ●), 1.30 (purple x), 1.36 (red ●), 1.40 (green ▲), 1.44 (pink ■) and 1.48 (blue ♦) in 1 mL solutions at temperature T=25 °C. Solid lines are the fits to eq (2.2).
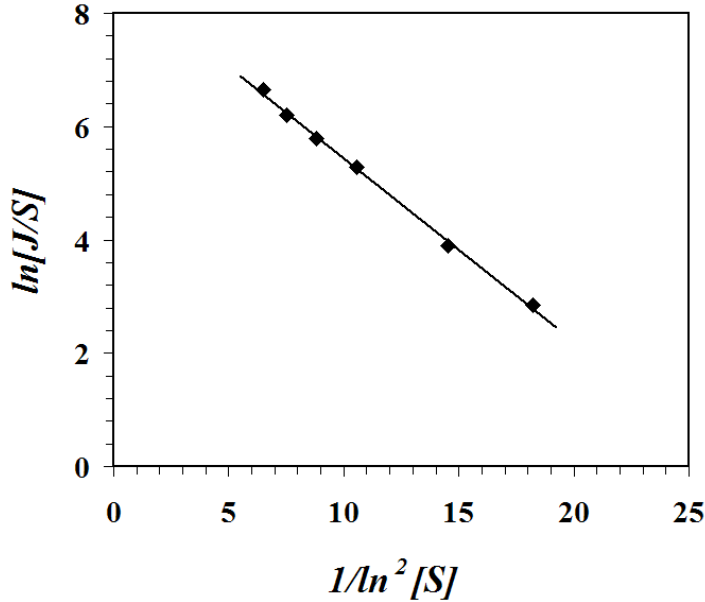
Figure 2.6: ln(J/S) against 1/ln2S for the induction time measurements enables the determination of the nucleation parameters A and B from eq 2.3. The obtained values are shown in **table 2.1**.

2.3.2. Metastable Zone Width measurements

Figure 2.7 shows the MSZW data of more than 150 experiments using a cooling rate of 0.4 °C/min at an INA concentration of 102 mg/mL. Again a large sample-to-sample variation is observed which is attributed to the stochastic nature of nucleation. At 1 mL scale, the MSZW displays a variation from 5 up to 23 °C. Similar to the induction time measurements, the experimental probability of detecting crystals within a metastable zone width ΔT can be determined using

$$P(\Delta T) = \frac{N^+(\Delta T)}{N}$$

(2.4)

where $N^+(\Delta T)$ is the number of experiments in which crystals are detected within the temperature range ΔT.

Figure 8 shows the experimental MSZW probability distribution determined using eq. 2.4 for the cooling rates 0.1, 0.4, 0.5 and 1.0 °C/min. Each cooling rate independently results in a separate estimate of the nucleation parameters A and B (**Table 2.1**). As can be seen from **Figure 2.8**, a higher cooling rate results in a lower probability $P(\Delta T)$ at the same temperature: crystals are detected at lower temperatures. Apart from this, the spread of the MSZW is a function of cooling rate; the higher the cooling rate, the higher the spread in the MSZW. Both are because at higher cooling rates the system has less time to respond to the prevailing supersaturation. It may also partly be caused by the difference between actual solution temperature in the vial and the set temperature of the cooling coil around the vial, which is displayed in the graph.

For a single cooling rate the experimental data can be described using a cumulative probability distribution $P(\Delta T)$[8]:

$$P(\Delta T) = 1 - \exp[-V \int_0^{t-t_g} J(t-t_g)d(t-t_g)]$$

(2.5)

Where J is the nucleation rate, V is the volume and t_g is the growth time which is now changing with the measured MSZW in a single measurement due to the increasing supersaturation during the measurement.

The cumulative probability distribution function of eq. 2.5 is then used to determine the nucleation parameters A and B from the experimentally determined probability distribution $P(\varDelta T)$ (eq. 2.4, **Figure 2.8**). For the sake of simplicity, we did not account for the temperature dependence of both nucleation parameter A and B. The nucleation parameters A and B obtained from the MSZW measurements at a cooling rate 0.5 °C/min of INA in 1 mL stirred solution are $A=2.8\times10^3$ m^{-3} s^{-1} ± 0.002 and $B=0.3516$ respectively.
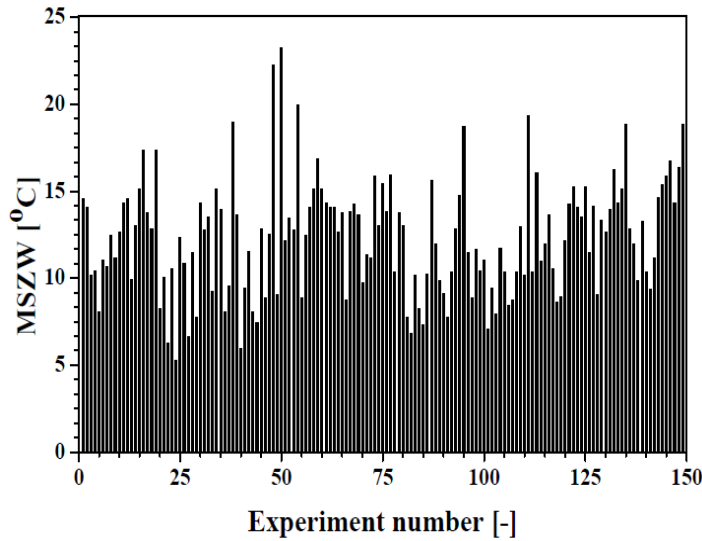
Figure 2.7: The MSZW in 150 measurements for an INA solution in ethanol with a concentration of 102 mg/mL and a saturation temperature of 35.8 °C using a cooling rate of 0.4 °C/min.
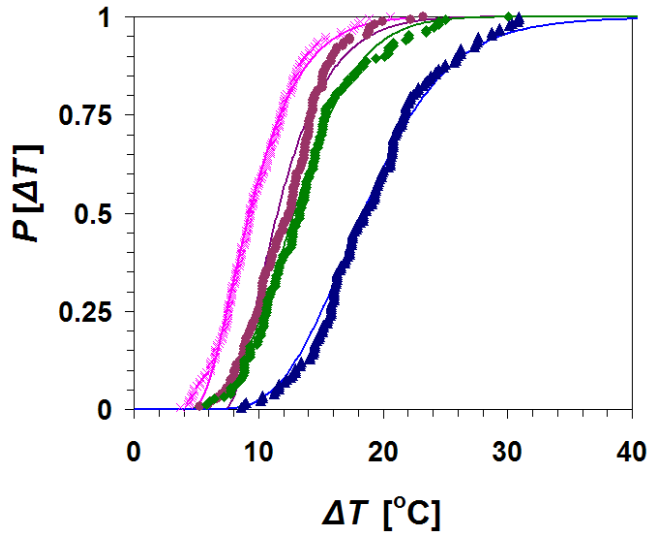
Figure 2.8: Experimentally determined probability distributions *P(ΔT)* of MSZW for INA at cooling rates of 1.0 (blue ▲), 0.5 (green ♦), 0.4 (brown ●) and 0.1 (pink x) °C/min in 1 mL solutions. The solids lines are fits to the experimental data using eq. (2.7). The experimentally determined probability distributions of MSZW at cooling rate of 0.2 °C/min is in close proximity to the 0.1 °C/min and therefore not shown.

Table 2.1: The kinetic parameter *A* and thermodynamic parameter *B* of the Classical Nucleation Rate equation determined from the induction time and the MSZW measurements. The values of Δ*B* from the fits are very small (<1%).

Induction Time Measurements			
	A $* 10^3$ [m^{-3}s^{-1}]	ΔA $* 10^3$ [m^{-3}s^{-1}]	B [-]
	6.6	+/- 0.05	0.32
Cooling rate (°C/min)			
0.1	0.42	≤ 0.01	0.02
0.2	0.65	≤ 0.01	0.009
0.4	1.3	≤ 0.1	0.010
0.5	2.8	≤ 0.1	0.35
1.0	5.8	≤ 0.1	0.89

As shown in table 2.1 the values of the thermodynamic parameter obtained for the smallest cooling rates i.e. 0.1, 0.2 and 0.4 °C/min during the MSZW measurements are very low as compared to higher cooling rates. Also for the smallest cooling rates i.e. 0.1, 0.2 and 0.4 °C/min, the values of the nucleation work $W*/kT$ for the supersaturations represented by the measured MSZW are less than one. This would indicate the occurrence of spinodal decomposition, which we believe, experimentally is not the case. It may mean that the current cumulative probability distribution function for the MSZW measurement (eq. 2.5) is not accurately describing the process.

2.3.3. Heterogeneous nucleation

Figure 2.9 shows the nucleation rate as a function of the supersaturation determined using the values A and B from **Table 2.1** both for the induction time measurements and the MSZW measurements. The figure shows that the experimentally determined nucleation rates approach a plateau value, which means that the nucleation work $W*/kT$ is close to 1. The nucleation work accounts for the energy needed to create a particular nucleus or the energy barrier for nucleation to occur.[2] The experimentally determined $W*/kT$ values for the supersaturation ratios S=1.26, 1.30, 1.36, 1.40, 1.44 and 1.48 are 5.83, 4.65, 3.38, 2.83, 2.41 and 2.08, respectively. The nucleus sizes $n*$ obtained for these supersaturation ratios are 50, 35, 22, 17, 13 and 11, respectively. Both the values of $W*/kT$ and nucleus size $n*$ are reasonable values. The classical nucleation theory leads to the following expressions for $n*$ and $W*/kT$ for heterogeneous nucleation[13]

$$W* = 16\pi v_o^2 \gamma_{ef}^3 / 3(kT)^2 \ln^2 S = (1/2)n* kT \ln S \qquad (2.6)$$

Figure 2.9 also shows the nucleation rate determined with the *A* and *B* values from MSZW measurements with different cooling rates. For the

cooling rates of 0.5 °C and 1.0 °C/min similar values for $W*/kT$ and nucleus size $n*$ are obtained compared to the induction time measurements.

The low values of experimentally obtained kinetic parameter A and the thermodynamic parameter B indicate that the heterogeneous nucleation is occurring. Heterogeneous nucleation is the type of primary nucleation for which the nuclei are formed at heterogeneous nucleation centers (dust particles, glass wall, stirrer etc).[13] The active heterogeneous surfaces in the case of INA in ethanol solution could be atmospheric dust or impurity particles present in the solution, the glass wall, the solution-air interface or the magnetic stirrer. To identify these heterogeneous surfaces a series of induction time experiments were carried out after filtering the INA solution with a 0.45 μm filter and also by using vials of which the interior glass walls were silanized.

Figure 2.10 shows the experimentally determined probability distributions *P(t)* of induction times for INA at supersaturation ratios S= 1.44 for filtered solutions, silanized vials and samples without both filtration and silanized vials. Solid lines are the fits to eq (2.2). The crystal nucleation rates obtained for INA in ethanol using silanized vials and with and without filtered solution at the supersaturation ratio S=1.44 are 631 ± 9, 233 ± 12 and 644 ± 5 m^{-3} s^{-1}, respectively. The nucleation rates of samples with and without silanized glass vials are within experimental error, while the filtered samples show a decreased nucleation rate. The nucleation rate decrease in case of the filtered samples is due to the removal of part of the dust particles from the solution, decreasing the concentration of heterogeneous particles. Similar results were obtained in case of the MSZW measurements. We conclude from these experiments that dust particles in the solutions rather than the glass walls or the liquid-air interface are responsible for the occurring heterogeneous nucleation.
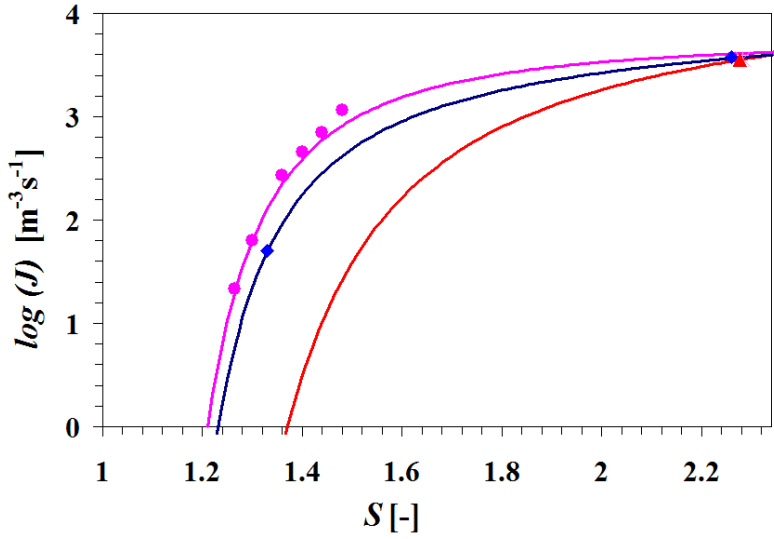
Figure 2.9: The nucleation rate *J* of INA from ethanol as a function of the supersaturation ratio *S* determined using the parameters *A* and *B* from the induction time measurements and the MSZW measurements. The solid dots (pink •) represent the experimentally determined nucleation rates using the induction time method at different supersaturation. The symbols for the MSZW method (cooling rates of 0.5 and 1.0 °C/min) indicate the lower and upper value of supersaturation for which crystals were detected in the MSZW experiments. Solid lines with the same color as the symbols represent the nucleation rates calculated from the determined nucleation rate parameters *A* and *B* from induction time and MSZW methods.

The heterogeneous nucleation rate in a solution containing heterogeneous particles can be represented by the following equation 2.2

$$J = C_a \times J_a$$
(2.7)

Where J is the nucleation rate, C_a is the concentration of active centres present in solution due to the heterogeneous particles and *J*a is the nucleation rate per active center.[2] We assume that we do not remove all heterogeneous particles by filtration and then we can calculate the ratio of active centers present in solution before and after filtration by using eq. (8)

$$\frac{J^-}{J^+} = \frac{C_a^-}{C_a^+}$$

(2.8)

where $J+$ and $J–$ are the nucleation rates of solution before and after filtration, respectively. The concentrations C_a^+ and C_a^- are the concentrations of active centers present in solutions before and after filtration, respectively. The ratio of the concentration of active centers after and before filtration is determined to be 0.37, which would mean that 63% of the active centers are removed by filtration. Nothing is known, however, about the actual concentration and functionality of the heterogeneous particles.[3] In order to thoroughly investigate the heterogeneous nucleation mechanism it is needed to add a known concentration of specifically functionalized templates.[3]
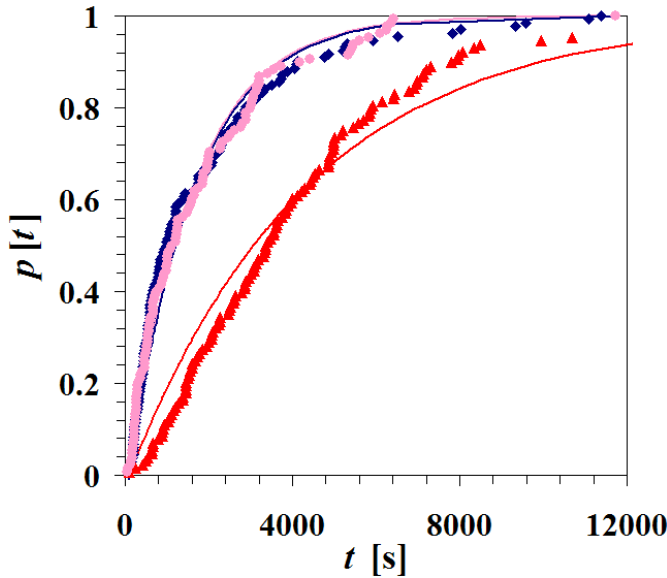
Figure 2.10: Experimentally determined probability distributions *P (t)* of induction times for INA at supersaturation ratios S= 1.44 in 1 mL Filtered solution (red　), solution in silanized vials (pink　) and sample without both filtration and silanized vials (blue ◆). Solid lines are the fits to eq 2.2 in order to obtain the nucleation rate.

2.4. Discussion

The induction time and metastable zone width methods are capable of obtaining high quality nucleation crystallization kinetics data for small volume stirred solutions. These two approaches can save significant experimental efforts and time in the development of crystallization processes on industrial scales.

One set of MSZW data was used to determine the nucleation parameters *A* and *B* of INA in ethanol. In case of the induction time measurements several sets of induction time measurements have to be done at different supersaturations to obtain these parameters. The MSZW method relatively quickly leads to the nucleation kinetics. As shown here, however, the cooling rate has a rather large effect on the determined nucleation parameter values. During the induction time measurement the temperature is kept constant while that in the MSZW measurement is decreasing. This decreasing temperature in the MSZW measurements may cause a temperature difference between cooling coil around the vials and the crystallization volume within the vials. This temperature difference would be difficult to accurately account for. A further inaccuracy is that in the MSZW measurements we did not account for the temperature dependence of both nucleation parameters *A* and *B*. Another reason might be that the cumulative probability distribution function is not sufficiently accurate to capture the MSZW distribution. These inaccuracies are also indicated by the difference in nucleation rate parameters obtained at different cooling rates (**Table 2.1**).

Heterogeneous nucleation is the most common phenomenon since most crystallization systems contains foreign particles such as dust particle, glass walls etc.[14, 15] For heterogeneous nucleation the value of the kinetic parameter (*A*) postulated in literature is in the order of 10^{15} to 10^{25} m^{-3} s^{-1}.[13] Similar to other experimental studies[3], the values of the kinetic parameter (*A*) obtained in the present paper are very low (<10^6) as compared to the postulated values. The kinetic parameter (*A*) is largely determined by the

attachment frequency of molecules to the nucleus and the concentration of the active nucleation sites in the solution.[16] A low concentration of heterogeneous particles (nucleation sites) may explain the low pre-exponential factor, which was measured with the filtered solutions. Nothing is known, however, about the actual concentration and functionality of the heterogeneous particles.[3] Another reason could be the self- association processes of INA in solution[9] where dominant presence of building units of 2 or more molecules might be responsible for the low attachment frequency to the nucleus. Again, in the future the heterogeneous nucleation research using the well-defined templates is needed to understand the occurring heterogeneous nucleation mechanism.

2.5. Conclusions

Both the induction time method as well as the MSWZ method results in an estimate of the nucleation rate parameters in stirred solutions. The MSZW method is less labour intensive, the induction time method seems to have higher accuracy and is easier to analyze. The MSZW has less control over temperature in the vials due to a possible temperature difference between cooling coil and crystallization volume while the temperature dependence of the kinetic factor *A* and the thermodynamic factor B are not accounted for in the model. Thus we conclude that the induction time method probably is more accurate. The values of the kinetic parameter *(A)* obtained in the present paper are low compared to the theoretical values. This could be due to both a lower than expected attachment frequency of building units to the nucleus and a lower than expected concentration of active nucleation sites in the solution. For the crystal nucleation of INA from ethanol the concentration of active nucleation sites in the solution could be reduced by filtering the solution.

2.6. Acknowledgement

2.7. References

(1) Mullin, J. W., Crystallization. Forth ed.; Butterworth-Heinemann: London, 2001.

(2) Kashchiev, D., Nucleation: Basic Theory with Application. ed.; Butterworth-Heinemann: Oxford, 2000.

(3) Davey, R. J.; Schroeder, S. L. M.; ter Horst, J. H., Nucleation of Organic Crystals—A Molecular Perspective. *Angewandte Chemie International Edition* 2013, 52, (8), 2166-2179.

(4) Ulrich, J.; Strege, C., Some aspects of the importance of metastable zone width and nucleation in industrial crystallizers. Journal of Crystal Growth 2002, 237-239, Part 3, (0), 2130-2135.

(5) Kadam, S. S.; Kramer, H. J. M.; ter Horst, J. H., Combination of a Single Primary Nucleation Event and Secondary Nucleation in Crystallization Processes. Crystal Growth & Design 2011, 11, (4), 1271-1277.

(6) Jiang, S.; ter Horst, J. H., Crystal Nucleation Rates from Probability Distributions of Induction Times. Crystal Growth & Design 2011, 11, (1), 256-261.

(7) Davey, R. J.; Garside, J., From molecules to crystallizers : an introduction to crystallization. ed.; Oxford Univ. Press: Oxford, 2000.

(8) Kadam, S. S.; Kulkarni, S. A.; Coloma Ribera, R.; Stankiewicz, A. I.; ter Horst, J. H.; Kramer, H. J. M., A new view on the metastable zone width during cooling crystallization. Chemical Engineering Science 2012, 72, (0), 10-19.

(9) Kulkarni, S. A.; McGarrity, E. S.; Meekes, H.; ter Horst, J. H., Isonicotinamide self-association: the link between solvent and polymorph nucleation. Chemical Communications 2012, 48, (41), 4983-4985.

(10) Aakeröy, C. B.; Beatty, A. M.; Helfrich, B. A.; Nieuwenhuyzen, M., Do Polymorphic Compounds Make Good Cocrystallizing Agents? A Structural Case Study that Demonstrates the Importance of Synthon Flexibility. Crystal Growth & Design 2003, 3, (2), 159-165.

(11) Eccles, K. S.; Deasy, R. E.; Fabian, L.; Braun, D. E.; Maguire, A. R.; Lawrence, S. E., Expanding the crystal landscape of isonicotinamide: concomitant polymorphism and co-crystallisation. CrystEngComm 2011, 13, 6923-6925.

(12) Li, J.; Bourne, S. A.; Caira, M. R., New polymorphs of isonicotinamide and nicotinamide. Chemical Communications 2011, 47, (5), 1530-1532.

(13) Kashchiev, D.; van Rosmalen, G. M., Review: Nucleation in solutions revisited. Crystal Research and Technology 2003, 38, (7-8), 555-574.

(14) Liu, X. Y., A new kinetic model for three-dimensional heterogeneous nucleation. The Journal of Chemical Physics 1999, 111, (4), 1628-1635.

(15) Lee, A. Y.; Lee, I. S.; Dette, S. S.; Boerner, J.; Myerson, A. S., Crystallization on Confined Engineered Surfaces: A Method to Control Crystal Size and Generate Different Polymorphs. Journal of the American Chemical Society 2005, 127, (43), 14982-14983.

(16) Kashchiev, D., Effect of carrier-gas pressure on nucleation. The Journal of Chemical Physics 1996, 104, (21), 8671-8677.

CHAPTER 3

Polymorphism Control through a Single Nucleation Event

This Chapter is published as

Abstract

Recently we identified that the single nucleus mechanism, in which all crystals in the suspension originate from the same parent single crystal, might occur more generally than is currently recognized, even in larger volumes. This has important implications for the control of industrial crystallization processes of polymorphic compounds. In this paper we used polymorphism as a tool to validate this single nucleus mechanism. INA crystallizes as form II in ethanol solutions, form I in nitromethane and form IV in nitrobenzene solutions. The metastable form I and form IV, furthermore, only very slowly transform to the stable form II in solvent mixtures of ethanol-nitromethane and ethanol-nitrobenzene. We performed multiple crystallization experiments in solvent mixtures of ethanol-nitromethane and ethanol-nitrobenzene, which all resulted in the formation of either pure form I or pure form II and either pure form II or pure form IV, respectively. In ethyl acetate, 4HAP crystallizes as form II at lower concentrations and as form I at higher concentrations. Crystallization of 4HAP as a function of concentration on a 3 mL scale results in either pure form I or pure form II. This can be well explained by the single nucleus mechanism. In terms of polymorphism the control can be achieved by controlling the primary nucleation event that leads to the single crystal, which in turn defines the crystal form of the secondary nuclei. Seeding approaches using only a single crystal would then lead to the avoidance of primary nucleation and thus control over the polymorph obtained.

3.1. Introduction

Crystal nucleation is the start of the phase transformation in crystallization and thus has a major impact on product quality aspects such as crystal size and polymorphic form.[1] A fundamental understanding of nucleation is needed for the rigorous control and prediction of the crystalline product quality of any crystallization processes on industrial scale.[2] Conventionally, the nucleation stage of an unseeded batch cooling crystallization process is thought to proceed through the formation of an abundance of crystal nuclei in the supersaturated mother liquor which subsequently grow out to macroscopically large crystals.[3] This is contradicted by the large variations in induction times and metastable zone widths (MSZW) measured for equally supersaturated samples.[3] Examples are becoming more and more available,[4, 5] for instance for Isonicotinamide on a 1 mL scale.[6]

Sodium chlorate crystals are optically active while the solute is achiral. Kondepudi et al.,[7] reported that an optically pure crystalline phase was obtained during sodium chlorate crystallization from a stirred and optically inactive solution. They attributed this chiral symmetry breaking to the secondary nucleation of a parent crystal.[7] This was confirmed visually[8] and can be seen as a validation of the occurrence of the single nucleus mechanism for this inorganic compound in water.

Recently, a Single Nucleus Mechanism was proposed that does explain and describe the variational differences for experiments under equal conditions.[3, 4, 6] During the Single Nucleus Mechanism a single parent crystal nucleates, grows and serves as the origin of secondary nuclei which further attrite to form the detectable crystalline phase.[5] By visual inspection it was identified that a number of crystallizing systems seem to follow this single nucleus mechanism: During the crystallization of Paracetamol in water, Isonicotinamide in butanol and ethanol and Succinic acid in water a single crystal was observed previous to the detection of the suspension. A more general occurrence of the Single Nucleus Mechanism has important

implications for the control of unseeded batch crystallization processes in for instance pharmaceutical industry. Secondary rather than primary nucleation, for instance, then plays a determining role in the control of the crystal size distribution and polymorphic outcome.

This paper describes the validation of the single nucleus mechanism by studying the polymorph crystallization behavior of INA and 4HAP. First, we determine the in-situ analysis tool to accurately determine polymorphic fractions as well as polymorphic transformation rates. Second, we establish the conditional regions for concomitant polymorphism. Finally, the polymorphic outcomes of batch cooling crystallizations of INA and 4HAP in the region of concomitant polymorphism are explored.

3.2. Experimental

3.2.1. Materials and Instrumentation.

Isonicotinamide and 4-Hydroxyacetophenone, both with a purity of ≥99% were obtained from Sigma Aldrich. Ethanol, nitromethane, nitrobenzene and ethyl acetate were used as solvent and were of ACS reagent grade with a purity of ≥99.5%, 99+%, 99+% and 99+% respectively. The 3 mL crystallization experiments were carried out in an 8 mL multiple reactors set up (Crystalline, Avantium, Amsterdam). For larger scale experiments, the 'EasyMax' system of Mettler Toledo was used. The crystallization volume was 100 mL.

A Hololab series 5000 Raman spectroscope (Kaiser Optical System, Inc.) coupled to the Crystalline facilitated the recording of Raman spectra of solutions and suspensions in one of the reactors of the Crystalline. The in situ Raman spectra were recorded using an excitation radiation of 785 nm and a NIR probe.

The final crystalline product was characterized using powder X-ray diffraction (XRD; Bruker D2 Phaser, 30kV and 30 mA) with CuKα radiation (λ= 1.5406 ˚A). Data were collected in the *2θ–θ* scanning mode with a scan speed of 2 degrees/min and a step size of 0.022 degrees *2θ*.

The solubility of INA in ethanol, nitromethane and nitrobenzene and the solubility of 4HAP in ethyl acetate at different concentrations were determined with the Crystal16 (Avantium, Amsterdam), following procedures described by ter Horst et al.[9]

3.2.2. Methods

3.2.2.1. Polymorphic fractions and transformation rates by Raman spectroscopy

100 mL clear saturated solutions of INA (at room temperature) in ethanol-nitromethane (EtOH-NM) and ethanol-nitrobenzene (EtOH-NB) solvent mixtures were prepared. For the polymorphic fraction calibration line, 100 mg/mL of polymorphic mixture of INA was placed in 3 mL of saturated solutions after which the Raman spectrum was recorder. The samples were stirred with a magnetic stirrer during the measurements. For the construction of the calibration line the Raman spectra of the clear saturated solution were measured before the addition of the crystals and subtracted from the suspension spectra. For polymorphic transformation rates two different experiments in a 70:30 vol% EtOH-NM and 90:10 vol% EtOH-NB were carried out: one by seeding a suspension of form I or form IV with form II crystals (5% with respect to yield), respectively and the other without seeding. Similar calibration and transformation rate experiments of two polymorphs of 4HAP in 3 mL saturated solutions of ethyl acetate were carried out at room temperature.

3.2.2.2. Conditional regions for concomitant polymorphism

INA. The six different polymorphs of INA were previously reported in literature.[10] It was recently reported that the self-association of INA in different solvents pushes the INA crystallization to produce a certain polymorphic

form.[10] When INA was crystallized from ethanol using different concentrated solutions (70 to 105 mg/mL) and subjected to a well-controlled cooling rate (0.3 °C/min), only form II was obtained reproducibly.[10] Using similar crystallization methods, only pure form I was crystallized from nitromethane with different concentrated solutions (2 to 10 mg/mL) while pure form IV was crystallized from nitrobenzene (concentrations 10 to 26 mg/mL).[10]

If the nucleation rates and growth rates of stable and metastable forms are equal, their formation probabilities will be nearly the same. Since for INA the solvents ethanol, nitromethane and nitrobenzene result in different INA polymorphs, concomitant polymorphism[11] was expected at some solvent mixture. Therefore, we performed series of crystallization experiments using ethanol-nitromethane and ethanol-nitrobenzene mixtures starting from 5vol% up to 95vol% of ethanol.

4-HAP. Two polymorphic forms of 4HAP were previously reported in the literature.[12] Form II was reported to be the stable form at room temperature (298 K) while form I was stable at temperatures above 351 K up to the melting point of 381.9 K.[12] When we crystallized 4HAP from ethyl acetate solutions, at high concentrations (≥600 mg/mL) the metastable form I crystallized while at low concentrations (≤250 mg/mL) the stable form II crystallized. Since for 4HAP different polymorphs form at different concentrations during cooling crystallization it was also expected that at some intermediate concentration of 4HAP in ethyl acetate the probability to form both polymorphs will be equal.

3.2.2.3. Cooling crystallization experiments

INA. Cooling crystallization experiments were carried out using different concentrations of INA in ethanol, nitromethane, nitrobenzene or mixtures thereof. The 3 mL starting suspension of INA in the solvent mixture was heated to 60 °C to establish a clear solution and then cooled down to 5 °C with a cooling rate of 0.5 °C/min while stirring (700 rpm) using a magnetic stirrer. The suspension was analyzed using in situ Raman spectroscopy. The

suspension was filtered through a 0.45 μm filter soon after solids were detected and the clear filtrate solutions were analyzed with Raman spectroscopy. The Raman spectrum of the clear filtrate was then subtracted from the suspension spectrum in order to determine the weight fraction of crystallized polymorphic forms using the calibration line. The crystalline product was also characterized using XRPD. Similar experiments were also performed at 100 mL scale.

Various cooling crystallization experiments under equal conditions (10 at 3 mL and 6 at 100 mL volume) were performed using INA (120 mg/mL) in EtOH-NM and INA (130 mg/mL) in EtOH-NB solvent mixtures.

We also performed five similar experiments at 3 mL scale but without stirring the samples in order to observe concomitant polymorphism in a single experiment. The experiments were performed using INA (120 mg/mL) in EtOH-NM and INA (130 mg/mL) in EtOH-NB solvent mixtures.

4HAP. A suspension of 4HAP in 3 mL ethyl acetate with a concentration between 250 and 600 mg/mL was heated to 50 °C with a heating rate of 1 °C/min and kept at that temperature for 1 hour. Then the clear solution was cooled with a cooling rate of 0.3 °C/min to 5 °C.

The crystallization behavior was recorded with the in situ Raman spectroscope. When a crystal suspension was observed the crystals were immediately filtered in vacuum and the dry solids were characterized using XRPD. Sixty cooling crystallization experiments under equal conditions were conducted using 4HAP with concentration between 250 and 600 mg/mL in ethyl acetate solvents to validate the single nucleus mechanism. Six similar experiments were also performed at larger scale (100 mL) with a concentration of 500 mg/mL of 4HAP.

3.3. Results and discussion

We can identify conditions at which the probability of formation for the different polymorphs is approximately equal. Crystallization of such a

polymorphic system via the single nucleus mechanism would result in a 100% pure polymorphic fraction, while the polymorphic outcome could vary from experiment to experiment (**Figure 3.1**). Crystallization of a polymorphic system following the conventional mechanism would result in impure polymorphic fractions (concomitant polymorphism) as shown in **Figure 3.1**. We thus study polymorph crystallization as a function of mixed solvent composition in the case of INA and of concentration in the case of 4HAP. In this way we can validate the single nucleus mechanism in these systems.
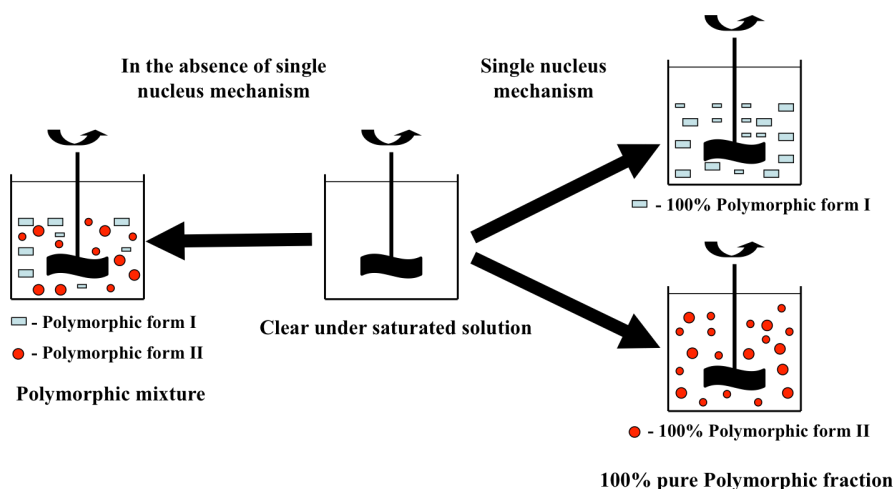
Figure 3.1: The outcome of a polymorph crystallization following a conventional pathway (left) and the Single Nucleus Mechanism (right) under conditions of concomitant polymorphism. Nucleation via the single nucleus mechanism would lead to 100% pure polymorphic fraction while the polymorphic outcome could vary from experiment to experiment. The conventional pathway would lead to concomitant polymorphism.

3.3.1. Polymorph Transformation

As we establish conditions for concomitant polymorphism it is important to exclude polymorph transformation processes to influence the results. We can exclude this if polymorph transformation is slow compared to the crystallization process. We thus studied the time required to transform the metastable form to the most stable form for both compounds.

INA. Seeding stable form II crystals (5% w/w of yield) in a suspension of metastable form I of INA in 70:30 vol% EtOH-NM at 25 °C resulted in a full transformation of form I to form II in 7 hours. The experiment without seeding showed a full transformation after only 24 hours. Similar studies were carried out using mixtures of stable form II and metastable form IV in 90:10 vol% EtOH-NB solutions leading to transformation times of 48 hours or more.

4HAP. A suspension of metastable form I only very slowly transform to stable form II (>72 hours). Complete transformation to stable form II starting with a suspended mixture (50% w/w) of form I and II was established only after 21 hours.

For the systems under investigation we thus found that the metastable polymorph only very slowly transform into the stable forms. This indicates that any polymorphic fraction determined early in a crystallization process is the result of nucleation and growth rather than of a transformation process.

3.3.2. Polymorph detection in suspension

To investigate the single nucleus mechanism we have to be able to detect small polymorphic fractions in suspension. In order to validate the polymorphic fraction in a suspension an in-situ analytical technique is required. The technique must be highly sensitive to different crystal structures, easy and fast to operate and sensitive enough to detect very small quantities of different polymorphic fractions. In-situ Raman spectroscopy is an ideal technique for this.[13]

INA polymorphs. Some Raman peaks of INA are relatively sensitive to the changes in the composition of the polymorphic fraction. As the pyridine-group does not play a major role in the hydrogen bonding of form II (dimer-like structure), while it does in the hydrogen bonding of form I and IV (chain-like structure), the position of the pyridine ring breathing region in the Raman spectra is different for both forms.[10] This ring breathing mode is the in-plane periodic expansion-contraction of the entire pyridine ring.[14] Pure Form II in a

suspension shows a peak for the pyridine ring breathing region at 995 cm^{-1} while pure form I in a suspension shows a peak at around 1002 cm^{-1} (7)[10] (**Figure 3.2**). Upon increasing the fraction of form I compared to form II in the suspension, the Raman peak intensity at 1002 cm^{-1} (form I) gradually increases while that at 995 cm^{-1} decreases. **Figure 3.2** shows that at a form I fraction of 5 and 95 wt% of INA it can already be identified that the suspension consists of 2 polymorphs.
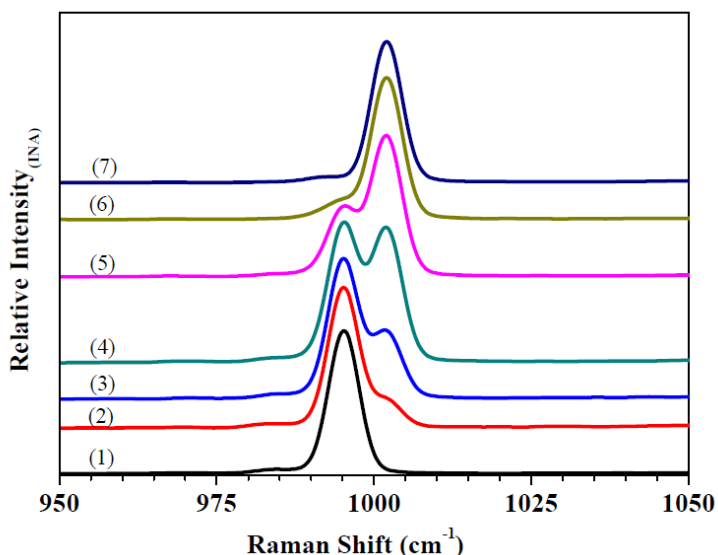
Figure 3.2: Raman spectra of different mixtures of form I and II of Isonicotinamide in an EtOH-NM suspension. (1) 0% Form I, (2) 5.0% Form I, (3) 30% Form I, (4) 50% Form I, (5) 70% Form I, (6) 95% Form I, and (7) 100% Form I.

In order to demonstrate the applicability and accuracy of Raman spectroscopy to the quantitative characterization of the polymorphs, a calibration curve was constructed from these suspension data (**Figure 3.3**). The calculation results for the 990-1010 cm^{-1} range showed a strong linear correlation (R^2=99.64%) between the peak intensity and the polymorphic form I fraction (**Figure 3.3**). Thus, Raman spectroscopy enables the detection of the polymorphic fraction of INA in a suspension right after its formation through

the determination of the relative peak heights. Similar experiments were carried out for form II and form IV of INA. A calibration curve was constructed with pure Form II in a suspension using the characteristic peak at 995 cm^{-1} and pure form IV in a suspension using the peak at around 1004 cm^{-1}.
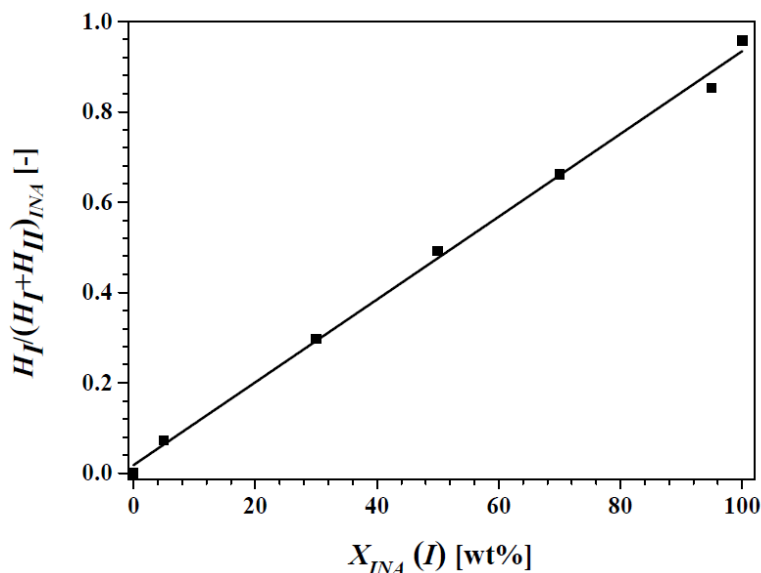
Figure 3.3: The calibration line constructed from the form I fraction and the relative peak height *HI/(HI+HII)* determined using Raman spectroscopy of the used INA suspension of form I and form II. Peak heights *HI* and *HII* were taken from the Raman spectrum of the suspension at respectively 1002 cm^{-1} and 995 cm^{-1}.

4HAP polymorphs. The two known forms of 4HAP exhibit different packing features as both polymorphs have different relative conformation of OH and C(O)-CH$_3$ groups.[12] The Raman spectra of the two forms show subtle differences between 1550 and 1700 cm^{-1}, which is the carbonyl region (**Figure 3.4**). The hydrogen bonded carbonyl group of 4HAP form II gives a peak at 1660 cm^{-1} while the hydrogen bonded carbonyl group of form I shows a peak at around 1642 cm^{-1}. **Figure 3.4** shows the region of the C-OH stretching vibrations for the Raman spectra of suspensions of mixtures of 4HAP form I and form II in ethyl acetate. Upon increasing the fraction of form I compared to

form II in the suspension, the Raman peak intensity at 1585 cm^{-1} and 1642 cm^{-1} (form I) gradually increases while that at 1570 cm^{-1} and 1660 cm^{-1} decreases.
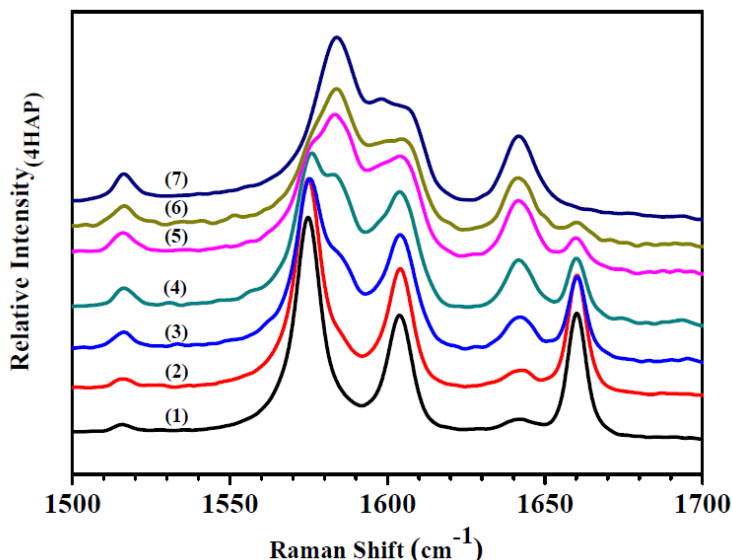
Figure 3.4: Raman spectra of mixtures of form I and II of 4HAP in an ethyl acetate suspension. (1) 0% Form I, (2) 5.0% Form I, (3) 30% Form I, (4) 50% Form I, (5) 70% Form I, (6) 95% Form I, and (7) 100% Form I.

To construct a calibration curve, similar to INA, binary mixtures of the two forms of 4HAP were suspended in a saturated solution. The peaks at 1570 cm^{-1}and 1642 cm^{-1} of form I and at 1585 cm^{-1} and 1660 cm^{-1} of form II were taken to construct the calibration curve. The calibration curve showed a strong linear correlation (R^2=99.05%) between the relative peak height and the polymorphic fraction (**Figure 3.5**). At a form I fraction of 5 and 95% it can already be identified that the suspension consists of 2 polymorphs. Hence Raman spectroscopy also enables the detection of the small polymorphic fraction of 4HAP in a suspension right after its formation.
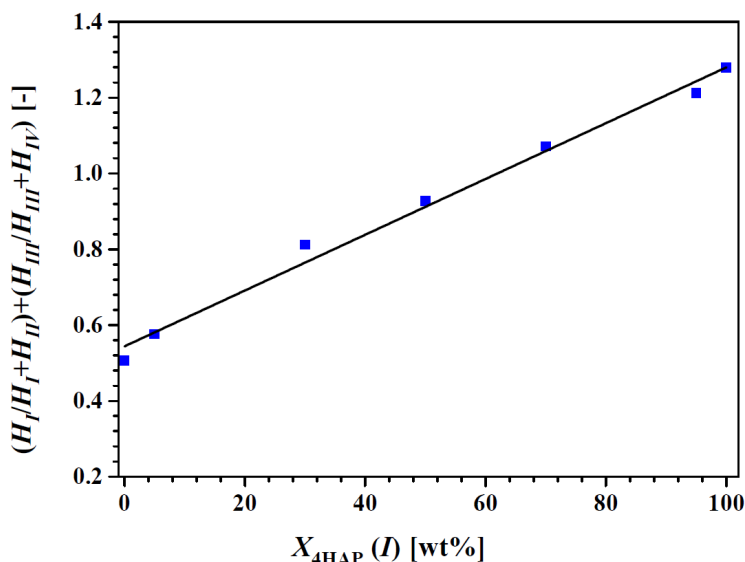
Figure 3.5: The calibration line constructed from the Raman spectra peak heights ($H_I/(H_I+H_{II})+ H_{III}/(H_{III}+H_{IV})$) of 4HAP suspensions of form I and II and the used form I fraction of 4HAP in the suspension. H_I, H_{II}, H_{III} and H_{IV} are the peak heights at 1570, 1585, 1642 and 1660 cm^{-1}, respectively. The solid line is the fit to the data.

3.3.3. Validation using Isonicotinamide polymorphs

The solvent mixture for concomitant polymorphism was established to be around 70:30 vol% EtOH-NM and 90:10 vol% EtOH-NB. When INA was crystallized from ethanol using differently concentrated solutions, only form II was obtained reproducibly (F**igure 3.6**).[10] Using similar crystallization methods, only pure form I was crystallized from nitromethane while only pure form IV was crystallized from nitrobenzene.[10]

We then performed 10 cooling crystallization experiments under equal conditions using 70:30 vol% EtOH-NM mixtures as a solvent and determined the polymorphic fraction as soon as crystals were detected using Raman (**Table 3.1**). The experimental weight fraction of form I and its significance were calculated using the constructed calibration curve with 70:30 vol% EtOH-

NM (**Figure 3.6**). Considering the margin of error (≤ ±4.1%) of the calibration line, all ten experiments using EtOH-NM resulted in a pure polymorphic phase of either form II or form I, see **Table 3.1** and **Figure 3.6** for the summary of results. These polymorphic fractions were verified using XRPD afterwards.
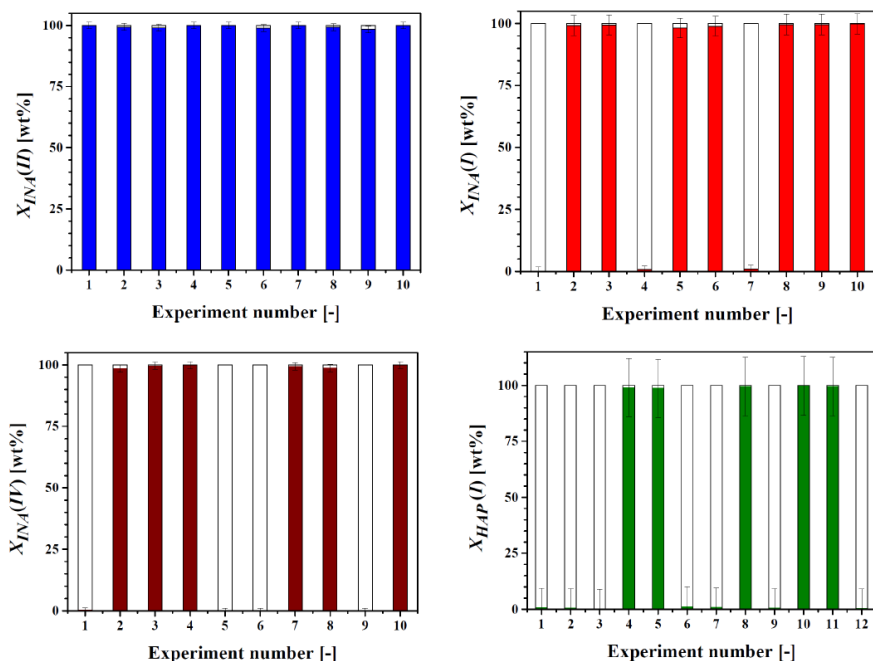
Figure 3.6: The polymorphic fractions of form II of INA in EtOH (100 vol% - blue columns), form I of INA in EtOH-NM solvent mixtures (70:30 vol% -red columns), form IV of INA in EtOH-NB solvent mixtures (90:10 vol% -brown columns) and form I of 4HAP in ethyl acetate (100 vol% -green columns). Considering the margin of error of the calibration line, all the experiments resulted in a pure polymorphic phase of either form II or form I or form IV in case of INA and either form I or form II in case of 4HAP.

We also performed 10 cooling crystallization experiments under equal conditions using 90:10 vol% EtOH-NB mixtures as a solvent and determined the polymorphic fraction as soon as crystals were detected using Raman (**Figure 3.6**). The experimental weight fraction of form IV and its significance was calculated using the constructed calibration curve with 90:10 vol% EtOH-

NB (**Figure 3.6**). All ten experiments using EtOH-NB resulted in a pure polymorphic phase of either form II or form IV. See **Table 3.2** and **Figure 3.6** for the summary of results. Within the error margin (≤ ±1.5%) all samples can be considered to be 100% pure. These polymorphic fractions were verified using X-ray powder diffraction afterwards.

Table 3.1: Final polymorphic outcome for the stirred cooling crystallization experiments of INA in EtOH-NM solvent mixtures.

EtOH fraction [vol%]	Total # of Experiment	Form I	Form II	Mixture
100	10	0	10	0
95	2	0	2	0
80	2	0	2	0
70	10	7	3	0
60	2	2	0	0

We further performed six larger scale (100 mL) crystallization experiments for the solvent mixtures 70:30 vol% EtOH-NM and 90:10 vol% EtOH-NB. In case of 90:10 vol% EtOH-NB two experiments resulted in pure form II and four in pure form IV. In case of 70:30 vol% EtOH-NM only one experiment resulted in pure form II and five in pure form I.

We further performed cooling crystallization experiments using 70:30 vol% EtOH-NM and 90:10 vol% EtOH-NB mixtures without stirring. In principle an unstirred experiment under these conditions should result in concomitant polymorphism since due to absence of secondary nucleation multiple primary nuclei can form. In case of 90:10 vol% EtOH-NB solvent mixtures all five experiments resulted in many small needle like crystals with a mixture of form II and form IV, as expected. In case of 70:30 vol% EtOH-NM two experiments

resulted in mixtures of polymorphs form I and form II, two in pure form I and one in pure form II.

Table 3.2: Final polymorphic outcome for the crystallization experiments of INA in EtOH-NB solvent mixtures.

EtOH fraction [vol%]	Total Experiment	Form II	Form IV	Mixture
100	10	10	0	0
97	2	2	0	0
94	2	2	0	0
90	10	4	6	0
85	2	0	2	0

The experiments suggest that in stirred solutions the single nucleus mechanism occurs, while unstirred solutions follow a conventional nucleation pathway resulting in concomitant polymorphism.

3.3.4. Validation using 4-Hydroxyacetophenone polymorphs

For 4HAP the concentration range for concomitant polymorphism was established to be between around 300 and 500 mg/mL of 4HAP in ethyl acetate. We performed 12 cooling crystallization experiments for each concentration under equal conditions in which we determined the weight fraction of form I in the crystal suspension using the established calibration line. All 12 experiments resulted in a close to pure polymorphic phase of either form II or form I, as determined by in situ Raman spectroscopy (**Figure 3.6**). Again, within the error margin (≤ ±13.1%) all samples can be considered to be 100% pure. The results were verified using X-ray powder diffraction. See **Table 3.3** for a summary of the 4HAP results.

We further performed six large-scale experiments (100 mL) at a concentration of 500 mg/mL. At this concentration the probability of

formation of both polymorphs was approximately equal. Four large-scale experiments resulted in pure form II and, surprisingly, two resulted in mixtures of form I and II. The polymorphic mixture cannot be due to a polymorph transformation as the transformation rate of form I to form II was shown to be too slow. A conventional nucleation mechanism for which in a larger volume multiple nuclei are formed in a short time, can lead to the formation of more than one polymorph. It could be conventional nucleation where multiple crystals of both polymorphs form in solution. It was previously shown that for larger volumes the fluctuation in metastable zone widths reduces to zero, indicating a transition from the single nucleus mechanism to a more conventional mechanism.[3] Another reason could be a liquid-liquid phase split in the 4HAP-ethyl acetate system as we observed a phase split in systems of 4HAP with solvents like water and water-ethanol mixtures. The liquid-liquid phase split region is a metastable region below the saturation temperature. Due to this metastable region the nucleation may proceed on the droplet surface and the single nucleus mechanism does not hold anymore.

We also performed five cooling crystallization experiments for 4HAP-ethyl acetate system with a concentration of 500 mg/mL at 3 mL scale without stirring. In case of 4HAP-ethyl acetate all five experiments resulted in mixtures of form I and form II.

Table 3.3: Final polymorphic outcome for the crystallization experiments of 4HAP in ethyl acetate solvent.

Concentration (mg/mL)	Total Experiment	Form I	Form II	Mixture
250	12	1	11	0
330	12	5	7	0
380	12	4	8	0
500	12	5	7	0
600	12	12	0	0

3.4. Discussion

3.4.1. Understanding crystal nucleation. The data generated on polymorphs of INA and 4HAP are highly supportive of our theory on the single nucleus mechanism. All experiments at small scale (3mL) resulted in a pure polymorphic phase of either form of INA and 4HAP. A single nucleus mechanism indicates pre-exponential factors of the classical nucleation rate equation orders of magnitude below those predicted by Classical Nucleation Theory (CNT).[3] These low pre-exponential factors are observed in many nucleation rate measurements.[4, 6, 15] Low pre-exponential factors might be resulting from low concentrations of a very active heterogeneous particles or low attachment frequency of molecules to the nucleus.[2]

3.4.2. Industrial importance. We have shown here that the single nucleus mechanism occurs for a number of systems on small and lab scale. Some observations indicate that the single nucleus mechanism might break down at larger scales (>1 L).[3] However, on industrial scales (>1000 L) at the cooling surface or the vapor-liquid surface at which evaporation takes place high local supersaturations will exist. Those will be the locations where crystal nucleation is most likely to take place. Thus, on industrial scales the occurrence of nucleation is bound to a small part of the industrial crystallizer, which would be advantageous for the single nucleus mechanism as compared to conventional nucleation. We thus expect that it is not unlikely to see the single nucleus mechanism to occur in industrial crystallization processes as well.

3.4.3. Industrial Control. The occurrence of the single nucleus mechanism on an industrial scale has strong implications for the control of the product quality from these industrial crystallization processes. In terms of crystal size distribution, control can be obtained by controlling the secondary rather than the primary nucleation event for which completely different control procedures are needed.[2] In terms of polymorphism we indicate that control

can be achieved by controlling the primary nucleation event that leads to the single crystal, which in turn defines the crystal form of the secondary nuclei. Seeding approaches using only a single crystal could then lead to the avoidance of primary nucleation and thus control over the polymorph obtained.

3.5. Conclusions

Crystallization of INA from the solvents ethanol, nitromethane and nitrobenzene results in respectively pure form II, pure form I and pure form IV. Because the transformation rate was measured to be relatively slow for INA as well as 4HAP this would not influence the polymorphic outcome from a relatively fast crystallization process. Nucleation experiments combined with polymorph detection could therefore be used to validate the single nucleus mechanism. Crystallization of INA from a 70:30 vol% mixture of EtOH-NM and 90:10 vol% mixture of EtOH-NB always resulted in either pure form I or pure form II. Similar to INA the crystallization of 4HAP at different concentrations in a 3 mL solution of ethyl acetate always resulted in either pure form I or II of 4HAP. At 100 mL scale four experiments resulted in pure form II and two resulted in the mixtures of form I and II. The data generated on polymorphs of INA and 4HAP are highly supportive to the proposed single nucleus mechanism and backing up our visual observations reported earlier.

3.6. Acknowledgement

3.7. References

(1) Mullin, J. W., Crystallization. 4th ed.; Butterworth-Heinemann: London, 2001.

(2) Kramer, H. J. M.; Jansens, P. J., Tools for Design and Control of Industrial Crystallizers – State of Art and Future Needs. Chemical Engineering & Technology 2003, 26, (3), 247-255.

(3) Kadam, S. S.; Kulkarni, S. A.; Coloma Ribera, R.; Stankiewicz, A. I.; ter Horst, J. H.; Kramer, H. J. M., A new view on the metastable zone width during cooling crystallization. Chemical Engineering Science 2012, 72, (0), 10-19.

(4) Jiang, S.; ter Horst, J. H., Crystal Nucleation Rates from Probability Distributions of Induction Times. Crystal Growth & Design 2011, 11, (1), 256-261.

(5) Kadam, S. S.; Kramer, H. J. M.; ter Horst, J. H., Combination of a Single Primary Nucleation Event and Secondary Nucleation in Crystallization Processes. Crystal Growth & Design 2011, 11, (4), 1271-1277.

(6) Kulkarni, S. A.; Kadam, S. S.; Meekes, H.; Stankiewicz, A. I.; ter Horst, J. H., Crystal Nucleation Kinetics from Induction Times and Metastable Zone Widths. Crystal Growth & Design 2013, 13, (6), 2435-2440.

(7) Kondepudi, D. K.; Kaufman, R. J.; Singh, N., Chiral Symmetry Breaking in Sodium Chlorate Crystallizaton. Science 1990, 250, (4983), 975-976.

(8) McBride, J. M.; Carter, R. L., Spontaneous Resolution by Stirred Crystallization. Angewandte Chemie International Edition in English 1991, 30, (3), 293-295.

(9) Horst, J. H. t.; Kashchiev, D., Determining the nucleation rate from the dimer growth probability. The Journal of Chemical Physics 2005, 123, (11), 114507.

(10) Kulkarni, S. A.; McGarrity, E. S.; Meekes, H.; ter Horst, J. H., Isonicotinamide self-association: the link between solvent and polymorph nucleation. Chemical Communications 2012, 48, (41), 4983-4985.

(11) Bernstein, J.; Davey, R. J.; Henck, J.-O., Concomitant Polymorphs. Angewandte Chemie International Edition 1999, 38, (23), 3440-3461.

(12) Bernardes, C. E. S.; Piedade, M. F. t. M.; Piedade, M. E. M. d., Polymorphism in 4'-Hydroxyacetophenone: Structure and Energetics. Crystal Growth & Design 2008, 8, (7), 2419-2430.

(13) Ono, T.; ter Horst, J. H.; Jansens, P. J., Quantitative Measurement of the Polymorphic Transformation of l-Glutamic Acid Using In-Situ Raman Spectroscopy. Crystal Growth & Design 2004, 4, (3), 465-469.

(14) Berg, E. R.; Freeman, S. A.; Green, D. D.; Ulness, D. J., Effects of hydrogen bonding on the ring stretching modes of pyridine. The journal of physical chemistry. A 2006, 110, (50), 13434-46.

(15) Davey, R. J.; Schroeder, S. L. M.; ter Horst, J. H., Nucleation of Organic Crystals—A Molecular Perspective. Angewandte Chemie International Edition 2013, 52, (8), 2166-2179.

CHAPTER 4

A Liquid-Liquid phase separation during Crystallisation of 4-Hydroxyacetophenone from solution

Submitted manusript

Abstract

An accurate understanding and representation of liquid-liquid phase separation (LLPS) in solutions of small molecules remains one of the challenging research areas in chemical processes. The unexpected presence of two distinct liquid phases during an industrial crystallization processes can seriously influence operation and product quality. In this study we show the effect of LLPS on the phase diagram and crystallization behaviour of 4-hydroxyacetophenone (4HAP) in water, water-ethanol mixtures and ethyl acetate solutions. The 4HAP in water and water/ethanol mixtures shows a stable LLPS and this stable region is influenced by the amount of ethanol used. Cooling crystallization experiments always resulted into mixtures of polymorphic fractions if the LLPS preceded 4HAP crystallization. For example in case of 4HAP in water-ethanol mixtures the crystallization outcome specially in the LLPS region was either a mixture of form I and form II or mixture of form I and hydrate H2 of 4HAP. The results suggest that the crystallization behaviour is strongly influenced by the presence of this LLPS. Due to the LLPS the nucleation may proceed on the droplet surface and the single nucleus mechanism does not hold anymore. The crystallization within the LLPS region seems to lead to agglomeration of the particles.

4.1. Introduction

Crystallization is an essential step in many processes in chemical industries, ranging from bulk chemicals to special products in order to meet customer demands on particle properties like particle size distribution, crystal shape, degree of agglomeration, caking behaviour, purity and filterability.[1] Sometimes, during the process of cooling crystallization, the product separates not as crystals but as an impure metastable liquid. This phenomenon is referred to as oiling out or liquid-liquid phase separation (LLPS). Oiling out is an often-unwanted effect during cooling crystallization processes. The LLPS has important effect on the crystallization process and in most cases affects the product properties like crystal size and form, affinity of agglomeration and hence the product purity.[2]

The LLPS was demonstrated for different g-crystallins[3, 4] in 1987 and lysozyme[5, 6] in 1994. The existence of a LLPS of methyl (E)-2-[2-(6-trifluoromethylpyridine-2-yloxymethyl)-phenyl]-3-methoxyacrylate in water-methanol solvent mixtures and its thermodynamic relation was studied experimentally by Bonnett et. al.,[2] and was also observed and studied in other systems.[7-11] The LLPS can occur prior to crystallization which can hinder the primary and secondary nucleation.[12] In the present work we study the LLPS during crystallization of 4-hydroxyacetophenone (4HAP) from solution.

4-hydroxyacetophenone (4HAP), also known as 4-hydroxybenzaldehyde, is known to have two anhydrous forms and three hydrated forms.[13] The selective and reproducible crystallization of two anhydrous and three hydrated forms from water-ethanol mixtures were previously studied.[14] These experiments showed the appearance of a colloidal dispersion in 4HAP solutions in H_2O mixture.[13] Our interest in the LLPS and the crystallization behaviour in the presence of a LLPS turned us to a deeper investigation into this complex system.

In the present work we report the adjustment of the LLPS by using solvent mixtures. We further describe the crystallization behaviour of 4HAP from solution in the presence and absence of the LLPS. The impact on the nucleation mechanisms is highlighted and the polymorphic outcome is discussed.

4.2. Materials and Methods

4.2.1. Materials and Instrumentation. 4-Hydroxyacetophenone (4HAP) with a purity of ≥99% was obtained from Sigma Aldrich. Ethanol and ethyl acetate were used as solvent and were of ACS reagent grade with a purity of ≥99.5% and 99+% respectively. The solubility of 4HAP in different solvents was determined using the Crystal16 (Avantium Amsterdam) following the procedure described by ter Horst et al.[15] The 3 ml crystallization experiments were carried out in an 8 ml multiple reactors set up (Crystalline, Avantium, Amsterdam). Four of the reactors of Crystalline are connected with an in situ camera with a resolution of 5-11 µm/pixel and a depth of field of 2.5 mm. A Hololab series 5000 Raman spectroscopy (Kaiser Optical System, Inc.) coupled to the Crystalline facilitated the recording of Raman spectra of solutions and suspensions in one of the reactors of the Crystalline. The in situ Raman spectra were recorded by excitation radiation at 785 nm using a NIR probe. The final crystalline product was characterized using powder X-ray diffraction (XRD; Bruker D2 Phaser, 30kV and 30 mA) with CuKα radiation (λ= 1.5406 ˚A). Data were collected in the 2θ–θ scanning mode with a scan speed of 2 min^{-1} and a step size of 0.022.

4.2.2. Methods

4HAP in water and water-ethanol mixtures. A binary phase diagram was constructed by doing a simple cooling crystallization experiments with in-situ camera to analyse the sample.

Cooling crystallization experiments were carried out using different concentrations of 4HAP in ethanol, water or mixtures thereof. The 3 ml starting

suspension of 4HAP in the solvent mixture was heated to 60 °C to establish a clear solution and then cooled down to 5 °C with a cooling rate of 0.5 °C/min while stirring (700 rpm) using a magnetic stirrer. During the heating and cooling cycles the presence of crystals, LLPS or both was observed using the in situ cameras and the suspension was analysed using in situ Raman spectroscopy. The temperature at which the suspension underwent a LLPS upon heating and the temperature at which a LLPS or crystallization occurred in the clear solution upon cooling were recorded. In a number of cases the suspension was filtered through a 0.45 μm filter soon after solids were detected and the crystalline product was characterized by XRPD.

Sixty cooling crystallization experiments using 90vol% water-ethanol and 80vol% water-ethanol solvent mixtures at 3 ml were performed using 4HAP with different concentrations.

4HAP in ethyl acetate. A suspension of 4HAP in 3 mL ethyl acetate with a concentration between 500 mg/mL was heated to 60 °C with a heating rate of 1 °C/min and kept at that temperature for 1 hour. Then the clear solution was cooled with a cooling rate of 0.3 °C/min to 5 °C. The crystallization behavior was recorded with the in situ camera. When a crystal suspension was observed the crystals were immediately filtered in vacuum and the dry solids were characterized using XRPD. 12 cooling crystallization experiments under equal conditions were conducted using 4HAP with concentration of 500 mg/mL in ethyl acetate solvents. Six similar experiments were also performed at larger scale (100 mL) with a concentration of 500 mg/mL of 4HAP.

4HAP, water and ethanol fraction in both liquid phases was determined by heating 4HAP in water (80%)-ethanol (20%) mixture in the L_S+L_H region until no solids were observed. The solution was held at the desired temperature until the two liquids was settled. The volume of both top and bottom liquid was measured by measuring the height of the liquid multiplied by the inner surface area of the vial. The water weight fraction was determined with the KF

Coulometer (Metrohm) and the 4HAP fraction of the top liquid was determined by evaporating the solvent at 80 °C for 2 days.

4.3. Results and discussion

We have investigated the system of 4-Hydroxyacetophenone (4HAP) in water, water-ethanol mixtures and ethyl acetate. In the first part we report the crystallization behaviour of 4HAP in ethyl acetate, water and water-ethanol mixtures. In the second part we discussed the crystallization conditions in presence and absence of LLPS and the phase diagram of 4HAP in water and water-ethanol mixtures. We also studied the role of LLPS on nucleation and crystallization of different forms of 4HAP and the effect of LLPS on single nucleus mechanism.

From previous studies 4HAP is known to form two anhydrous polymorphic forms as well as three hydrated forms.[13, 14] The two anhydrous forms are enantiotropically related where form II is more stable below 293-308K while form I is more stable above this temperature, although an earlier report gives a temperature of around 277 K.[14] At room temperature the hydrate H1 (4HAP.1.5H2O) is reported to be the most stable hydrate in water.[13] At this temperature the metastable hydrate H2 (4HAP.3H2O) transformed slowly into hydrate H1. A colloidal phase was reported to influence crystallization behaviour leading to the identification of hydrate H3 of yet unknown stoichiometry.[13]

4.3.1. Cooling crystallization of 4HAP in Ethyl acetate

We performed 12 cooling crystallization experiments for 265 mM/M of 4HAP in ethyl acetate under equal conditions. During the crystallization experiments of 4HAP in ethyl acetate, a single crystal was observed before the formation of crystal suspension (**Figure 4.1**). This single parent crystal further grows and serves as the origin of secondary nuclei, which further grow to form the detectable crystalline phase. All 12 experiments resulted in a close to pure

polymorphic phase of either form II or form I, as determined by in situ Raman spectroscopy. See a summary of the results in **table 4.1**.

We further performed six large-scale experiments (100 mL) at a concentration of 265 mM/M. From previous study we know that at this concentration the probability of formation of both polymorphs was approximately equal.[16] Four large-scale experiments resulted in pure form II and, surprisingly, two resulted in mixtures of form I and II.

(a) At 60 °C   **(b) At 27 °C**   **(c) At 15 °C**

Slow cooling with 0.2 °C/min
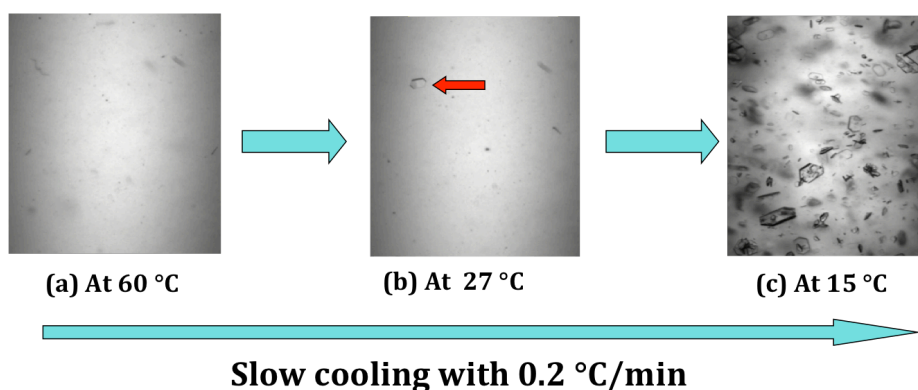
Figure 4.1: In-situ images from a stirred cooling crystallization experiments of 4HAP (265 mM/M) in ethyl acetate at 3 ml scale. a) The clear supersaturated solution; b) The single parent crystal; and c) the suspension after attrition of the single parent crystal and growth of the secondary nuclei. The red arrow indicates the single parent crystal.

4.3.2. Cooling crystallization of 4HAP in water/ethanol (90-10% vol/vol)

Twenty cooling crystallization were performed using water/ethanol mixture (90-10% vol/vol) as a solvent. Out of 20 experiments of 4HAP from water/ethanol mixtures (90-10% vol/vol), four resulted in 4HAP form I and sixteen resulted in the mixtures of form I and hydrate H2. **Figure 4.2** shows in-

situ images from a cooling crystallization experiment of 4HAP in Water-ethanol Mixture (90-10% vol/vol).

(a)   (b)
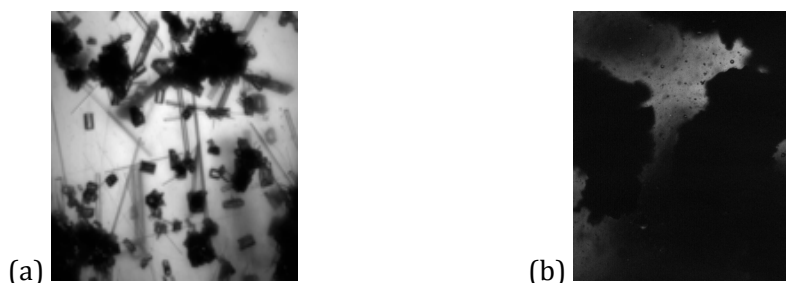
Figure 4.2: In-situ images from cooling crystallization experiments of 4HAP in water-ethanol mixture (90-10% vol/vol). (a) Form I (agglomerates) together with the hydrate H2 (needles) from water, (b) Crystallization leads to agglomeration of the particles of 4HAP form I after the LLPS at 70 mM of 4HAP in water/ethanol mixture (90-10% vol/vol).

When a clear solution was cooled in water-ethanol mixture (90-10 vol%), a cloud point with a LLPS occurs at 55 °C. Initially the droplets were about 10-15 μm in size which grows to 100 μm with decreasing temperature. After cooling the solution further to 21 °C, crystals appeared at the interface of the dispersed drops. The solution was further cooled to 15 °C until it completely crystallized (**Figure 4.3**). When this crystal suspension further heated, a LLPS was observed before the measurement of the clear point (35 °C). The crystals eventually dissolved in solution and the liquid splits into two phases. At 37 °C, a solution completely shows only two liquid phases. The LLPS, upon further heating, became a single clear phase at 57 °C. **Figure 4.3** shows the images of this process recorded at 1) 60 °C, 2) 55 °C and 3) 21 °C**,** 4) 14 °C and 5) 37 °C. The LLPS is a stable region in case of 4HAP in water-ethanol mixture (80-20% vol/vol). The stable LLPS was also observed for water/ethanol (80-20% vol/vol) and pure water systems.
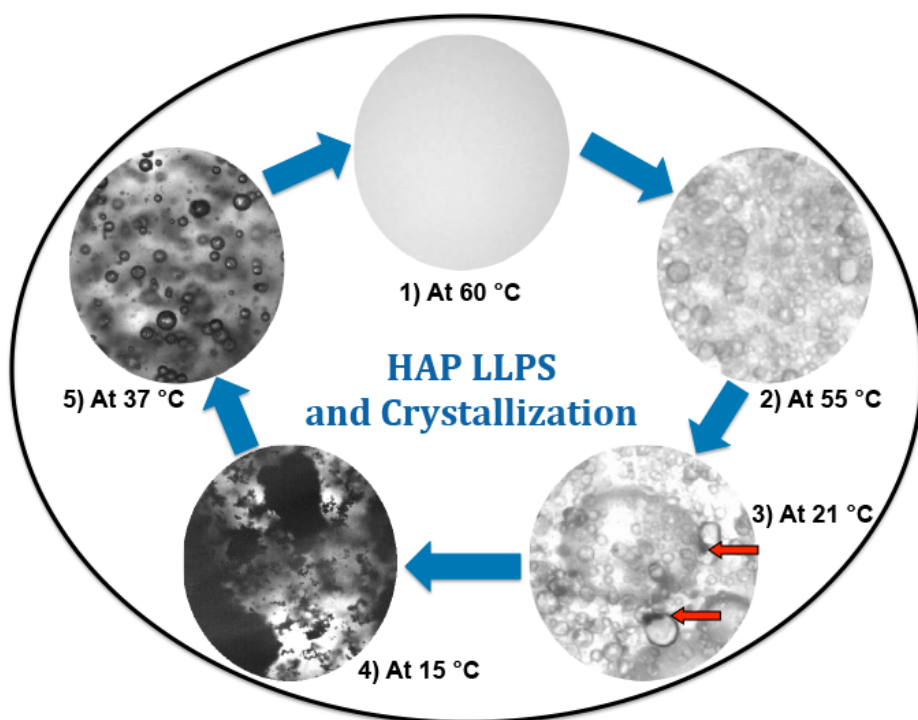
Figure 4.3: Observation of a sample having a composition of 25 mM/M in 90-10v% water-ethanol mixtures upon slowly (0.2 °C/min) decreasing and increasing the temperature. 1) At 60°C a clear single liquid is observed, 2) upon cooling a LLPS appeared at 55°C. Droplets were about 10-100 μm in size, 3) After further cooling down to 21 °C, crystals appeared on the droplet surface, indicated by the red arrows, 4) A completely crystallized suspension at 15 °C, 5) Upon heating, the suspension turns into a Liquid-Liquid system at 35 °C. Droplets are about 10-50 μm in size.

4.3.3. Cooling crystallization of 4HAP in water/ethanol (80-20% vol/vol)

Twenty cooling crystallization were also performed using water/ethanol mixture (80-20% vol/vol) as a solvent. Out of 20 cooling crystallization experiments using water ethanol mixture (80-20% vol/vol), seven experiments resulted in pure form I, two resulted in pure form II, eight resulted in the mixtures of form I and for II and three resulted in the mixtures of form I and hydrate H2. See the summary of results in **Table 4.1**.
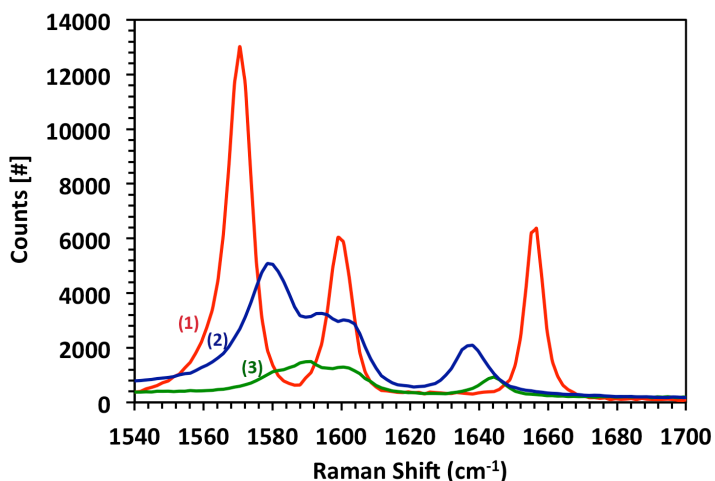
Figure 4.4: Raman spectra's of solids samples of 4HAP polymorphs, (1) Form II Solids (2) Form I Solids (3) hydrate H2 (4HAP.3H2O). 4HAP form II shows peaks at 1660 cm^{-1} is the carbonyl (CO) stretching vibration peak, at 1595 cm^{-1} is the hydrogen bonded CO and peak at 1565 cm^{-1} is the skeletal vibrations of the aromatic ring.[17] The carbonyl stretching vibration peaks are shifted to a lower wavenumber in case of form I and hydrate H2.
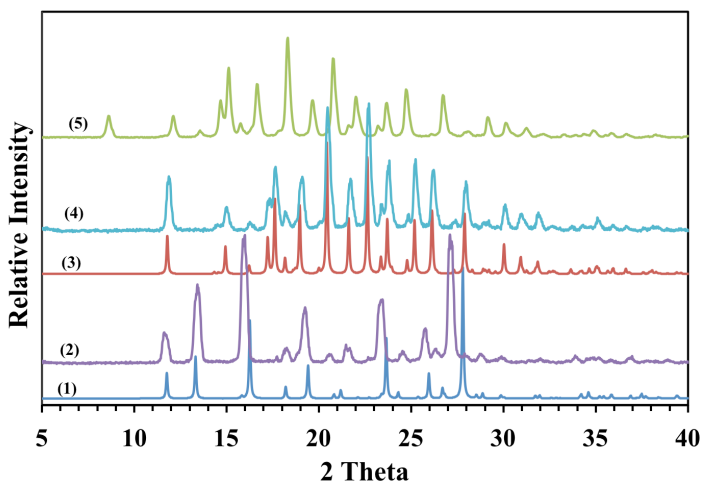
Figure 4.5: XRPD of solids samples of 4HAP polymorphs, (1) Reference form I_CSD (4503536.cif) (2) Form I Solids (3) Reference form II_CSD (4503538.cif) (4) Form II Solids (5) hydrate H2.

The crystals obtained with crystallization via the LLPS were also analysed with Raman spectroscopy. **Figure 4.4** shows Raman spectra of the carbonyl region of 4HAP from water and water-ethanol mixtures. The 4HAP form II peaks at 1660 cm^{-1}, 1595 cm^{-1} and 1565 cm^{-1} are the peaks of carbonyl stretching vibrations, hydrogen bonded carbonyl group and skeletal vibrations of the aromatic ring[17], respectively. The carbonyl peaks shifts to lower wavenumber in case of form I (1638 cm-1) and hydrate H2 (1642 cm^{-1}) as compared to carbonyl group of 4HAP form II. The cooling crystallization experiments using water ethanol mixture (80-20% vol/vol) results in either pure form I or form II or mixtures of form I and hydrate H2. The solids were further verified by the XRPD.

Table 4.1: Final polymorphic outcome of 4HAP from water, water-ethanol mixtures and ethyl acetate as a solvent.

Solvent used	Scale (ml)	Total experiments	Form I	Form II	Hydrate H2	Mixture
4HAP in Water (0-12 mM of 4HAP)	3	20	0	0	10	10 (Form I + Hydrate H2)
4HAP in Water-ethanol (90-10 wt%) (6-40 mM of 4HAP)	3	20	4	0	0	16 (Form I + Hydrate H2)
4HAP in Water-ethanol (80-20wt%) (15-80 mM of 4HAP)	3	20	7	2	0	8 (Form I + Form II) 3 (Form I + Hydrate H2)
4HAP in ethyl acetate (265 mM of 4HAP)	3	12	5	7	0	0
4HAP in ethyl acetate (265 mM of 4HAP)	100	6	0	4	0	2 (Form I + Form II)

4.3.4. Cooling crystallization of 4HAP in water

Out of 20 cooling crystallization experiments of 4HAP in water, seven experiments resulted in pure form I, two resulted in pure form II, eight resulted in the mixtures of form I and for II and three resulted in the mixtures of form I and hydrate H2. See the summary of results in **Table 4.1**.
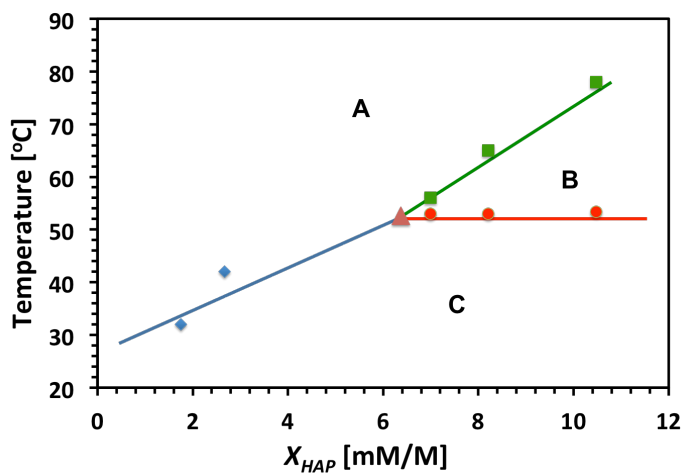
Figure 4.6: Phase diagram of 4HAP in water. Region (A) is the single liquid region where the solution is stable. Region (B) is the region where a liquid–liquid phase separation (LLPS) occurs into a 4HAP-rich and a 4HAP-lean liquid phase. Region (C) is the region where crystals and liquid co-exists. The solid green squares (■) are the points at which the liquid separate into two liquids (4HAP-rich and a 4HAP-lean liquid phase). The lower left blue squares (♦) indicate equilibrium between a solid and a liquid phase. The solid circles (●) represent the line at which the solid and the two liquids are in equilibrium. The solid triangle (▲) indicates the composition in the light liquid phase when 3 phases are in equilibrium. The lines are drawn as a guide to the eye.

In order to further explore the LLPS of 4HAP in water and water-ethanol mixtures, we explore the temperature and composition at which the 4HAP shows clear single liquid region of 4HAP solution, also a temperature and

composition at which LLPS appear and disappear and finally the temperature and composition at which the crystallization starts. To determine the temperature where the solute rich phase formed and to confirm its liquid-like structure, a set up with an in-situ camera was used.

The obtained phase diagram information of 4HAP in water is presented in **figure 4.6**. It shows three regions. The first region (A) is the single liquid region where the solution is stable. In the second region (B), a liquid–liquid phase separation (LLPS) occurs into a 4HAP-rich and a 4HAP-lean liquid phase. The droplets had an initial mean size of approximately 10-15 μm, which increased to 100 μm with decreasing temperature. If the stirrer was switched off the two phases eventually settled as two continuous liquid phases. At lower temperatures the LLPS disappears and a normal suspension appears where crystals and liquid co-exists (C).

Between the concentrations ranges 0-6 mM/M of 4HAP in water, hydrates H2 of 4HAP were formed when water was used as solvent. Above 6 mM/M of 4HAP in water the crystallization experiments resulted in the mixtures of form I and hydrate H2.

After adding 10 and 20 vol% of ethanol in water the solubility of 4HAP increases with a factor of 5 and 10 respectively (**Figure 4.6, Figure 4.7** and **Figure 4.8**). The phase diagram of 4HAP in water-ethanol (90-10 vol%) and water-ethanol (80-20 vol%) are presented in **figure 4.7** and **figure 4.8**, respectively. It clearly appears that in both cases the liquid-liquid phase boundary lies above the solubility curve. As the solubility of 4HAP increases with the amount of ethanol in water, the LLPS also shifts to higher temperature and concentration with increasing amount of ethanol so as the line at which the solid and the two liquids are in equilibrium also shifts higher.
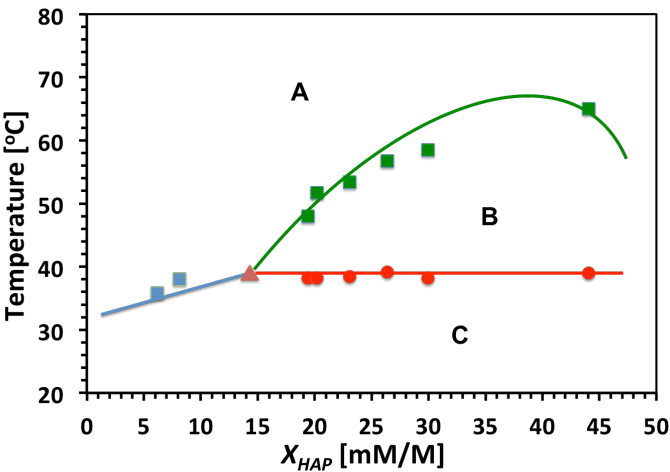
Figure 4.7: Phase diagram of 4HAP in a water-ethanol mixture (90-10 vol/vol%). Region (B) is the region where a liquid–liquid phase separation (LLPS) occurs into a 4HAP-rich and a 4HAP-lean liquid phase. Region (C) is the region where crystals and liquid co-exists. The solid green squares (■) are the points at which the liquid separate into two liquids (4HAP-rich and a 4HAP-lean liquid phase). The lower left blue squares (◆) indicate equilibrium between a solid and a liquid phase. The solid circles (●) represent the line at which the solid and the two liquids are in equilibrium. The solid triangle (▲) indicates the composition in the light liquid phase when 3 phases are in equilibrium. The lines are drawn as a guide to the eye.

Table 4.2: Fractions of the solute rich and solvent rich liquid in the L_S+L_H region at 35 °C of 260 mg/ml 4HAP in water (80%)-ethanol (20%).

|	L_S Weight Fraction	L_H Weight Fraction	K
Water	0.78	0.367	0.47
Ethanol	0.15	0.141	0.94
4HAP	0.07	0.492	7.03
Total	1.00	1.00	

L_S- Solvent rich phase; L_H- Solute rich phase
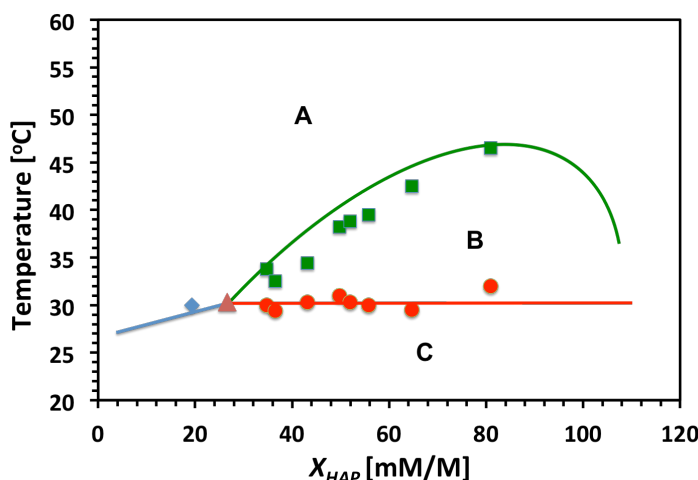
Figure 4.8: Phase diagram of 4HAP in water-ethanol mixture (80-20 vol/vol%). Region (A) is the single liquid region where the solution is stable. Region (B) is the region where a liquid–liquid phase separation (LLPS) occurs into a 4HAP-rich and a 4HAP-lean liquid phase. Region (C) is the region where crystals and liquid co-exists. The solid green squares (■) are the points at which the liquid separate into two liquids (4HAP-rich and a 4HAP-lean liquid phase). The lower left blue squares (◆) indicate equilibrium between a solid and a liquid phase. The solid circles (●) represent the line at which the solid and the two liquids are in equilibrium. The solid triangle (▲) indicates the composition in the light liquid phase when 3 phases are in equilibrium. The lines are drawn as a guide to the eye.

In order to estimate the boundaries of the LLPS region the value of low and high concentrations of LLPS droplet formation were experimentally determined. A sample containing 260 mg/ml of 4HAP in water-ethanol (80-20 vol%) was used which is in the LLPS region at 35 °C. Two liquid phases separate upon leaving the sample unstirred. The compositions and weights of the low-density solvent rich phase L_S (78-15 wt% water-ethanol) and the high-density solute rich phase L_H (37-14 wt% water-ethanol) is shown in **table 4.2**. The result also shows that 4HAP favours water deficit phase (ethanol rich

phase) than water rich phase. The top liquid contained mainly solvent and only 7wt% 4HAP. This solvent rich liquid (L_s) decreased when the 4HAP concentration is increased. The bottom liquid was the solute rich solvent that contained 49wt% of 4HAP. The composition of the solvent and solute in the L_s+L_H region depended on the temperature.
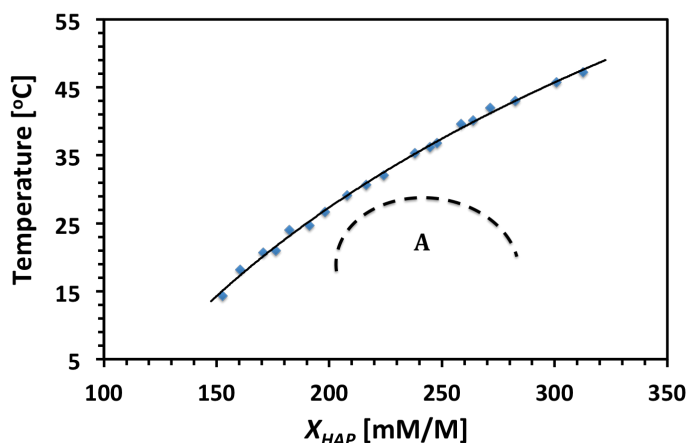
Figure 4.9: Phase diagram of 4HAP in ethyl acetate. The solid squares represent the average value of several saturation temperature measurements of a single sample. The line is a fit of the Van't Hoff equation to the experimental data. The dashed line indicates the liquid–liquid region at which the liquid separates into two liquids (A).

In case of 4HAP in ethyl acetate four large-scale experiments (100 ml) resulted in pure form II and, surprisingly, two resulted in mixtures of form I and II. 4HAP does not follow single nucleus mechanism in presence of LLPS and results in polymorphic fractions. The polymorphic mixture cannot be due to a polymorph transformation as the transformation rate of form I to form II was shown to be too slow.[16] The reason could be a liquid-liquid phase split in the 4HAP-ethyl acetate system as we observed a phase split in systems of 4HAP with solvents like water and water-ethanol mixtures. The liquid-liquid phase split region is a metastable region below the saturation temperature (**Figure**

4.9). Due to this metastable region the nucleation may proceed on the droplet surface and the single nucleus mechanism does not hold anymore.[16] Another reason could be as per conventional nucleation mechanism for which in a larger volume multiple nuclei are formed in a short time, can lead to the formation of more than one polymorph. It could be conventional nucleation where multiple crystals of both polymorphs form in solution.

4.4. Discussion

We have investigated the effect of LLPS on the crystallization of 4HAP in water, water-ethanol mixtures and ethyl acetate. Techniques, such as in-situ cameras and Raman spectroscopy are used to determine the temperature at which the LLPS occurs and the crystal forms present in solution and XRPD was used to investigate the final crystallization outcome. The increase in the amount of one solvent in a mixed-solvent solution dramatically influences the phase distribution of a solute between the liquid phases. The temperature and concentration of LLPS region increases with increase in the amount of ethanol. At water to ethanol ratio of 90:10, the size of the region is significantly enlarged. However, this region becomes largest at water to ethanol ratio of 80:20. The onset of crystallization of 4HAP in pure water was around 50 °C at a concentration of 45-80 mg/ml, while it shifts to 40 °C at a concentration of 100-300 mg/ml of 4HAP in water to ethanol ratio of 90:10 and 30 °C at a concentration of 100-300 mg/ml of 4HAP in case of water to ethanol ratio of 80:20.

The results show that the crystallization of 4HAP from water and water-ethanol mixtures resulted into form I, form II, mixtures of form I and form II and form I and hydrate H2 ($4HAP.3H_2O$). The amount of ethanol dramatically influences the distribution of the solute over the liquid phases by changing the solubility of 4HAP in solvent mixtures and results in the crystallization of anhydrated forms of 4HAP. We observed the crystal forming at the interface of water deficit (ethanol rich) phase, which could lead to the

formation of anhydrated polymorphic forms of 4HAP. Although many of the experiments resulted in the mixtures of polymorph of form I and form II and also form I and hydrate H2. The results suggest that the crystallization behaviour is strongly influenced by the presence of this LLPS. The crystallization within the LLPS region seems to lead to agglomeration of the particles. The consequence of the formation of LLPS is that it changes the kinetic pathway of crystal nucleation significantly. Moreover, the metastable LLPS hinder the primary and secondary nucleation and the single nucleus mechanism does not hold anymore which was the case of 4HAP in ethyl acetate. In many experiments under identical conditions we obtained crystals of pure polymorphic form of 4HAP as well as mixtures of stable and metastable polymorph of 4HAP. For 4HAP in water and water-ethanol mixtures the LLPS region was stable region below the saturation temperature where the nucleation starts. Due to this LLPS region the nucleation proceed with different mechanism. We can however not rule out that the polymorphic outcome is determined in the growth stage of the process after liquid-like clusters are formed on the surface.

4.5. Conclusion

In this study, in-situ cameras were used to determine the disappearance and reappearance temperatures of LLPS. The unexpected presence of two liquid phases can be a serious problem during industrial crystallization processes. We have studied the effect of LLPS on crystallization of 4HAP in water and water-ethanol mixtures. Observation by Crystalline in situ camera of the nucleation of droplets of the supersaturated solution of 4HAP shows the crystal forming at the interface of the droplets. Crystallization experiments of 4HAP in water resulted in either hydrate of 4HAP or mixtures of hydrate and pure form I. In case of 4HAP in water ethanol mixtures the crystallization outcome was either anhydrous form I and form II or mixtures of both and mixtures of form I and hydrate of 4HAP. The data generated on polymorphs of

4HAP suggest that LLPS hinder the primary and secondary nucleation and the single nucleus mechanism does not hold anymore. The amount of ethanol also dramatically influences the phase distribution of a solute between the liquid phases by changing the solubility of 4HAP in solvent mixtures.

4.6. Reference

(1) Lee, A. Y.; Erdemir, D.; Myerson, A. S., Crystal Polymorphism in Chemical Process Development. Annual review of chemical and biomolecular engineering 2011, 2, (1), 259-280.

(2) Bonnett, P. E.; Carpenter, K. J.; Dawson, S.; Davey, R. J., Solution crystallisation via a submerged liquid-liquid phase boundary: oiling out. Chemical Communications 2003, (6), 698-699.

(3) Thomson, J. A.; Schurtenberger, P.; Thurston, G. M.; Benedek, G. B., Binary liquid phase separation and critical phenomena in a protein/water solution. Proceedings of the National Academy of Sciences of the United States of America 1987, 84, (20), 7079-7083.

(4) Broide, M. L.; Berland, C. R.; Pande, J.; Ogun, O. O.; Benedek, G. B., Binary-liquid phase separation of lens protein solutions. Proceedings of the National Academy of Sciences of the United States of America 1991, 88, (13), 5660-5664.

(5) Ishimoto, C.; Tanaka, T., Critical Behavior of a Binary Mixture of Protein and Salt Water. Physical Review Letters 1977, 39, (8), 474-477.

(6) Taratuta, V. G.; Holschbach, A.; Thurston, G. M.; Blankschtein, D.; Benedek, G. B., Liquid-liquid phase separation of aqueous lysozyme solutions: effects of pH and salt identity. The Journal of Physical Chemistry 1990, 94, (5), 2140-2144.

(7) Veesler, S.; Revalor, E.; Bottini, O.; Hoff, C., Crystallization in the Presence of a Liquid–Liquid Phase Separation. Organic Process Research & Development 2006, 10, (4), 841-845.

(8) Codan, L.; Casillo, S.; Bäbler, M. U.; Mazzotti, M., Phase Diagram of a Chiral Substance Exhibiting Oiling Out. 2. Racemic Compound Forming Ibuprofen in Water. Crystal Growth & Design 2012, 12, (11), 5298-5310.

(9) Murata, K.-i.; Tanaka, H., Liquid–liquid transition without macroscopic phase separation in a water–glycerol mixture. Nat Mater 2012, 11, (5), 436-443.

(10) Yang, H.; Rasmuson, Å. C., Investigation of Batch Cooling Crystallization in a Liquid–Liquid Separating System by PAT. Organic Process Research & Development 2012, 16, (6), 1212-1224.

(11) Lafferrère, L.; Hoff, C.; Veesler, S., In Situ Monitoring of the Impact of Liquid–Liquid Phase Separation on Drug Crystallization by Seeding. Crystal Growth & Design 2004, 4, (6), 1175-1180.

(12) Liu, X. Y., A new kinetic model for three-dimensional heterogeneous nucleation. The Journal of Chemical Physics 1999, 111, (4), 1628-1635.

(13) Bernardes, C. E. S.; da Piedade, M. E. M., Crystallization of 4′-Hydroxyacetophenone from Water: Control of Polymorphism via Phase Diagram Studies. Crystal Growth & Design 2012, 12, (6), 2932-2941.

(14) Simões, R. G.; Bernardes, C. E. S.; da Piedade, M. E. M., Polymorphism in 4-Hydroxybenzaldehyde: A Crystal Packing and Thermodynamic Study. Crystal Growth & Design 2013, 13, (7), 2803-2814.

(15) ter Horst, J. H.; Deij, M. A.; Cains, P. W., Discovering New Co-Crystals. Crystal Growth & Design 2009, 9, (3), 1531-1537.

(16) Kulkarni, S. A.; Meekes, H.; ter Horst, J. H., Polymorphism Control through a Single Nucleation Event. Crystal Growth & Design 2014, 14, (3), 1493-1499.

(17) Vijayan, N.; Ramesh Babu, R.; Gunasekaran, M.; Gopalakrishnan, R.; Kumaresan, R.; Ramasamy, P.; Lan, C. W., Studies on the growth and characterization of p-hydroxyacetophenone single crystals. Journal of Crystal Growth 2003, 249, (1–2), 309-315.

CHAPTER 5

Isonicotinamide self-association: the link between solvent and polymorph nucleation

This Chapter is published as

Abstract

We show that, in a controlled and reproducible way, specific solvents lead to specific polymorphic forms of isonicotinamide. We argue on the basis of Raman and FTIR spectroscopy that the hydrogen bonding in solution kinetically drives the nucleation towards a specific form. This generally may lead to good understanding and control of polymorphism and crystal nucleation.

5.1. Introduction

The ability to control and predict crystal nucleation is of paramount importance from the viewpoint of crystal engineering, materials synthesis and crystalline product quality.[1-3] In this communication we demonstrate the reproducible effect of solvents on the formation of isonicotinamide (INA) polymorphs. We establish that in solvents with strong hydrogen bond acceptors, the dominant configuration of the INA molecules with respect to each other is that of amide-pyridine heterosynthons (head-to-tail chains) (**Figure 5.1**). Similarly, solvents with strong hydrogen bond donors lead to dominancy of amide-amide homosynthons (head-to-head dimers). This self-association in solution controls the polymorph nucleation of INA by controlling the building unit attaching to the nucleus.
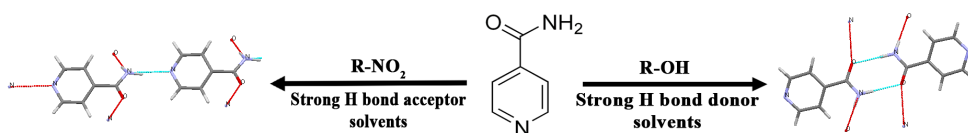
Figure 5.1: In solutions INA can be present as a single molecule (middle), in a chain-like structure (left) or in a dimer-like structure (right).

Polymorphism can be defined as the ability of a single chemical compound to form more than one crystal structure.[4] Polymorphism of active pharmaceutical ingredients is the subject of intense interest in both science and industry.[4, 5] On the one hand, this is because crystalline product quality aspects such as drug efficacy, bioavailability and safety are affected by the polymorphic form present. On the other hand, polymorphs have economic and intellectual property implications.

Often through empirical research, effects of solvent, supersaturation and impurities are observed on polymorph formation.[6] Recently, next to the two known forms of INA,[7] a third form was reported which incidentally and irreproducibly formed during a co-crystal screen from a multicomponent

solution.[8] More recently, the difficult to control evaporative crystallization process yielded two new forms of INA.[9] Form IV was obtained only as a mixture together with form II and/or V. For form V yields were often poor, typically 10%, and in some cases it could not be obtained.

The crystal nucleation of INA is a most interesting process because of the strongly differing packing of form II and the other forms. Isonicotinamide Form II has been reported to be the most stable form at room temperature.[8] In the structure of form II the amide groups form homosynthons (dimers),[8] which in turn are hydrogen bonded through the oxygen atom and the remaining hydrogen of the amide group. Interestingly, the pyridine group does not participate in hydrogen bonding in the crystal structure of form II, contrary to all other currently known forms of INA. These consist of differently packed head-to-tail chains connected through heterosynthons of the amide and the pyridine group.

The classical view of crystal nucleation is that building units attach to and detach from clusters of molecules.[10] This attaching building unit could be a single molecule, a specifically bound dimer of two molecules or even a larger cluster. How the solute is dominantly present in solution could thus strongly influence the crystal nucleation process. It was for instance reported that 2,6-dihydroxybenzoic acid[11] associates in dimers in toluene and catemers in chloroform. Crystallization from these solvents leads to the dimer crystal structure form 1 in case of toluene and to the catemer crystal structure form 2 in case of chloroform.

In our study on the crystallization behavior of INA we chose to use cooling crystallization, thereby enabling us to precisely control the crystallization conditions such as supersaturation and temperature. When INA was crystallized from ethanol, methanol and 2-propanol using differently concentrated solutions and different well-controlled cooling rates, only form II was obtained reproducibly. Using similar crystallization methods, only pure form I was crystallized from nitromethane while pure form IV was crystallized

from nitrobenzene. Similar experiments were carried out using weak proton donor and accepting solvents like dioxane and acetone. These experiments resulted in stable form II. Forms III and V were not observed during any of these experiments. The obtained pure forms I and IV were meta-stable because they very slowly transformed (>48 hours) into the stable form II. See **table 5.1** for a summary of these results.

While the pyridine group does not play a major role in the hydrogen bonding of form II (dimer like structure), it does in the hydrogen bonding of forms I and IV (chain like structure). Therefore, we expected the Raman spectra of solid samples of the different INA polymorphs to show differences in the pyridine region between 970 and 1010 cm^{-1}. The Raman peak between 970-1010 cm^{-1} is the ring breathing mode of the pyridine which includes ring vibrations and ring bond stretching.[12] The Form II gives a peak at 991 cm^{-1} while forms I and IV show a peak maximum at respectively 995 and 997 cm^{-1}. Due to the similarities in crystal structure, the peak of form IV is shifted slightly to a higher wave number compared to form I.

Similar to the solid phase Raman spectra, the pyridine region in the solution spectra is also related to the pyridine group of INA being present in either a chain form or a non-chain form; the latter is then either a dimer or a single molecule. **Figure 5.2** shows Raman spectra of dissolved INA in different solvents. The spectra of clear INA solutions in nitrobenzene show a single peak with a maximum at 997 cm^{-1}. This coincides with the peaks of the solid form IV. Strikingly, in this solvent the peak at 991 cm^{-1} representing un-hydrogen bonded pyridine groups is absent. The Raman spectra of clear solutions in acetone also show only one peak, but now at a position of 991 cm^{-1}, indicating the absence of chains. Those of clear solutions in methanol show two distinct peaks; The first peak at 991 cm^{-1} can again be due to an unassociated single molecule or the dimer-like structure of INA in which pyridine does not interact with any other group. Since also the hydroxyl-group of methanol can hydrogen bond with the pyridine group of INA, the second peak at 997 cm^{-1} can be due to

the presence of chain-like structures, the hydrogen bonding of INA and methanol[13] or both interactions. The Raman spectra of clear solutions in ethanol and 2-propanol closely resemble that in methanol and thus indicate similarly structured INA solutions, while that in nitromethane resemble that in nitrobenzene. In nitromethane and nitrobenzene thus the chain-like associates are dominantly present, while in acetone and 1,4-dioxane they are absent. In the solvents methanol, ethanol and 2-propanol mixed associates are present. See **table 5.1** for a summary of the Raman results.
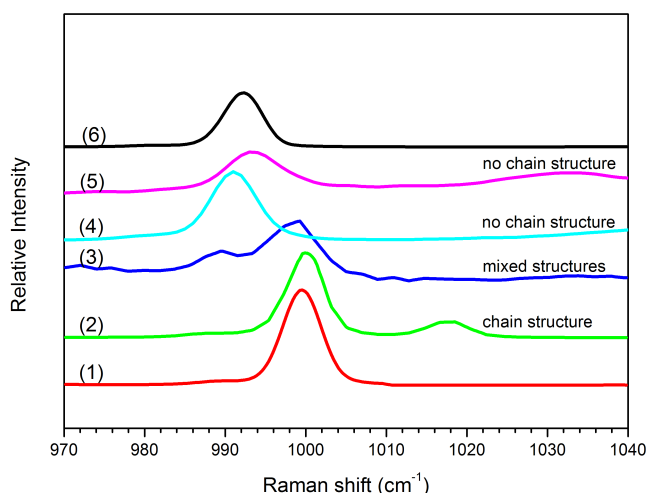
Figure 5.2: Raman spectra of INA in different solvents and of solid samples. (1) Form IV Solid; (2) In nitrobenzene; (3) In methanol; (4) In acetone; (5) In chloroform (6) Form II solids. There is a relation between the hydrogen bonding of the pyridine group in the crystal form (dimer or chain) obtained and in the solution from which it is crystallized.

With ATR-FTIR spectroscopy the type of hydrogen bonding of the amide group of INA in solutions could be identified.[14] **Figure 5.3** shows the FTIR spectra of INA solutions in nitromethane and methanol. The peak with a maximum at 1692 cm^{-1} for the INA-nitromethane solution is the carbonyl stretching vibration of INA. This shifts to a slightly lower wave number for INA

solutions in methanol. In the INA-methanol solution the carbonyl group of INA can hydrogen bond with the -NH$_2$ of another INA molecules or with the hydroxyl group of methanol.[15] The shift can thus be due to the presence of dimers, the hydrogen bonding of INA and methanol or both interactions. A similar but more substantial peak shift was observed in the spectrum of form II solids (dimers) compared to that of Form I and form IV solids (chains). The spectrum in methanol contains an additional peak around 1630 cm^{-1}. This peak is characteristic for the N-H bending vibration of the primary amine which is only observed in solution in the presence of amide-to-amide homosynthons.[16] The strong bending of N-H in the dimers leads to an increased intensity of the peak, while a chain structure of INA leads to a lower intensity of N-H bending peak. A high peak intensity in this area thus reflects the presence of dimers rather than chains. This is also observed in the spectra of the solids. Thus, INA dimers are present in methanol, but not in nitromethane. The FTIR spectra of clear solutions of INA in ethanol, 2-propanol, acetone and 1,4-dioxane resemble that in methanol and thus indicate the presence of dimers. The spectra in nitrobenzene resemble those in nitromethane, which indicates the absence of dimers. See **table 5.1** for a summary of the IR results.

To further understand the hydrogen bonding interactions in the solutions with strong donor and acceptor solvents, we performed quantum mechanical calculations of single and associated pairs of molecules. In the cases of the hydrogen bond accepting solvents nitrobenzene and nitromethane the –NO$_2$ groups were found to only bond with the outward pointing –NH$_2$ group of INA with maximum affinities of -5.12 kJ/mol per hydrogen bond. This is weaker than the dimer bonding of INA (-14.3 kJ/mol per hydrogen bond). However, since no strong bonding of these solvents and the pyridine of INA is possible, the self-association of INA into chains would dominate in nitrobenzene and nitromethane. Thus, INA in these solvents would be prone to form chains. Indeed, the spectroscopy results indicate that dominantly the chain-like structure of INA is present in those solvents. This then directs the

crystallization into chain-like crystal structures (form I from nitromethane, form IV from nitrobenzene). Why different chain-like forms are obtained from nitromethane and nitrobenzene is probably a delicate balance determined by solvent interactions with the chains in solution.
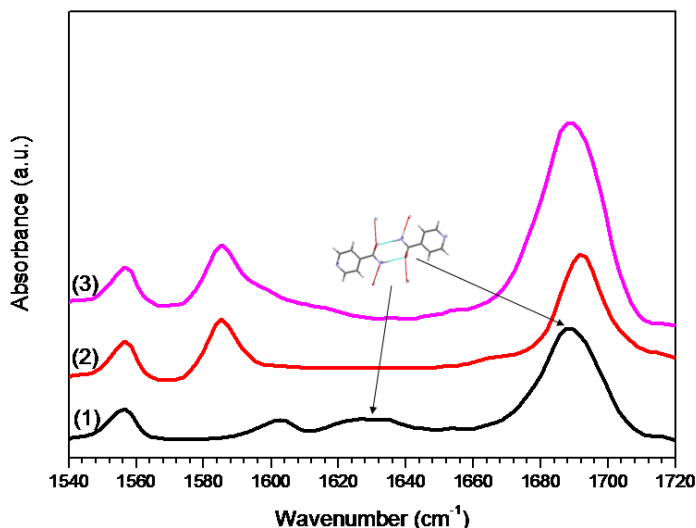
Figure 5.3: FTIR spectra of solutions of INA in (1) methanol, (2) nitromethane and (3) chloroform.

Contrarily, for the hydrogen bond donating solvent methanol we found that it binds very strongly to the pyridine group (-16.8 kJ/mol), slightly stronger than the self-associated chain structure of INA (-14.6 kJ/mol). It binds less strongly to the amide group (-11.2 kJ/mol). We expect the head-to-tail chains therefore to be absent in methanol. INA in these solvents would thus be prone to dimerize and to nucleate as form II, the dimer crystal structure.

We investigated more solvents to identify one in which both the chain-like structure and the dimer structure are absent. Surprisingly, this was found to be the case, as shown in **figure 5.2 and 5.3**, in the solvent chloroform, a weak hydrogen bond acceptor. This may mean that INA is dominantly present as unassociated single molecules. Indeed, crystallization of INA from chloroform resulted in a solid phase (form VI) of which the XRPD pattern was

different from that of the other known forms.

In the last few years the two-step nucleation mechanism[17] received a lot of attention. Crystal nucleation following this mechanism proceeds by the formation of an unordered metastable state or by a density fluctuation in which the crystalline state emerges. This preceding phase is highly concentrated. If crystal nucleation follows this mechanism the effect of solvent on the formation of different polymorphs would not be expected to be prominent. Apparently, in the case of INA, the two-step mechanism is not occurring but nucleation rather follows the classical route. An alternative for the classical route might be occurring in the case of a dominant presence of long chains of INA. Eventually these polymer-like chains might collapse to form clusters of INA, similar to what was observed in simulations of strongly polar stockmayer fluids.[18]

Table 5.1: Spectroscopy results for the association of INA in solvents and the form obtained from crystallization experiments

Solvents	HB$_i$	Raman	FTIR	Summary	Crystallization
		Chain	Dimer		
Nitrobenzene	SA	Yes	No	Chain	IV
Nitromethane	SA	Yes	No	Chain	I
Acetone	WA	No	Yes	Dimer	II
1,4-Dioxane	WA	No	Yes	Dimer	II
Chloroform	WA	No	No	Single molecule	VI (New)
2-Propanol	SD	Yes	Yes	Chain/ Dimer	II
Methanol	SD	Yes	Yes	Chain/ Dimer	II
Ethanol	SD	Yes	Yes	Chain/ Dimer	II

[I] Hydrogen bonding HB capabilities the solvent: Strong acceptor (SA), weak acceptor (WA), strong donor (SD).

We demonstrated that the structural outcome of the crystallization process of INA is directed by the association and self-association processes in solutions, which are largely influenced by the hydrogen bonding capacity of the solvent. Our results thus may suggest that a systematic analysis method of the association processes in solutions would be beneficial in polymorph discovery and preparation but also in the search for new multicomponent crystals such as salts and co-crystals.

5.2. Notes and references

5.3. References

(1) Davey, R. J.; Allen, K.; Blagden, N.; Cross, W. I.; Lieberman, H. F.; Quayle, M. J.; Righini, S.; Seton, L.; Tiddy, G. J. T., Crystal engineering - nucleation, the key step. CrystEngComm 2002, 4, (47), 257-264.

(2) Parveen, S.; Davey, R. J.; Dent, G.; Pritchard, R. G., Linking solution chemistry to crystal nucleation: the case of tetrolic acid. Chemical Communications 2005, (12).

(3) Chattopadhyay, S.; Erdemir, D.; Evans, J. M. B.; Ilavsky, J.; Amenitsch, H.; Segre, C. U.; Myerson, A. S., SAXS Study of the Nucleation of Glycine Crystals from a Supersaturated Solution. Crystal Growth & Design 2005, 5, (2), 523-527.

(4) Bernstein, J., Polymorphism in Molecular Crystals. ed.; Clarendon Press: Oxford, 2002.

(5) Lee, A. Y.; Erdemir, D.; Myerson, A. S., Crystal Polymorphism in Chemical Process Development. Annual Review of Chemical and Biomolecular Engineering 2011, 2, (1), 259-280.

(6) Kitamura, M., Strategy for control of crystallization of polymorphs. CrystEngComm 2009, 11, (6), 949-964.

(7) Aakeröy, C. B.; Beatty, A. M.; Helfrich, B. A.; Nieuwenhuyzen, M., Do Polymorphic Compounds Make Good Cocrystallizing Agents? A Structural Case Study that Demonstrates the Importance of Synthon Flexibility. Crystal Growth & Design 2003, 3, (2), 159-165.

(8) Li, J.; Bourne, S. A.; Caira, M. R., New polymorphs of isonicotinamide and nicotinamide. Chemical Communications 2011, 47, (5), 1530-1532.

(9) Eccles, K. S.; Deasy, R. E.; Fabian, L.; Braun, D. E.; Maguire, A. R.; Lawrence, S. E., Expanding the crystal landscape of isonicotinamide: concomitant polymorphism and co-crystallisation. CrystEngComm 2011, 13, 6923.

(10) Kashchiev, D., Nucleation: Basic Theory with Application. ed.; Butterworth-Heinemann: Oxford, 2000.

(11) Davey, R. J.; Blagden, N.; Righini, S.; Alison, H.; Quayle, M. J.; Fuller, S., Crystal Polymorphism as a Probe for Molecular Self-Assembly during Nucleation from Solutions: The Case of 2,6-Dihydroxybenzoic Acid. Crystal Growth & Design 2000, 1, (1), 59-65.

(12) Bakiler, M.; Bolukbasi, O.; Yilmaz, A., An experimental and theoretical study of vibrational spectra of picolinamide, nicotinamide, and isonicotinamide. Journal of Molecular Structure 2007, 826, (1), 6-16.

(13) Kreyenschmidt, M.; Eysel, H. H.; Asthana, B. P., Study of the pyridine–methanol system using four-channel Raman spectroscopy: Concentration dependence of frequencies, line widths and integrated intensities. Journal of Raman Spectroscopy 1993, 24, (10), 645-652.

(14) Kuznetsova, L. M.; Furer, V. L.; Maklakov, L. I., Infrared intensities of N-methylacetamide associates. Journal of Molecular Structure 1996, 380, (1-2), 23-29.

(15) Furer, V. L., Hydrogen bonding in ethyl carbamate studied by IR spectroscopy. Journal of Molecular Structure 1998, 449, (1), 53-59.

(16) Biemann, L.; Haber, T.; Maydt, D.; Schaper, K.; Kleinermanns, K., Fourier transform infrared spectroscopy of 2'-deoxycytidine aggregates in $CDCl_3$ solutions. Journal of Chemical Physics 2011, 134, (11), 115103-115103.

(17) Vekilov, P. G., The two-step mechanism of nucleation of crystals in solution. Nanoscale 2010, 2, (11), 2346-2357.

(18) Wolde, P. R. t.; Oxtoby, D. W.; Frenkel, D., Chain formation in homogeneous gas-liquid nucleation of polar fluids. The Journal of Chemical Physics 1999, 111, (10), 4762-4773.

CHAPTER 6

Self-association in Solution for Polymorph preparation and control

Submitted manusript

Abstract

In the early drug discovery and development stage a systematic approach based on scientific principles is important to typically uncover stable and metastable polymorphic forms. With Raman and FTIR spectroscope we demonstrated a new approach in which the structural outcome of the crystallization process of a number of organic compounds is guided by the self-association processes in solutions, which are largely influenced by the solvent. The method based on self-association of molecules in solution may not only help to discover new polymorphs but can also be used for solvent selection for reproducible production of polymorphs. Not only the published forms of isonicotinamide (INA) were found, but also new form was identified. Raman and IR can be used to characterize hydrogen bonding association processes in solutions of compounds containing amide and pyridine groups. We not only crystallized the known forms of INA (form I, form II, form IV) but also crystallized a new form of INA (form VI). In solutions nicotinamide (NA) showed three different associates present, out of which we crystallized two known forms. The spectroscopic behavior of similar solutes like NA and INA can be quite different in the same solvent resulting in a different association behavior. Due to the intramolecular interaction of picolinamide (PA) pyridine with NH_2, there were no indications of additional associates in solution and all solutions resulted in only one form of PA. Two different associates of pABA were present in solution and the crystallization always resulted in the formation of only stable form I (dimer associate). Despite the strong indication of ring associate presence the building units do not result in form II (ring structure). Next to the building units, the relative stability of the polymorphs and the heterogeneous particles in solution are important for polymorph crystallization.

6.1. Introduction

Polymorphism is the ability of a single chemical compound to form more than one crystal structure. Particularly, variations in solubility between different polymorphs of an Active Pharmaceutical Ingredient can affect for instance drug efficacy, bioavailability and safety.[1] A well-known example is Ritonavir of which the more stable and less soluble polymorph appeared in the marketed formulation which had a much smaller dissolution rate and bioavailability compared to the existing marketed polymorph.[2] The company has to reintroduced the improved formulation product to the market resulting in huge loss of profits.[2, 3] Intellectual Property rights in the pharmaceutical sector make it vital to identify, analyze, and patent every solid form (polymorph) of a potential new API.[1] Therefore, polymorph discovery is the subject of intense interest in the pharmaceutical industry.[1, 4]

Discovery of polymorph is one aspect but it is also important to industrially obtain a particular known polymorph under controlled and reproducible conditions.[1] Polymorphism issues like poor yield as well as reproducibility issues are very common[5]. For example in case of isonicotinamide crystallization, form V yields were often poor, typically 10% and 90% was stable form II, and in some cases the form IV could not be obtained.[5] Recently in 2008, Neupro (transdermal rotigotine) patches were recalled because of the crystallization in the patches after formation of a new polymorph that resembled snowflake-like crystals.[6] In 2010, a popular blood thinner Coumadin (warfarin sodium 2-propanol solvate) was withdrawn due to the variation in the 2-propanol levels, which affect the crystallinity of warfarin sodium.[7]

One of the determining factors in polymorph crystallization may be the molecular association process occurring in solutions.[8-11] For example tetrolic acid forms dimers in chloroform, whereas in ethanol dimers were absent while there were indications of solute solvent interactions.[11, 12] Crystallization from

chloroform leads to one of the dimer containing polymorph of tetrolic acid, while crystallization from ethanol leads to a catemeric form.[11, 12] Another example where association processes seem important is Isonicotinamide (INA) which forms amide-pyridine heterosynthons (head-to-tail chains) in solvents like nitromethane and forms both amide-amide homosynthons (head-to-head dimers) and heterosynthons (head-to-tail chains) in solvents like methanol.[10] This self-association in solution controls the polymorph crystallization by controlling the crystal building unit.[10] A systematic study of these processes would possibly identify a variety of building units for the polymorphs. These building units then can be controlled using the choice of solvent or solvent mixtures.[8] The solute self-associates or building units will be a function of, among others; the solvent used and can be either a single molecule or differently associated molecules like dimers, tetramers and caterers.[8]

High Throughput Experimentation (HTE) is an less effective technique to discover polymorphs as well as to come to polymorph crystallization control.[13] Such a HTE is based on Trial-and-Error by trying as many conditions and solvents as possible and possibly lacks a systematic approach based on scientific principles. We want to incorporate self-association in solution analysis method in the screening procedure in order to make it more effective and faster.

In this paper we demonstrate the potential of spectroscopic techniques for analyzing solutions to determine association differences. Solvents strongly influence the associates in solution and thus determine the building units which in turn could determine the polymorph that crystallizes out. A spectroscopic solution study thus enables the choice of a wide range of solvents to explore polymorphic phase space in polymorph discovery. We chose to work with relatively well studied systems to focus on solution association and its relation to polymorphism rather than on discovering new polymorphs. As model compounds we chose Isonicotinamide (INA),

Nicotinamide (NA), Picolinamide (PA), p-Aminobenzoic acid (pABA), Carbamazepine (CBZ) and Diprophylline (DPL). We identified a range of solvents with various hydrogen bond acceptor donor capabilities. We studied association processes in solutions with aid of Raman, IR and NMR. Then we performed crystallization experiments to establish the polymorphic outcome under varying conditions. Last we discuss the combination of association and crystallization results.

6.2. Materials and Methods

INA, NA, PA, pABA, CBZ and DPL with a purity of ≥99%, ≥99.5%, 98%, ≥97% 99.0% and ≥99%, respectively, were obtained from Sigma Aldrich. Ethanol, methanol, diethyl amine, diethyl ether, pentane, clyclohexane, toluene, chloroform, acetonitrile, 1,4-dioxane, ethyl acetate, acetone, Dimethyl formamide, dimethyl suphoxide, nitromethane, nitrobenzene and pyridine were of ACS reagent grade with a purity of ≥99+%. Ultra pure water was also used as a solvent in one case.

6.2.1 Raman & infrared

A Hololab series 5000 Raman spectroscopy (Kaiser Optical System, Inc.) and an ATR-FTIR spectrometer (Bruker Optics GmbH, Germany) facilitated the recording of Raman and IR spectra. The peak maximum determines the position of the peak of specific polymorph. Raman detection limit is determined to be approximately 1.0 mg/ml. The detection limit was calculated with Raman spectra at 785 nm excitation radiation using a NIR probe with a exposure time of 20 sec.

6.2.2. X-ray powder diffraction (XRPD)

X-ray powder diffraction (XRPD) pattern was recorded in Bragg-Brentano geometry in a Bruker D5005 diffractometer equipped with Huber incident-beam monochromator and Braun PSD detector. Data collection was carried out

at room temperature using monochromatic Cu Kα1 radiation (λ = 0.154056 nm) in the 2θ region between 5° and 90°, step size 0.038 degrees 2θ. The sample powders were deposited on a Si <510> wafer and were rotated during measurement. Data evaluation was done with the Bruker program EVA.

6.2.3. Nuclear Magnetic Resonance spectroscopy (NMR)

NMR spectra were recorded with either Bruker Avance-400 or Varian-Inova-300 spectrometer operating at 400, 128, and 100 MHz (1H NMR) or 300, 96, 75 MHz respectively. The NMR chemicals shifts are reported in ppm, referencing to the residual solvent peak.

6.2.4 Self-association in different solutions

A suspension of INA, NA, PA, pABA, CBZ and DPL in 5 ml ethanol, methanol, diethyl amine, diethyl ether, pentane, cyclohexane, toluene, chloroform, acetonitrile, 1,4-dioxane, ethyl acetate, acetone, nitromethane, nitrobenzene and pyridine was stirred for 24 hours at a temperature of 20 °C. The suspension was filtered through a 0.45 µm filter. The clear filtrate was used to record Raman and ATR-FTIR spectrums.

6.2.5. Crystallization

At first the solubility of INA, NA, PA, pABA and DPL in 15 solvents were determined with the Crystal16 (Avantium, Amsterdam), following procedure described by ter Horst et al.[14] The solubility results are used to determine concentrations for the crystallization experiments. The 3 ml crystallization experiments were carried out in an 8 ml multiple reactor set up (Crystalline, Avantium, Amsterdam). The 3 ml starting suspension of INA, NA, PA, pABA and DPL in the 15 above mentioned solvents were heated to 60°C to establish a clear solution and then cooled down rapidly to 20°C with a cooling rate of 5 °C/min while stirring (700 rpm) using a magnetic stirrer. At some point in time, the sample started to crystallize at a constant temperature. The sample

was then filtered and the solids were analyzed by Raman and XRPD to identify the final polymorphic outcome. All the experiments were repeated with different concentrations depending on the solubilities in different solvents.

6.3. Results

First, we analyze the self-association of isonicotinamide (INA), nicotinamide (NA), picolinamide (PA), p-Aminobenzoic acid (pABA), carbamazepine (CBZ) and diprophylline (DPL) in different solvents using spectroscopic techniques (part 1). Second, we performed cooling crystallization experiments from various solvents and analyzed the polymorphic outcome (part 2). Then we establish the relation between solvent type used, self-associates in solution and polymorphic outcome (part 3). **Figure 6.1** shows the molecular structures of the model compounds used.
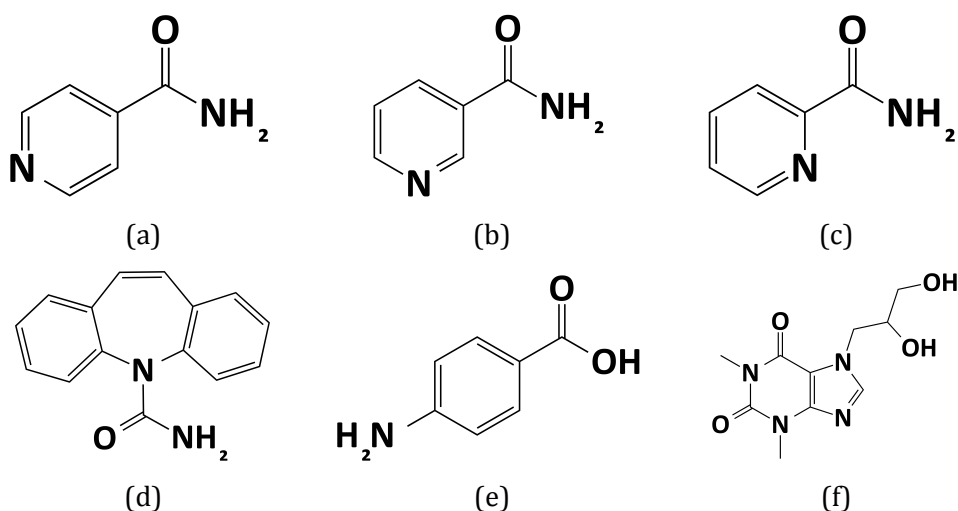
Figure 6.1: The molecular stuctures of (a) Isonicotinamide (INA) (b) Nicotinamide (NA), (c) Picolinamide (PA), (d) Carbamazepine (CBZ), (e) p-Aminobenzoic acid (pABA), and (f) Diprophylline (DPL).

Part 1: Solute self-association

Isonicotinamide. INA has two important functional groups, one is amide group and the other is pyridine group. **Table 6.1** and **Figure 6.2** shows information from the Raman spectra in different solvents. The solvent used influences the pyridine region of INA in the Raman spectra around 1000 cm^{-1}. The Raman spectra of clear solution of INA in nitromethane, nitrobenzene and pyridine show a single peak with a maximum at 1002 cm^{-1}. Those of clear solutions of INA in acetone, 1,4-dioxane, ethyl acetate, acetonitrile, chloroform and diethyl amine also show only one peak, but now at a position of 994 cm^{-1}. The Raman spectra of clear solutions of INA in ethanol and methanol show two distinct peaks at a position of 994 cm^{-1} and 1002 cm^{-1}. From these 3 characteristic Raman spectra of clear INA solutions we can deduce three types of solvent (1, 2 and 3) for INA reflecting the difference in hydrogen bonding of the pyridine. We define solvent type 1 having a peak at 994 cm^{-1} in the solution Raman spectra, solvent type 2 having both peaks at 994 cm^{-1} and 1002 cm^{-1} in the solution Raman spectra and solvent type 3 have a peak at 1002 cm^{-1} in the solution Raman spectra.

  Figure 6.3 and **Table 6.1** give details of the FTIR spectra of the amide region of INA solutions. The FTIR spectra of clear solutions of INA in acetone, 1,4-dioxane, acetonitrile, ethyl acetate, ethanol, methanol and diethyl amine show a small but significant peak at 1630 cm^{-1}, while those of chloroform, nitromethane, nitrobenzene and pyridine do not. From these 2 characteristic IR spectra of clear INA solutions we can deduce two types of solvent (A and B) for INA reflecting the difference in hydrogen bonding of the amide group in solutions.[10] Solvent type A has IR spectra containing the NH-bending peaks in INA solution while solvent type B does not.

The FTIR peaks around 1630 cm^{-1} and 1690 cm^{-1} are the N–H bending vibration of the primary amine and carbonyl stretching vibrations of INA,

respectively. The FTIR peaks at 1555 cm^{-1} and 1590 cm^{-1} are the stretching vibrations of ring carbons C6 and C5.
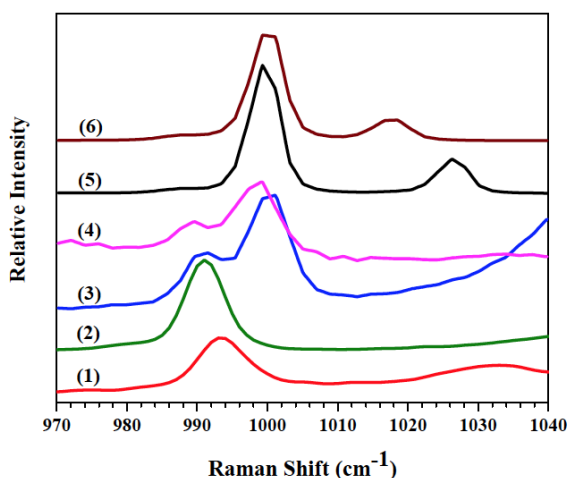
Figure 6.2: Raman spectra of solutions of INA. Solvent type 1: chloroform (1), acetone (2). Solvent type 2: methanol (3), ethanol (4). Solvent type 3: nitromethane (5), nitrobenzene (6).
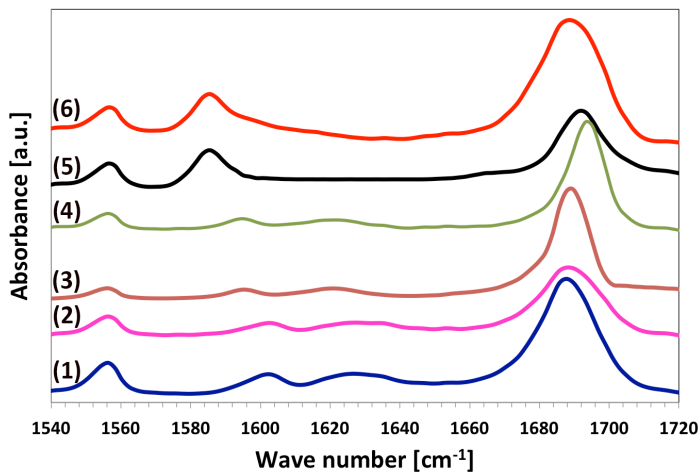
Figure 6.3: FTIR spectra of solutions of INA. Solvent type A: methanol (1), ethanol (2), 1,4-dioxane (3), acetone (4). Solvent type B: nitromethane (5), Chloroform (6). The small but significant peak around 1630 cm^{-1} represents the NH bending vibrations of INA.

The peak with a maximum at 1692 cm^{-1} for the INA–nitromethane solution is the carbonyl stretching vibration of INA. This shifts to a slightly

lower wavenumber for INA solutions in methanol, ethanol and 1,4-dioxane. In the INA–methanol or ethanol solution the carbonyl group of INA can hydrogen bond with the –NH₂ of another INA molecule or with the hydroxyl group of methanol or ethanol.[15]

The combination of these Raman and IR results identifies 3 x 2 = 6 solvent type possibilities for INA. Ethanol is identified as solvent type 2A for instance since INA in ethanol shows two pyridine peaks (994 cm⁻¹ and 1002 cm⁻¹) in Raman spectra (solvent type 2) while the IR spectra contain the NH bending vibration peak (solvent type A). Only chloroform was identified as solvent type 1B, with Raman peak at 994 cm⁻¹ (solvent type 1) and no NH bending vibration peak with FTIR spectroscopy (solvent type B). The solvent type 2B, with Raman peaks at 994 cm⁻¹ and 1002 cm⁻¹ and no NH bending vibration peak with FTIR spectroscopy and solvent type 3A, with Raman peak at 1002 cm⁻¹ and NH bending vibration peak with FTIR spectroscopy were not identified. So from the 6 possible solvent types we identified 4 using our list of solvents. The different solvent types indicate distinct hydrogen bonding in the INA solutions, which may lead to different crystallization behavior.

Nicotinamide

Nicotinamide (NA) differs from INA in the position of the pyridine group, which for NA is on the meta-position in respect to the amide group. **Figure 6.4** shows the pyridine region (1020 to 1045 cm⁻¹) of the Raman spectra of different NA solutions. The region shows a single peak with a maximum at 1033 cm⁻¹ for NA dissolved in nitromethane (solvent type 1). The spectra in chloroform, 1,4-dioxane, acetonitrile and ethyl acetate for this region resemble that in nitromethane. The region also shows only one peak for NA in acetone, but now at a position of 1038 cm⁻¹ (solvent type 3). In ethanol two distinct peaks at a position of 1030 cm⁻¹ and 1038 cm⁻¹ are visible (solvent type 2). The peak at 1030 cm⁻¹ slightly shifts to a lower wavenumber for NA solutions in ethanol compared to NA in acetonitrile, acetone and 1,4-dioxane solutions. In

the NA–ethanol solution the shift can be because of the pyridine of NA hydrogen bonding with the hydroxyl group of ethanol or pyridine of NA hydrogen bonding with the NH_2 group of another NA. The Raman spectroscopic behavior of NA in methanol (not shown in **Figure 6.4**) closely resembles that in ethanol indicating similarly associated NA pyridine groups in these solutions. So from the Raman spectra of clear solution of NA we can deduce that the two types of associates (two peak positions) result in three types of solvent (1, 2 and 3) in which either a single type of associate or both associates are present.

Table 6.1: Raman and FTIR Spectroscopy results for the association of INA, NA and PA in solvents.

Compound	Raman peaks at	FTIR peaks	
		NH_2 Bending peak	**No NH_2 Bending peak**
INA	994 cm^{-1}	Solvent-1A Acetone, 1,4-dioxane, Acetonitrile, Ethyl acetate, Diethyl amine	Solvent-1B Chloroform
	994 cm^{-1} + 1002 cm^{-1}	Solvent-2A Ethanol, Methanol	Solvent-2B None
	1002 cm^{-1}	Solvent-3A None	Solvent-3B Nitromethane, Nitrobenzene, Pyridine
NA	1033 cm^{-1}	Solvent-1A None	Solvent-1B Chloroform, acetonitrile, 1,4-dioxane, ethyl acetate, nitromethane
	1033 cm^{-1} + 1038 cm^{-1}	Solvent-2A Ethanol, Methanol	Solvent-2B None
	1038 cm^{-1}	Solvent-3A Acetone	Solvent-3B None
PA	994 cm^{-1} (No chain)	Solvent-1A Ethanol, methanol, diethyl amine, diethyl ether, acetonitrile, 1,4-dioxane, ethyl acetate, acetone, nitromethane	Solvent-1B None
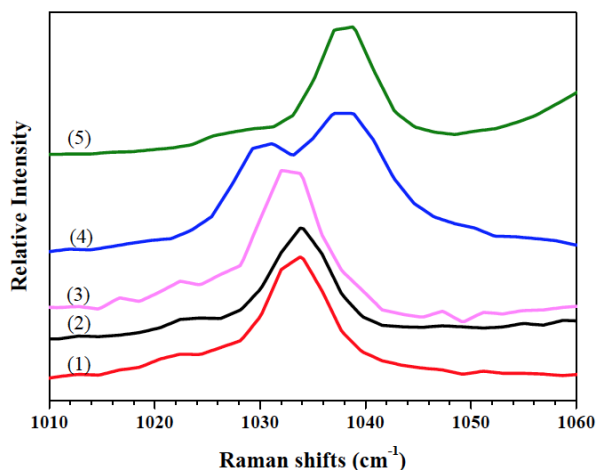
Figure 6.4: Raman spectra of solutions of NA. Solvent type 1: acetonitrile (1), nitromethane (2), 1,4-dioxane (3). Solvent type 2: ethanol (4). Solvent type 3: acetone (6).
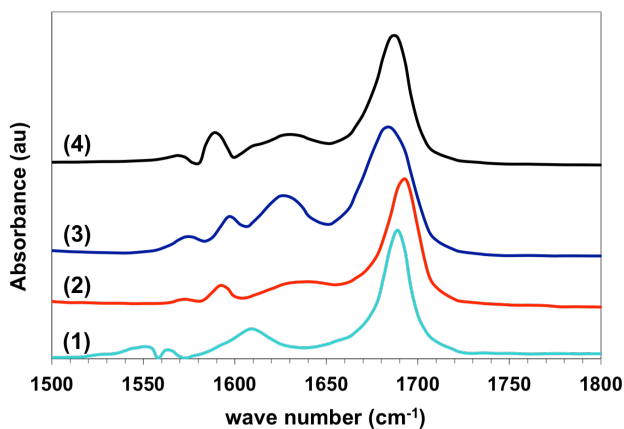
Figure 6.5: FTIR spectra of solutions of NA. Solvent type B: nitromethane (1), Solvent type A: acetone (2), ethanol (3), methanol (4). The peak around 1630 cm^{-1} represents the NH bending vibrations of NA.

Figure 6.5 shows the FTIR spectra of NA solutions in nitromethane, acetone, methanol and ethanol. The spectra in methanol, ethanol and acetone contain an additional peak around 1630 cm^{-1}. As in the case of INA, this peak is characteristic for the N-H bending vibration of the primary amine and thus indicates the presence of NA dimers in the solution.[16] The FTIR spectra of clear solutions of NA in ethanol closely resemble that in methanol and acetone, thus indicate similarly structured amide groups of NA in these solutions (solvent type A), while the amide group behavior in chloroform, 1,4-dioxane, acetonitrile and ethyl acetate resembles that in nitromethane (solvent type B). So from the IR spectra of clear NA solutions we can deduce two types of solvent (A and B) for NA.

The combination of these Raman and IR results again identifies 3 X 2 = 6 types of possible solvents for NA. NA in Ethanol for instance shows two Raman peaks at 1030 cm^{-1} and 1038 cm^{-1} (solvent type 2) and the presence of NH bending vibration peak with FTIR (solvent type A) making ethanol solvent type 2A. Acetone was identified as solvent type 3A, with Raman peak at position at 1038 cm^{-1} and NH bending vibration peak with FTIR. The solvents nitromethane, acetonitrile, 1,4-dioxane and ethyl acetate were identified as solvent type 1B, containing peaks at 1033 cm^{-1} with Raman spectroscope and no NH bending vibration peak with FTIR. The solvent type 1A, 2B and 3B were not identified for NA. So from the 6 possible solvent types we identified 3 using our list of solvents.

Picolinamide

Picolinamide (PA) has its pyridine group on the ortho-position in respect to the amide group. **Figure 6.6** shows the Raman spectra of the pyridine region of dissolved PA between 980 cm^{-1} to 1005 cm^{-1} in different solvents. All spectra in the figure show a single peak with a maximum at 994 cm^{-1}, similar to those of PA in methanol, diethyl amine, diethyl ether, acetonitrile, 1,4-dioxane, ethyl acetate and nitromethane not shown in the figure. This indicates a similarly

hydrogen bonded pyridine of PA in all used solutions. The Raman analysis of the pyridine region indicates that in our list only one type of solvent exists for PA.
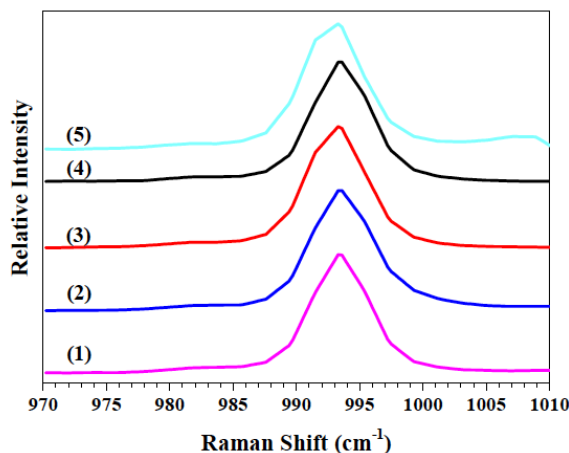
Figure 6.6: Raman spectra of PA in different solvents and of solid samples. (1) In nitromethane; (2) In ethanol; (3) In acetone; (4) In methanol and (5) In acetonitrile. The peak 994 cm^{-1} represents the ring breathing mode of pyridine group.
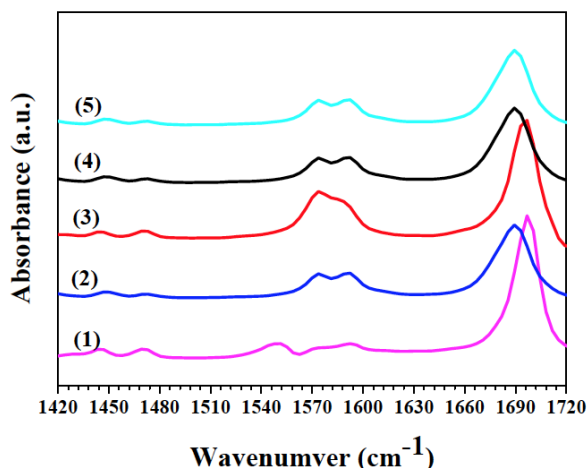
Figure 6.7: FTIR spectra of solutions of PA (1) In nitromethane; (2) In ethanol; (3) In acetone; (4) In methanol; (5) In acetonitrile. The peaks at 1576 and 1592 cm^{-1} represents the NH bending vibrations of PA.

Figure 6.7 shows the FTIR spectral region of the amide group of PA in solutions for PA solutions in nitromethane, acetone, acetonitrile, methanol and ethanol. These spectra contain two peaks in the region 1560-1600 cm^{-1}, which are characteristic for the N-H bending vibration of the primary amine.[17] The peaks with a maximum at 1696 cm^{-1} for the PA–nitromethane, acetone and acetonitrile solutions are the carbonyl stretching vibration of PA. This shifts to a slightly lower wavenumber for PA solutions in methanol and ethanol possibly reflecting the hydrogen bonding of the carbonyl with the hydroxyl group of methanol or ethanol.

The combination of these Raman and IR results identifies only 1 type of solvent for PA indicating only one type of associate present in solution. See **Table 6.1** for a summary of the results.

Carbamazepine.

Figure 6.8 shows the FTIR spectra of the carbonyl region (1600 to 1700 cm^{-1}) of dissolved CBZ in 1,4-dioxane, acetonitrile, chloroform, methanol and ethanol. The FTIR spectra in ethanol and methanol show two distinct carbonyl peaks at a position of 1663 cm^{-1} and 1689 cm^{-1}. Those in acetonitrile show a single peak with a maximum at 1689 cm^{-1}. The spectra in 1,4-dioxane and chloroform also show only one peak, but now at a position of 1696 cm^{-1} and 1681 cm^{-1}, respectively. From the IR spectra of clear CBZ solutions we can deduce four types of solvent (A, B, C and D) for CBZ influencing the hydrogen bonding of the amide group in solutions. The N-H bending vibration of the primary amine shows a peak at 1603 cm^{-1} wavenumber and shifts to lower wavenumber for differently associated forms.[18]

p-Amino benzoic acid. We investigated pABA in the same list of solvents to identify different self-associates in solution. The Raman spectra of clear solutions of pABA in ethanol and methanol show a single peak with a maximum at 1274 cm^{-1}. The Raman spectra of clear solutions of pABA in

acetonitrile, acetone, nitromethane and pyridine shows a single peak with a maximum at 1286 cm^{-1}. So from the Raman spectra of clear solution of pABA we can deduce two types of solvent (A and B) for pABA influencing the hydrogen bonding of the amide group in solutions. So there may be two different associates of pABA present in all above-mentioned solvents. See **Table 6.2** for a summary of the results.
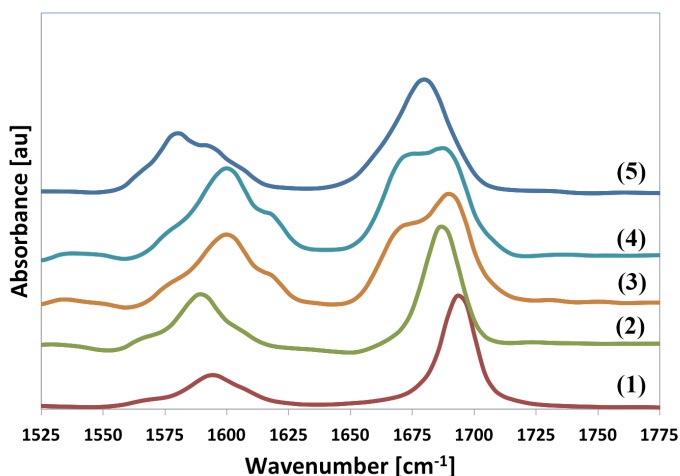
Figure 6.8: FTIR spectra of solutions of CBZ (1) In 1,4-dioxane; (2) In acetonitrile; (3) In methanol; (4) In ethanol; and (5) In chloroform. The peaks between 1650 and 1725 cm^{-1} represent the carbonyl stretching vibrations of CBZ.

Diprophylline. The DPL was very poorly soluble in all 15 solvents. Only in ethanol, methanol, isopropanol, dimethyl formamide (DMF), dimethyl sulfoxide (DMSO) and water it was possible to obtain sensible spectra. In all other selected solvents the solubility of DPL was below the detection limit of Raman spectroscope. The CO stretching vibrations of the carbonyl group of DPL between 1750-1600 cm^{-1} shows significant substantial differences in different solutions. The Raman spectra of clear solutions of DPL in ethanol, methanol and isopropanol show a peak with a maximum at 1642 cm^{-1} while those in DMF, water and DMSO show a peak with a maximum at 1652 cm^{-1}. The

1642 cm⁻¹and 1652 cm⁻¹ peaks represent the bonded carbonyl group of DPL. So from the Raman spectra of clear solution of DPL we can deduce that two solvents (A and B) for DPL influencing the hydrogen bonding of the carbonyl group in solutions. See **Table 6.2** for a summary of the results.

Table 6.2: Spectroscopy results for the association of pABA and DPL in solvents using Raman spectroscope and CBZ in solvents using FTIR spectroscope.

Raman peaks at	p-Amino benzoic acid (pABA)		Diprophylline (DPL)	
	1274 cm⁻¹	1286 cm⁻¹	1642 cm⁻¹	1652 cm⁻¹
	Solvent-1 Ethanol, Methanol	Solvent-2 Acetonitrile, Acetone, Nitromethane and Pyridine	Solvent-1 Ethanol, Methanol, isopropanol	Solvent-2 DMF, water, DMSO
Carbamazepine (CBZ)				
FTIR peaks at	1689 cm⁻¹	1663 cm⁻¹ + 1689 cm⁻¹	1696 cm⁻¹	1681 cm⁻¹
	Solvent-A Nitromethane, acetonitrile	Solvent-B Ethanol, methanol	Solvent-C 1,4-dioxane	Solvent-D Chloroform

Part 2: Crystallization of model compounds from different solutions

In this part we report the outcome of the crystallization experiments of INA, NA, PA, CBZ, pABA and DPL for all identified solvents and solvent types.

INA shows single molecule, head-to-head dimers and head-to-tail chains in solution as self-associates, which results in the formation of form I, form II, form IV and form VI polymorphs. INA Form II is reported to be the most stable at room temperature.[10] In this polymorph the amide group forms homosynthons with other amide groups (head-to-head dimers), while the pyridine groups are not involved in the hydrogen bonding. Form I, III, IV and V contain heterosynthons between the amide and the pyridine group (head-to-

tail chains). The Raman spectra of pure solid form I, II and IV shows a pyridine ring breathing peaks at peak position 1002 cm^{-1}, 994 cm^{-1}, and 1004 cm^{-1}, respectively.

Crystallization of INA from ethanol with different concentrations leads to the formation of the stable form II. The solvents nitromethane and nitrobenzene lead to the formation of metastable forms I (chains) and form IV (chains) respectively.[10] Crystallization from the solvents acetone, ethyl acetate, acetonitrile leads to the stable form II (dimers).[10] Interestingly cooling crystallization experiment of INA in chloroform resulted in a new polymorphic form identified by XRPD, DSC and TGA.[10] Crystallization of INA from 1,4-dioxane with 15 mg/ml and 20 mg/ml resulted in the formation of stable form II, while crystallization using 25, 30, 35 and 40 mg/ml resulted in the formation of metastable form I.
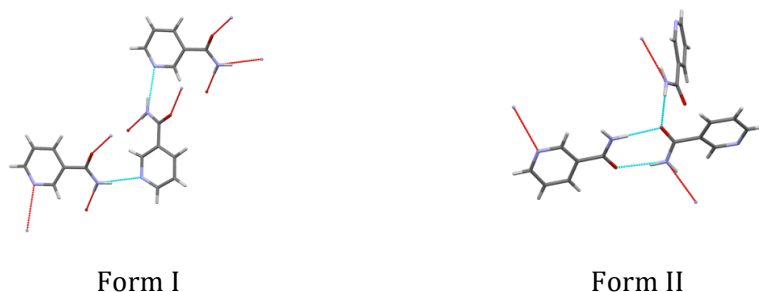
Form I   Form II

Figure 6.9: The hydrogen bond motifs in the NA crystal structures. Form I arranges in head-to-tail chains and form II arranges in dimers.

NA self-associates into two different structures chains with bounded pyridine (form I) and dimers (form II). The **Figure 6.9** shows the crystal structure of two previously known NA polymorph.[19] NA Form I has been reported to be the most stable form at room temperature[19]. In the structure of form I the amide groups form heterosynthons (head-to-tail chains) with the pyridine group. The NA form II consist of differently packed head-to-head dimers connected through homosynthons of the amide groups (head-to-head dimers). The form

II crystal structure also consist the hydrogen bonding between the pyridine group and amide group.

Crystallization of NA from ethanol with different concentrations leads to the formation of the stable form I, whereas the crystallization of NA from methanol leads to the formation of metastable form II. Crystallizations from the solvents chloroform, acetonitrile and 1,4-dioxane, ethyl acetate and nitromethane resulted in the formation of stable forms I. NA from acetone resulted in the formation of metastable form II.
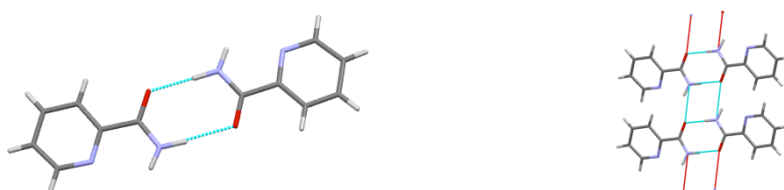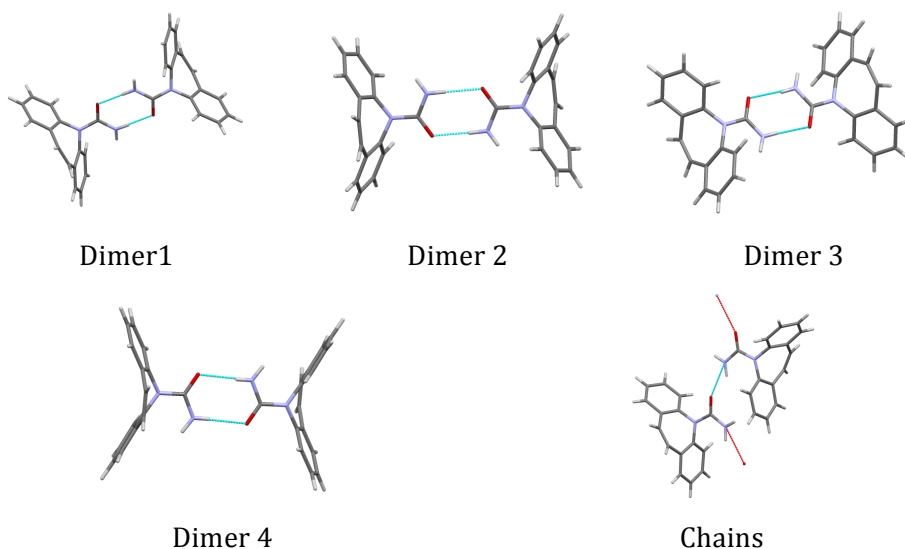

Figure 6.10: The hydrogen bond motifs in the PA crystal structures. Both forms arranges in head-to-head dimers of PA molecules, no polymorphs with head-to-tails of PA are known.

Both polymorphic forms of PA contain dimers as the main supramolecular unit[20], characterized by head to head arrangement with a pair of hydrogen bonds of the amide group (**Figure 6.10**).

In case of PA, we analyzed only one type of self-associates in all 9 solvents used. In other solvents the PA appeared to be poorly soluble leading to concentrations below the detection limit of Raman and FTIR spectroscopy. Crystallization of PA from ethanol, methanol, diethyl amine, diethyl ether, acetonitrile, 1,4-dioxane, acetone, ethyl acetate and 1,4-dioxane resulted in the formation of stable form I.

CBZ self-associates into chains with bounded pyridine (form V)[21] and dimers (form I, II, III and IV).[18, 22] **Figure 6.11** shows the crystal structure of five previously known CBZ polymorph.[21] CBZ Form III has been reported to be the most stable form at room temperature.[19] The CBZ form II consist of differently

packed head-to-head dimers connected through homosynthons of the amide groups (head-to-head dimers). In the structure of form V the NH_2 of amide group of one molecule forms a chain with the carbonyl group of other molecule.

Dimer1   Dimer 2   Dimer 3

Dimer 4   Chains

Figure 6.11: The hydrogen bond motifs in the CBZ crystal structures. Four forms arrange in dimers of CBZ molecules, one polymorphs with chains of CBZ are known.

Crystallization of CBZ from acetonitrile and nitromethane leads to the formation of the stable form III, whereas the crystallization of CBZ from ethanol and methanol also form the stable form III. Solvent like 1,4-dioxane resulted in the formation of metastable forms II. CBZ from chloroform resulted in the formation of metastable form IV.
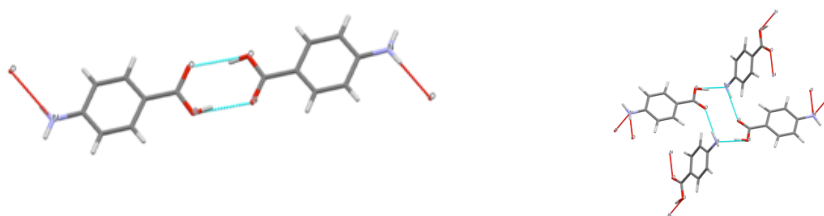
Figure 6.12: The hydrogen bond motifs in the pABA crystal structures. Both forms I arranges in head-to-head dimers and form II is a ring like structure of

pABA molecules.

pABA form a head-to-head dimers in which the carboxylic group of one molecule interacts with the carboxylic group of other molecule[23]. pABA also forms a ring like structure in which the CO group interacts with the amine group and 4 molecule forms a ring like structure (**Figure 6.12**).[23, 24] Form I (dimer structure) is the most stable form whereas form II (ring structure) is the metastable form at room temperature.

The solution spectra of pABA in acetonitrile, acetone, nitromethane and pyridine resembles that in with form I and the crystallization using these solvents always resulted in the formation of stable form I, as expected.[9] The crystallization from ethanol and methanol solvents also resulted in the formation of stable form I.

The DPL was very poorly soluble in all 15 solvents and was only some extent detectable in ethanol and methanol. In all other selected solvents the concentration of DPL was below the detection limit of Raman and FTIR spectroscope. The crystallization of DPL using ethanol, methanol and isopropanol resulted in the formation of metastable form (ssRII) structure while the crystallization of DPL using DMF, water and DMSO resulted in the formation of stable form (RI).

Part 3: Link between solvent type, self-associates in solution and polymorph obtained

From the Raman spectra of pure solids of INA we know that the peak at 994 cm^{-1} corresponds to the non-hydrogen bonded pyridine of INA, while the peak at 1002 cm^{-1} corresponds to the hydrogen-bonded pyridine of INA.[10] The FTIR region around 1630 cm^{-1} is characteristic for the N–H bending vibration of the primary amine which is only observed in solution in the presence of amide-to-amide homosynthons.[16] From this we can conclude that solvent type A

indicates solutions containing INA dimers while solvent type B indicates solutions containing INA chains or single molecules.

Crystallization of INA from ethanol leads to the formation of the stable form II, which is a crystal structure containing head-to-head dimers. The solution spectra INA in ethanol (Solvent-2A) shows two peaks at the same position of self-associates of dimers and chains forms. Nitromethane and nitrobenzene (Solvent-3B) enable the association of INA into chains leading to the formation of metastable forms I and form IV respectively. The form I and IV crystal structures both contain chains of INA. INA is present as head-to-head dimers through hydrogen bonding of the amide-group in the solvent acetone (Solvent-1A). Crystallization from this solvent leads to the stable form II. In case of the solvent chloroform (Solvent-1B), the Raman and IR spectra of INA chloroform solution shows no peak shifts or extra NH bending peak. This may mean that neither chain-like nor dimer-like associates are present in chloroform and that INA is dominantly present as unassociated single molecules. Indeed, the crystallization experiment of INA in chloroform resulted in a new polymorphic form.[10] In 1,4-dioxane (Solvent-1A), INA was dominantly present as dimer like associates and the crystallization experiments of INA at concentrations of 15 mg/ml and 20 mg/ml resulted in form II (head-to-head dimers). But the crystallization of INA from 1,4-dioxane at a concentration of 25, 30, 35 and 40 mg/ml resulted in the formation of metastable form I (head-to-tail chains). So out of 6 possible solvent types from which we identified 4 using our list of solvents and crystallized four different polymorphs (INA form I, form II, form IV and new form) using these solvents. We did not find solvents of type 2B and 3A in case of INA. See **Table 6.3** for summary of results.

The temperature and solvent dependence of hydrogen-bonding interactions of INA has further been studied experimentally using ^{1}H NMR. **Figure 6.13** shows the ^{1}H NMR spectra of INA in four different solutions. The

shifts of NH_1 and NH_2 are substantially different when using ethanol as a solvent, showing a chemical shift difference of around 1.2 ppm in the measured temperature range from 25 to 70 °C. This indicates that the kinetics of interconversion of the H1 and H2 hydrogen's of the amide group is slow compared to the chemical shift difference in Hz of the two peaks. This in turn points to a strong self-association or solvent interaction of at least one of this hydrogen's in the entire temperature range. In the solvent nitromethane and a temperature range of 25 to 50 °C the hydrogen's of the amide group show the same chemical shift behavior, however, above 50 °C a coalescence point is observed and the H1 and H2 hydrogen's have the same chemical shift. These increased interconversion kinetics indicate a change in the solvent interaction or self-association. In the solvent chloroform the hydrogen's of the amide group show the same chemical shift behavior, however, above 40 °C a coalescence point is observed and the H1 and H2 hydrogen's have the same chemical shift. When chloroform is added to the ethanol the shifts of NH_1 and NH_2 are substantially different when using ethanol as a solvent, showing a chemical shift difference of around 1.4 ppm in the measured temperature range from 25 to 70 °C. This in turn points to a change in self-association or solvent interaction of at least one of this hydrogen's in the entire temperature range as compared to pure ethanol.

As explained in the previous sections that in ethanol, nitromethane and chloroform three different associate of INA are present in solution. The NMR results also shows that the 1H shifts of amide NH2 are different in all three solvents. In the solvent the coalescence is at a lower temperature as compared to nitromethane, which might indicate the presence of unassociated INA in chloroform. The nitromethane shows coalescence at 60 °C and ethanol does not show coalescence until 70 °C, which might indicate the presence of stable associates in ethanol as compared to a metastable in nitromethane.
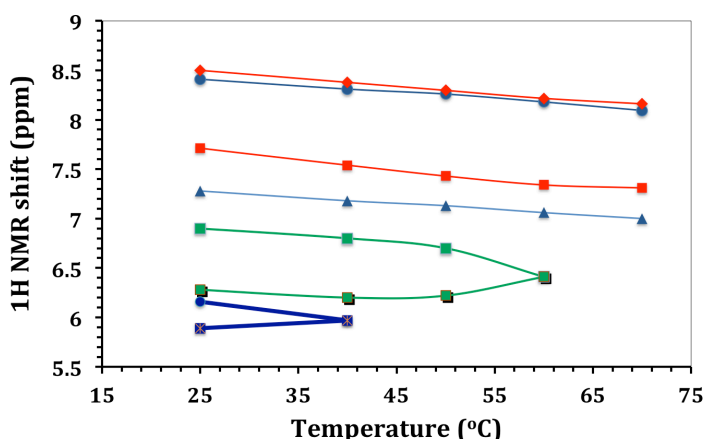
Figure 6.13: Effect of temperature on the ^{1}H NMR hydrogen shifts of dissolved INA in ethanol, nitromethane and chloroform. (1) NH_1 (■) and NH_2 (■) hydrogens of INA in ethanol (2) NH_1 (●) and NH_2 (▲) hydrogens of INA in mixtures of ethanol-chloroform (60-40 vol%), (3) NH_1 (■) and NH_2 (■) hydrogen's of INA in nitromethane and (4) NH_1 (●) and NH_2 (■) hydrogen's of INA in chloroform.

The Raman and FTIR spectra of clear solution of NA we can deduce that three different associates are dominantly present. NA in ethanol, methanol (Solvent-2A) self-associates into both dimers and chains. Crystallization of NA from ethanol leads to the formation of the stable form I, which is a crystal structure containing head-to-tail chains. While crystallization of NA from methanol leads to the formation of the metastable form II, which is a crystal structure containing head-to-head dimers. Solvents like chloroform, acetonitrile, nitromethane, ethyl acetate and 1,4-dioxane (Solvent-1B) enable the association of NA into chains leading to the formation of stable forms I. In case of acetone (Solvent-3A), NA is present as a crystal structure containing head-to-head dimers and crystallization from acetone leads to the formation of metastable form II. We have 6 possible solvent types from which we identified 3 using our list of solvents and crystallized two different polymorphs (NA form I, and form II) using these solvents. See **Table 6.3** for summary of results.

Table 6.3: Outcome of the crystallization experiments of INA, NA, PA, CBZ, pABA, and DPL in different type of solvents.

Compound	Solvent Type	Building units in solution	Polymorph obtained	Remarks
Isonicotinamide (INA)	Solvent-1A	Dimers	Form II (dimer), Form I (chain)	Form I only obtained using 1,4-dioxane at conc. of 25-40 mg/ml
	Solvent-1B	No dimers or chains	Form VI (single molecule)	New polymorph (5-25 mg/ml)
	Solvent-2A	Dimers and chains	Form II (dimer)	70 -135 mg/ml
	Solvent-3B	Chains	Form I (chain), Form IV (chain)	Form I from nitromethane(2-10 mg/ml) and form II from nitrobenzene (10-26 mg/ml)
Nicotinamide (NA)	Solvent-1B	Chains	Form I (chain)	Stable form
	Solvent-2A	Dimers and chains	From I (chain), From II (dimer)	Form I from ethanol (65-100 mg/ml), form II from methanol (80-120 mg/ml)
	Solvent-3A	Dimers	Form II (dimer)	10-50 mg/ml
Picolinamide (PA)	Solvent-1A	Dimers	Form I (dimer)	Stable form
Carbamazepine (CBZ)	Solvent-A	Dimer 3	Form III (dimer 3)	Stable form (60-100 mg/ml)
	Solvent-B	Dimer 3	Form III (dimer 3)	Stable form (32-120 mg/ml)
	Solvent-C	Dimer 2	Form II (dimer 2)	Metastable form (100 mg/ml)
	Solvent-D	Dimer 1	Form I (dimer 1)	Metastable form (5-25 mg/ml)
p-Amino benzoic acid (pABA)	Solvent-1	Dimers	Form I (dimer)	Stable form (110-300 mg/ml)
	Solvent-2	Ring structure	Form I (dimer)	Stable form
Diprophylline (DPL)	Solvent-1	ssRII structure	Form ssRII	Metastable form
	Solvent-2	RI structure	Form RI	Stable form

PA shows only one type of self-associates with amide and pyridine and always resulted in the formation of stable form I in all the solvents used (Solvent-1A). Interestingly, in all solvents the FTIR spectra indicate that the amide functional groups are present as hydrogen bonded to another amide. There was no evidence of another associate leading to second types of solvent (1B). The pyridine group of PA is at ortho position and the intramolecular interaction between NH_2 and pyridine are dominant in solution. The FTIR spectra of amide show an additional peak of bending vibrations of NH. The peak at 1594 cm^{-1} is due to the presence of self-associates[17] (amide-amide dimers) while the other peak at 1576 cm^{-1} is due to the bending of the NH group as a result of the intramolecular hydrogen bond with the pyridine on the ortho position. Because of these intramolecular interactions the pyridine was unavailable to make any other hydrogen bonds to form chains with other molecules of PA. Similar intramolecular interactions were observed previously during the co-crystal formation of PA with carbamazepine.[25] See **Table 6.3** for summary of results.

PA shows only one type of self-associates with amide and pyridine and always resulted in the formation of stable form I in all the solvents used (Solvent-1A). Interestingly, in all solvents the FTIR spectra indicate that the amide functional groups are present as hydrogen bonded to another amide. There was no evidence of another associate leading to second types of solvent (1B). The pyridine group of PA is at ortho position and the intramolecular interaction between NH_2 and pyridine are dominant in solution. The FTIR spectra of amide show an additional peak of bending vibrations of NH. The peak at 1594 cm^{-1} is due to the presence of self-associates[17] (amide-amide dimers) while the other peak at 1576 cm^{-1} is due to the bending of the NH group as a result of the intramolecular hydrogen bond with the pyridine on the ortho position. Because of these intramolecular interactions the pyridine was unavailable to make any other hydrogen bonds to form chains with other molecules of PA. Similar intramolecular interactions were observed previously during the co-

crystal formation of PA with carbamazepine.[25] See **Table 6.3** for summary of results.

The FTIR spectra of clear solution of CBZ we can deduce that four different associates are dominantly present. CBZ in ethanol, methanol show two peaks (Solvent-B), one can be because of the self-associates and the other can be because of the solvent-solute interactions. Crystallization of CBZ from ethanol and methanol leads to the formation of the stable form III, which is a crystal structure containing head-to-head dimers. Solvents like acetonitrile and nitromethane (Solvent-A) enable the association of CBZ into dimers leading to the formation of stable forms III. In case of 1,4-dioxane (Solvent-C), CBZ is present as a crystal structure containing head-to-head dimers and crystallization from 1,4-dioxane leads to the formation of metastable form II. Crystallization of CBZ from chloroform (Solvent-D) also results in the formation of dimers but a different metastable form I. We deduce four different associates of CBZ from different solvents and were able to get three different polymorphs. See **Table 6.3** for summary of results.

The Raman spectra of -COH stretching vibration of form I shows a peak at 1286 cm^{-1}, while the –COH stretching vibration of form II shows a peak at around 1274 cm^{-1}.[26] The solution spectra show both associates present in different solutions, like dimers in acetonitrile, acetone, nitromethane and pyridine and rings in ethanol and methanol. The C-OH stretching peaks of pABA in ethanol and methanol resembles that with pure solid form II.[23] The crystallization of pABA from these solvents always resulted in the formation of stable form I (dimer structure). The final crystallization outcome could be because of slow kinetics of metastable form II and thermodynamic which might be playing an important role during the crystallization of pABA. See **Table 6.3** for summary of results.

In case of DPL the compound is very poorly soluble in all 15 selected solvents, which might indicate that the solvent selection is very important in

order to study the self-associates to control and prepare polymorphs. The crystallization of DPL using ethanol, methanol and isopropanol resulted in the formation of metastable form (ssRII) structure while the crystallization of DPL using DMF, water and DMSO resulted in the formation of stable form (RI). See **Table 6.3** for summary of results.

6.4. Discussion

We showed that the association of INA, NA, PA, CBZ and DPL in solutions plays a significant role in determining the dominant building units directing the structural outcome of the crystal nucleation of polymorphs. For example in case of INA, out of 6 possible solvent types from which we identified 4 using our list of solvents and crystallized four different polymorphs (INA form I, form II, form IV and new form) using these solvents. Not only the known form of INA was prepared but also a new form of INA was discovered from chloroform. There are other factors than association, which also has influences on polymorphic outcome, like heterogeneous template, relative stability, and other kinetic factors like supersaturation. For example in 1,4-dioxane (INA-1A solvent type), INA was dominantly present as dimer like associates and the crystallization experiments of INA resulted in form II (head-to-head dimers) and metastable form I (head-to-tail chains) at different concentrations.

In case of NA, out of 6 possible solvent types from which we identified 3 using our list of solvents and crystallized two different polymorphs (NA form I, and form II) using these solvents. Interestingly the spectroscopic behavior of similar solutes like NA and INA can be quite different in the same solvent resulting in a different association behavior and crystallization behavior. Form example acetone is solvent type 1A for INA, resulting in the formation of stable form II (dimer) while in case of NA it is solvent type 3A resulting in the formation of metastable form II (dimer).

PA shows only one type of self-associates with amide and pyridine and always resulted in the formation of stable form I in all the solvents used (Solvent-1A). Interestingly, in all solvents the FTIR spectra indicate that the amide functional groups are present as hydrogen bonded to another amide. There was no evidence of another associate leading to second types of solvent (1B). The pyridine group of PA is at ortho position and the intramolecular interaction between NH_2 and pyridine are dominant in solution. The intramolecular interaction of PA makes the pyridine unavailable to hydrogen bond with other molecules of PA. This is the reason we get only one type of PA with Raman spectroscopy and finally only one type of polymorphs from all solvents used.

The four different associates of CBZ from different solvents and were able to get three different polymorphs. In case of DPL the crystallization using ethanol, methanol and isopropanol resulted in the formation of metastable form (ssRII) structure while the crystallization of DPL using DMF, water and DMSO resulted in the formation of stable form (RI).

The Raman spectra of pABA two different associates present in solution and the crystallization always resulted in the formation of only stable form I (dimer structure). The final crystallization outcome could be because of slow kinetics of metastable form II and thermodynamic which might be playing an important role during the crystallization of pABA.

In the early drug discovery and development stage there are many common techniques employed that are designed to typically uncover stable and metastable polymorphic forms.[27] These approaches are based on crystallization mode diversity like, crystallizations through solvent evaporations, anti-solvent crystallization, slow and fast cooling to induce precipitation, and slurring of solids for extended periods of time. The other approach is based on solvent diversity.[27] These methods are typical throughout the pharmaceutical industry and have been incorporated into practices for

polymorph screening.[27] But these approaches of polymorph discovery and development are more random and not based on scientific principles. The method based on self-association of molecules in solution may not only help to discover new polymorphs but can also help in reproducible production of polymorphs.[8, 10]

Other than building units, the relative stability of polymorph, heterogeneous particles in solution are important in order to nucleate and grow stable as well as metastable polymorphs.[28] In solution the metastable form can transform to stable form.[29] The heterogeneous particles can reduce the energy barrier of the metastable form in order to nucleate the metastable polymorph other than stable form.

6.5. Conclusion

We demonstrated that the structural outcome of the crystallization process of INA, NA, PA, CBZ and DPL are directed by the association and self-association processes in solutions, which are largely influenced by the hydrogen bonding capacity of the solvent. Our results thus suggest that a systematic analysis method of the association processes in solutions method would be beneficial in polymorph discovery and preparation. The self-association method offer the ability to develop a more fundamental understanding of the crystallization process, based on knowledge generated from large numbers of experiments on diverse compounds and conditions. In this article the self-association method that we have developed is described. Not only the published forms of INA were found, but also new form was identified. We used Raman spectroscopy of solutions as a novel analytical tool in combination with FTIR and NMR to identify the self-association of INA, NA, PA, CBZ, pABA and DPL in different solvents. This new systematic method could also be applied to discover new multicomponent crystals such as salts and co-crystals.

6.6. Acknowledgements

6.7. References

(1) Lee, A. Y.; Erdemir, D.; Myerson, A. S., Crystal Polymorphism in Chemical Process Development. Annual review of chemical and biomolecular engineering 2011, 2, (1), 259-280.

(2) Bauer, J.; Spanton, S.; Henry, R.; Quick, J.; Dziki, W.; Porter, W.; Morris, J., Ritonavir: An Extraordinary Example of Conformational Polymorphism. Pharmaceutical research 2001, 18, (6), 859-866.

(3) Lee, A. Y.; Erdemir, D.; Myerson, A. S., Crystal polymorphism in chemical process development. Annual review of chemical and biomolecular engineering 2011, 2, 259-80.

(4) Bernstein, J., Polymorphism in Molecular Crystals. ed.; Clarendon Press: Oxford, 2002.

(5) Eccles, K. S.; Deasy, R. E.; Fabian, L.; Braun, D. E.; Maguire, A. R.; Lawrence, S. E., Expanding the crystal landscape of isonicotinamide: concomitant polymorphism and co-crystallisation. CrystEngComm.

(6) Chen, J. J.; Swope, D. M.; Dashtipour, K.; Lyons, K. E., Transdermal rotigotine: a clinically innovative dopamine-receptor agonist for the management of Parkinson's disease. Pharmacotherapy 2009, 29, (12), 1452-67.

(7) Gao, D.; Maurin, M. B., Physical chemical stability of warfarin sodium. AAPS pharmSci 2001, 3, (1), E3.

(8) Davey, R. J.; Schroeder, S. L. M.; ter Horst, J. H., Nucleation of Organic Crystals—A Molecular Perspective. Angewandte Chemie International Edition 2012, 52, (8), 2166-2179.

(9) Davey, R. J.; Blagden, N.; Righini, S.; Alison, H.; Quayle, M. J.; Fuller, S., Crystal Polymorphism as a Probe for Molecular Self-Assembly during Nucleation from Solutions: The Case of 2,6-Dihydroxybenzoic Acid. Crystal Growth & Design 2000, 1, (1), 59-65.

(10) Kulkarni, S. A.; McGarrity, E. S.; Meekes, H.; ter Horst, J. H., Isonicotinamide self-association: the link between solvent and polymorph nucleation. Chemical Communications 2012, 48, (41), 4983-4985.

(11) Parveen, S.; Davey, R. J.; Dent, G.; Pritchard, R. G., Linking solution chemistry to crystal nucleation: the case of tetrolic acid. Chemical Communications 2005, (12), 1531-1533.

(12) Chen, J.; Trout, B. L., Computational study of solvent effects on the molecular self-assembly of tetrolic acid in solution and implications for the polymorph formed from crystallization. The journal of physical chemistry. B 2008, 112, (26), 7794-802.

(13) Gardner, C. R.; Almarsson, O.; Chen, H.; Morissette, S.; Peterson, M.; Zhang, Z.; Wang, S.; Lemmo, A.; Gonzalez-Zugasti, J.; Monagle, J.; Marchionna, J.; Ellis, S.; McNulty, C.; Johnson, A.; Levinson, D.; Cima, M., Application of high throughput technologies to drug substance and drug product development. Computers & Chemical Engineering 2004, 28, (6–7), 943-953.

(14) ter Horst, J. H.; Deij, M. A.; Cains, P. W., Discovering New Co-Crystals. Crystal Growth & Design 2009, 9, (3), 1531-1537.

(15) Furer, V. L., Hydrogen bonding in ethyl carbamate studied by IR spectroscopy. Journal of Molecular Structure 1998, 449, (1), 53-59.

(16) Biemann, L.; Häber, T.; Maydt, D.; Schaper, K.; Kleinermanns, K., Fourier transform infrared spectroscopy of 2′-deoxycytidine aggregates in CDCl3 solutions. The Journal of Chemical Physics 2011, 134, (11), -.

(17) Borba, A.; Albrecht, M.; Gomez-Zavaglia, A.; Lapinski, L.; Nowak, M. J.; Suhm, M. A.; Fausto, R., Dimer formation in nicotinamide and picolinamide in the gas and condensed phases probed by infrared spectroscopy. Physical Chemistry Chemical Physics 2008, 10, (46), 7010-7021.

(18) Grzesiak, A. L.; Lang, M.; Kim, K.; Matzger, A. J., Comparison of the four anhydrous polymorphs of carbamazepine and the crystal structure of form I. Journal of pharmaceutical sciences 2003, 92, (11), 2260-71.

(19) Li, J.; Bourne, S. A.; Caira, M. R., New polymorphs of isonicotinamide and nicotinamide. Chemical Communications 2011, 47, (5), 1530-1532.

(20) Evora, A. O. L.; Castro, R. A. E.; Maria, T. M. R.; Rosado, M. T. S.; Silva, M. R.; Canotilho, J.; Eusebio, M. E. S., Resolved structures of two picolinamide polymorphs. Investigation of the dimorphic system behaviour under conditions relevant to co-crystal synthesis. CrystEngComm 2012, 14, (24), 8649-8657.

(21) Arlin, J.-B.; Price, L. S.; Price, S. L.; Florence, A. J., A strategy for producing predicted polymorphs: catemeric carbamazepine form V. Chemical Communications 2011, 47, (25), 7074-7076.

(22) Getsoian, A.; Lodaya, R. M.; Blackburn, A. C., One-solvent polymorph screen of carbamazepine. International Journal of Pharmaceutics 2008, 348, (1–2), 3-9.

(23) Gracin, S.; Rasmuson, Å. C., Polymorphism and Crystallization of p-Aminobenzoic Acid. Crystal Growth & Design 2004, 4, (5), 1013-1023.

(24) Stevens, J. S.; Byard, S. J.; Seaton, C. C.; Sadiq, G.; Davey, R. J.; Schroeder, S. L., Proton transfer and hydrogen bonding in the organic solid state: a combined XRD/XPS/ssNMR study of 17 organic acid-base complexes. Physical chemistry chemical physics : PCCP 2014, 16, (3), 1150-60.

(25) Habgood, M.; Deij, M. A.; Mazurek, J.; Price, S. L.; ter Horst, J. H., Carbamazepine Co-crystallization with Pyridine Carboxamides: Rationalization by Complementary Phase Diagrams and Crystal Energy Landscapes. Crystal Growth & Design 2009, 10, (2), 903-912.

(26) Yang, X.; Wang, X.; Ching, C. B., In situ monitoring of solid-state transition of p-aminobenzoic acid polymorphs using Raman spectroscopy. Journal of Raman Spectroscopy 2009, 40, (8), 870-875.

(27) Morissette, S. L.; Almarsson, O.; Peterson, M. L.; Remenar, J. F.; Read, M. J.; Lemmo, A. V.; Ellis, S.; Cima, M. J.; Gardner, C. R., High-throughput crystallization: polymorphs, salts, co-crystals and solvates of pharmaceutical solids. Adv Drug Deliv Rev 2004, 56, (3), 275-300.

(28) Caridi, A.; Kulkarni, S. A.; Di Profio, G.; Curcio, E.; ter Horst, J. H., Template-Induced Nucleation of Isonicotinamide Polymorphs. Crystal Growth & Design 2014, 14, (3), 1135-1141.

(29) Kulkarni, S. A.; Meekes, H.; ter Horst, J. H., Polymorphism Control through a Single Nucleation Event. Crystal Growth & Design 2014, 14, (3), 1493-1499.

CHAPTER 7

Self-association during heterogeneous nucleation onto well-defined templates

This Chapter is published as

Abstract

We investigated the interplay between self-associates in solution and surface templating by studying the crystallization behaviour of isonicotinamide (INA) and 2,6-dihydroxy benzoic acid (DHB) in the presence of self-assembled monolayers (SAM). The end group of the SAM as well as the hydrogen bonding capabilities of the solvent and self-association of INA and DHB were found to be important in polymorph crystallization on SAMs. In the case of INA in ethanol, both chain and dimer self-associates are present in the solution. In the absence of SAMs the polymorph form II (dimer structure) is the crystallization outcome. In ethanol the 4-mercaptopyridine and 4-mercaptobenzoic acid SAMs organize INA chain associates at the template surface and enable the crystallization of form I while the 16-mercaptohexadecanoic acid SAM results in the crystallization of form II. Raman spectroscopy suggests that molecular interactions between INA and the SAM are responsible for the formation of specific polymorphs. XRPD results in the identification of the orientation of the crystal on the surface that further verified the results obtained by Raman spectroscopy. In nitrobenzene and nitromethane INA associates in solution only as chains and crystallization results in the formation of form IV and form I, respectively (both chain forms). The crystals formed in the bulk solution and on SAMs were the same, which seems to indicate that the self-association in nitrobenzene and nitromethane are not influenced by the presence of templates. In the case of DHB in toluene and chloroform, all three SAMs nucleated only one type of polymorph (stable form 2). In the case of toluene the polymorphic outcome was stable form 2 instead of metastable form 1, which is favoured in toluene in the absence of the SAMs. Again, Raman spectroscopy and XRPD suggest that DHB-SAM molecular interactions may be responsible for the formation of form 2.

7.1. Introduction

An industrial crystallization has to be carefully controlled in order to meet crystal product quality demands like crystal form, particle size distribution, crystal shape and purity.[1] A fundamental understanding of crystal nucleation is of major importance for the control and prediction of product quality from industrial crystallization processes.[2, 3] Polymorphism is the ability of a compound to self-assemble into different crystal structures.[4-6] Although many factors are known to influence the nature of the crystallized polymorph, for example supersaturation and temperature, a fundamental understanding of the mechanism is still lacking.[4, 7] Understanding the principles which influence the nature of the polymorph that crystallizes will improve the prediction and control of crystallization of desired polymorphs.[8-10]

To some extent polymorph control can be achieved by choosing a solvent that results in solute association related to the preferred polymorphic form.[8, 11] In solution different intermolecular interactions between like (solute-solute) and unlike (solute-solvent) molecules occur leading to the formation of different associates or building units.[8] The solute self-associates or building units will be a function of, among other factors, the solvent used.[8] The dominant building unit can be either a single molecule or differently associated molecules like dimers, tetramers and catemers. For example 2,6-dihydroxy benzoic acid (DHB) forms dimers in toluene and catemers in chloroform.[12] Crystallization from toluene leads to form 1 which is constructed of dimers while crystallization from chloroform leads to form 2 constructed of the catemer.[12] Isonicotinamide (INA) forms amide-pyridine heterosynthons (head-to-tail chains) in solvents like nitromethane and forms both amide-amide homosynthons (head-to-head dimers) and amide-pyridine heterosynthons (head-to-tail chains) in solvents like methanol.[13] This self-association in solution controls the polymorph crystallization by controlling the crystal building unit.[13]

It is also known that templates or organized substrates can be used to facilitate the formation of specific types of polymorphs.[14-16] Heterogeneous nucleation is the type of primary nucleation for which the nuclei are formed at surfaces such as dust particles, glass walls and stirrers.[17, 18] On an industrial scales these dust particles or small impurities are very difficult to remove. A more practical approach is to add effective particles or well-defined surfaces to control polymorph crystallization. Self-assembled monolayers (SAMs) have been used to control crystallization.[14, 17, 19-22] One type of SAM involves the use of thiol molecules assembled with a head group (thiol) bound to a substrate (gold), a chain or backbone and the free end group pointing outwards. The SAM surface can act as template for nucleation and crystal growth through functional group interactions and by providing a surface for the nucleation and growth of crystals.[14]

The interplay between template interaction and solution association is still not well understood. We chose SAMs with strong hydrogen bond acceptor and donor surface groups to favour specific molecular interactions between the solute and surface to enable the crystallization of polymorphs structurally related or unrelated to the associates in solution. The solution crystallization and template-induced nucleation may provide an understanding of polymorph nucleation from solution and also the underlying surface chemistry that controls nucleation and growth.

7.2. Experimental

7.2.1. Materials. INA (isonicotinamide) and DHB (2,6-dihydroxy benzoic acid) with a purity of ≥99% and ≥99.5% respectively, were obtained from Sigma Aldrich. The solvents ethanol, nitromethane, nitrobenzene, chloroform and toluene were used as received and were of ACS reagent grade with a purity of ≥99.5%, 99+% and 99+% respectively. 4MP (4-mercaptopyridine), 4MBA (4-mercaptobenzoic acid) and MHDA (16-mercaptohexadecanoic acid) were purchased from Sigma Aldrich. Gold coated (100 nm thick coating of gold)

glass substrates with a size of 25×120 mm were purchased from Evaporated Metal Films Corporation, New York and used as SAM substrate.

7.2.2. SAM preparation. Self-assembled monolayer (SAM) surfaces were prepared by immersing gold coated glass substrates in 10 mM solutions of 4MP, 4MBA, and MHDA in ethanol for 18 hours, following the SAM preparation procedure described by Yang et al.[14] After removing the substrates from solution, they were rinsed with copious amounts of toluene and then carefully blow-dried with ultrahigh purity nitrogen.

7.2.3. Cooling Crystallization on immerged SAMs. During INA crystallization experiments using ethanol, four concentrations (70, 87, 93 and 96 mg/mL) were used. The solids were suspended in 10 mL of ethanol and complete dissolution was obtained after heating the solution up to 60 °C. The samples were then cooled to 40 °C with a cooling rate of 0.1 °C/min and the SAM was carefully placed into the solution in an almost vertical position to prevent any crystals forming in the bulk solution attaching to the SAM surface. The solution was further cooled to 10 °C with a cooling rate of 0.1 °C/min and crystallization occurred either on the SAM, in the bulk solution or both. The SAM was removed from the solution in order to investigate the connected crystals. The SAM was carefully washed with ethanol to avoid nucleation of other crystals due to evaporation of the adhering solution. In all cases force was needed to remove the crystals from the SAM surface. The crystals were further analyzed with Raman spectroscopy and XRPD. The crystals formed in the bulk solution were also collected and analyzed. The same procedure was followed for INA in nitromethane (2 to 10 mg/mL) and nitrobenzene (10 to 20 mg/mL) and DHB in chloroform (60 to 90 mg/mL) and toluene (30 to 45 mg/mL). The experiments were repeated three times for each solvent and concentration to check the reproducibility of polymorph formation. Every crystal that nucleated and grew on the SAM surface was analyzed by XRPD to determine their orientation with respect to the SAM.

The transformation of metastable to stable polymorphic forms of INA and DHB were studied. A suspension of metastable form I of INA only very slowly transform to stable form II (>24 hours only trace of form II be seen) whereas form IV transforms to stable form II after 21 hours. In the case of DHB the transformation from metastable to stable form takes more than 72 hours. The crystals produced from the cooling procedure above were quickly removed following their nucleation and growth, minimizing the possibility of any transformation.

7.2.4. Crystal-SAM interface

The Raman microscope (Kaiser Optical Systems, Inc.), equipped with a 785 nm exciting line using a 600 grooves/mm grating and a 100× microscope objective, was used to obtain a Raman spectrum of the crystal-SAM interface. This objective gives a working distance of 0.27 mm and spot size of ~5 μm. The spectra were collected from 100 to 4000 cm^{-1}. The SAM surface with the attached crystals was placed on a microscope slide and placed under the microscope. Manual focusing of Raman spectroscope was used to locate the interface position within the crystalline sample. The same sample was measured number of times to locate the surface. Once found, a Raman spectrum was then obtained using the Raman instrument. Longer exposure times (20 sec) were used to obtain Raman spectra of a decent quality. The spectrum of the interface either shows an additional peaks or peak shifts when compared to the pure solid forms. Raman spectra were obtained for samples of each of the pure polymorphs away from the interface for comparison. It is clear that the relevant Raman spectra of the interface regions are spectroscopically distinct from the bulk indicating that the shifts observed are likely due to surface interactions.

7.2.5. Crystal orientation on the SAM surface

Each crystal on the SAM surface was picked up very carefully, collected and analysed using XRPD. Keeping track of the orientation of the crystals on the SAM, they were carefully removed from the SAM surfaces and each crystal was separately analysed by XRPD to determine the crystal surface connecting with the SAM. The XRPD pattern of the crystals bound to the SAM showed preferred orientation of the crystal face of the compound with respect to the SAM surface. X-ray powder diffraction data were collected using a PANalytical X'Pert PRO Theta/Theta powder X-ray diffraction system with a Cu tube and X'Celerator high-speed detector. All the XRPD patterns were added as electronic supplementary information.

7.3 Results

First, we describe the experimentally determined self-association of INA and DHB in different solvents. Then we focus on the crystallization outcome of INA and DHB from different solvents and on a number of templates. Finally, we discuss the competition between self-association and templates during crystallization. **Figure 7.1** shows the molecular structures of INA and DHB.


Figure 7.1: The molecular structures of INA and DHB.

7.3.1. Solvent dependent self-association of INA and DHB

The crystal structures of five polymorphs of INA have previously been reported in the literature.[23, 24] Form II is reported to be the most stable at room temperature. In this polymorph the amide group forms a homosynthon with the amide group of another INA, while the pyridine groups are not involved in

hydrogen bonding. Forms I, III, IV and V consist of differently packed head-to-tail chains connected through heterosynthons of the amide and the pyridine group with subtle differences in the crystal structure between each polymorph.[23, 24]

Figure 7.2 shows Raman solution spectra of dissolved INA in different solvents. Similar to the solid phase Raman spectra, the pyridine region in the solution spectra is related to the pyridine group of INA being present in either a chain form (1002 cm^{-1}) or a non-chain form (994 cm^{-1}); the latter is then either a dimer or a single INA molecule, possibly associated with the solvent. A similar IR spectral analysis leads to information on the hydrogen bonding of the amide group of INA in solutions.[13] In ethanol, for instance, INA self-associates in both head-to-head amide group dimers and head-to-tail amide-pyridine chains while in nitrobenzene and nitromethane only chains are present.
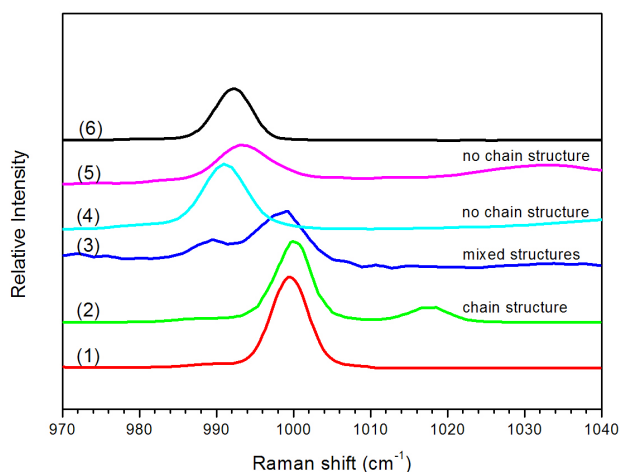
Figure 7.2: Raman spectra of isonicotinamide in different solvents and of solid samples. (1) Form I crystals; (2) In nitromethane; (3) In ethanol; (4) In acetone; (5) In chloroform (6) Form II crystals.[13]

Self-association of INA plays a key role in the crystallization outcome of INA.[13] For example, INA in ethanol self-associates into both dimers and chains. In this case, since different building units are present, the polymorphic outcome is determined by the competing processes of cluster formation of the different associates. In ethanol the dimer associates dominate and form the dimer structure form II.[13] Solvents like nitromethane and nitrobenzene enable the association of INA into chains leading to the formation of metastable forms I and form IV respectively. The form I and IV crystal structures both contain chains of INA.[13]

DHB also shows solvent dependent self-association.[25] DHB forms hydrogen bonded catemers in chloroform and dimers in toluene.[12] Crystallization of DHB from chloroform solutions at low supersaturation results in the most stable form 2 consisting of catemers. Crystallization of DHB from toluene always yields the metastable form 1 consisting of dimers.[12]

7.3.2. Crystallization of INA and DHB in the presence of SAM templates

The SAM components 4MP, 4MBA and MHDA consist of a thiol group, which connects to the gold surface, a backbone and either a pyridine or a carboxylic acid group that defines the character of the SAM surface onto which crystals would form. The pyridine group on the SAM serves as an hydrogen bonds acceptor while the carboxyl group on SAM can donate and accept hydrogen bonds via the acidic OH group and the C=O group.[14]

7.2.2.1 Isonicotinamide (INA)

Upon cooling crystallization of INA from ethanol in the presence of the 4MBA SAM, two different types of crystals were observed in the vials (**Figure 7.3**). The first type crystallized on the SAM while the other crystallized in the bulk solution. Analysis of crystals with Raman spectroscopy and XRPD showed that the bulk solution crystals were form II, as expected. However, the crystals formed on the SAM were identified as form I crystals (**Table 7.1**).
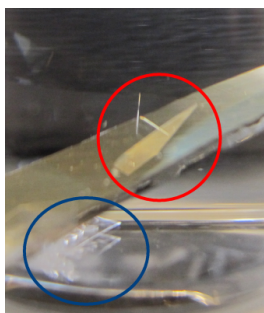
Figure 7.3: Cooling crystallization of INA from ethanol in the presence of the 4MBA SAM. The tilted surface contains the SAM onto the gold-coated surface. The INA form I crystals on the 4MBA SAM are marked with a red circle while INA form II crystals in the bulk solution are marked with a blue circle.

Similarly, upon cooling crystallization from ethanol the crystals obtained on the 4MP SAM were form I, whereas form II was crystallized in the bulk of the solution. The crystals obtained on the MHDA SAM surface were form II, the same as obtained from the bulk solution. Thus, although the 4MBA SAM and MHDA SAM have the same functionalized surface of carboxylic acids, two different polymorphs were obtained (**Table 7.1**).

Upon cooling crystallization of INA from nitrobenzene, crystals formed on the 4MP SAM. These crystals were form IV, the same form as crystallized in the bulk solution. In this solvent no crystals were obtained on the 4MBA and MHDA SAM while form IV crystals were formed in the bulk. Upon cooling crystallization of INA from nitromethane, form I was crystallized on 4MP and 4MBA SAMs as well as in bulk solution. There were no crystals formed on the MHDA SAM as the form I crystals were only formed in the bulk solution. See **Table 7.1** for a summary of the results.

Table 7.1: Polymorphic outcomes for cooling crystallization of INA and DHB from different solvents in the presence of 4MP, 4MBA and MHDA SAMs. The dashes indicate experiments without any crystal formation on the SAM. The table also shows experimentally derived solution associates of INA and DHB found in previous studies.[13, 25]

Compound	Solvent	Self-Association	Form in Bulk	SAM component	Form on SAM	Crystal-SAM interface	Connecting crystal faces on SAM
INA	Ethanol	Dimer + Chain	Dimer (Form II)	4MP (Pyridine)	Form I (Chain)	NH$_2$ of INA-Pyridine of 4MP	(0 2 0)
			Dimer (Form II)	4MBA (Ar-COOH)	Form I (Chain)	i) NH$_2$ of INA-CO of 4MBA and ii) INA CO-OH of 4MBA	(4 0 -2)
			Dimer (Form II)	MHDA (C$_{16}$H$_{32}$COOH)	Form II (Dimer)	Pyridine of INA-COOH of MHDA	(1 0 0) and (4 1 0)
INA	Nitrobenzene	Chain	Chain (Form IV)	4MP (Pyridine)	Form IV (Chain)	NH$_2$ of INA-Pyridine of 4MP	(1 0 0) and (0 0 2)
			Chain (Form IV)	4MBA (Ar-COOH)	-	-	-
			Chain (Form IV)	MHDA (C$_{16}$H$_{32}$COOH)	-	-	-
INA	Nitromethane	Chain	Chain (Form I)	4MP Pyridine	Form I (Chain)	NH$_2$ of INA-Pyridine of 4MP	-
			Chain (Form I)	4MBA (Ar-COOH)	Form I (Chain)	NH$_2$ of INA-CO of 4MBA	-
			Chain (Form I)	MHDA (C$_{16}$H$_{32}$COOH)	-	None	-
DHB	Chloroform	Catemers	Catemer (Form 2)	4MP Pyridine	Form 2 (Catemer)	OH of DHB-Pyridine of 4MP	(2 1 0)
			Catemer (Form 2)	4MBA (Ar-COOH)	Form 2 (Catemer)	i) OH of DHB-CO of 4MBA and ii) CO of DHB-OH of 4MBA	(2 1 0)
			Catemer (Form 2)	MHDA (C$_{16}$H$_{32}$COOH)	Form 2 (Catemer)	i) OH of DHB-CO of MHDA and ii) CO of DHB-OH of MHDA	(2 1 0)
DHB	Toluene	Dimer	-	4MP Pyridine	Form 2 (Catemer)	i) OH of DHB-pyridine of 4MP	(2 1 0)
			Dimer (Form 1)	4MBA (Ar-COOH)	Form 2 (Catemer)	i) OH of DHB-CO of 4MBA and ii) CO of DHB-OH of 4MBA	(2 1 0)
			-	MHDA (C$_{16}$H$_{32}$COOH)	Form 2 (Catemer)	i) OH of DHB-CO of MHDA and ii) CO of DHB-OH of MHDA	(2 1 0)

With aid of Raman spectroscopy coupled to a microscope, Raman spectra of the SAM-crystal interfaces could be obtained. For INA, the region of the NH_2 and CO stretching vibrations of (respectively 3030 -3090 cm^{-1} and 1580 -1680 cm^{-1}) as well as the ring breathing region of INA pyridine (950 -1050 cm^{-1}) reflect how the crystals are molecularly connected to the SAM surface.[13] The Raman spectra of the SAM-crystal interfaces are compared with that of INA form I and form II in **Figure 7.4** and **Figure 7.6** for INA crystals on the 4MP, 4MBA and MHDA SAMs. Analysis of XRPD data of the crystals bound to the SAM showed preferred orientation of the crystal face of the compound with respect to the SAM surface, which further verified the results obtained by Raman spectroscopy.
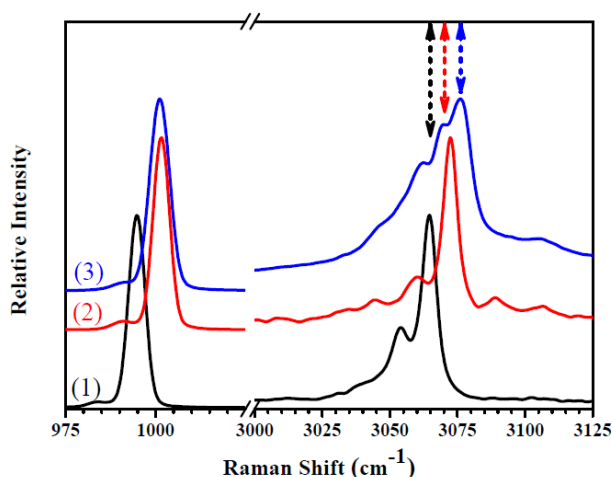
Figure 7.4: Raman spectra of INA crystals showing the NH_2 stretching vibrations (3000-3125 cm^{-1}) and pyridine ring breathing mode (975 -1100 cm^{-1}) vibrations. (1) Pure form II, (2) Pure form I, (3) interface region of form I on the 4MP surface in ethanol. The arrow indicates the position of an additional peak in (3). This additional peak is positioned at higher wavenumbers compared to pure form I reflecting interactions between the pyridine of the 4MP SAM and the amide group of INA.
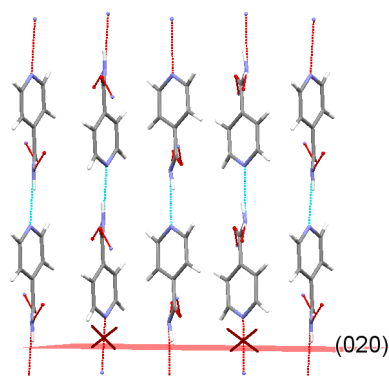
Figure 7.5: The 4MP SAM and the INA crystal grown from ethanol are connected through the (0 2 0) face of INA form I. The NH_2 group of INA is pointing towards the pyridine group of the 4MP SAM. The red crosses indicate molecules in an orientation without hydrogen bonding with the template surface.

The Raman spectrum of the template-crystal interface for the INA form I crystal formed on the 4MP SAM in ethanol shows that the pyridine ring-breathing mode (990-1010 cm^{-1}) has the same peak position as that of INA form I (**figure 7.4)**. Compared to INA form I and form II the NH_2 stretching vibration region (3000-3125 cm^{-1}) shows an additional peak at slightly higher wavenumber for the interface spectrum. An explanation for this extra peak is the occurrence of additional interactions compared to the internal crystal. One such interaction that would create an additional peak is hydrogen bonding between the pyridine group of the 4MP SAM and the NH_2 group of INA. The shift to the higher wavenumber could be because the pyridine N^+ stretching vibrations of 4MP are between 3300 to 1900 cm^{-1}. The NH_2 group of INA is a strong hydrogen bond donor, which can interact with pyridine of 4MP, which is strong hydrogen bond acceptor. We further analysed the same crystals using XRPD in order to find out the crystal orientation on the surface. In the case of INA on the 4MP surface it was found that the interface is the (0 2 0) face.

Figure 7.5 shows the (0 2 0) face with the NH_2 group of INA points towards the surface. This is consistent with our hypothesis from the Raman spectroscopy results that hydrogen bonding interactions between the pyridine

group on the SAM surface and INA amide groups play a key role in the formation of INA form I on the 4MP SAM.

In the case of the interface between form I grown from ethanol and the 4MBA SAM, the NH_2 stretching vibrations of INA between 3040-3100 cm^{-1} show an additional peak as compared to pure form I (**Figure 7.6**). An explanation for this extra peak at 3069 cm^{-1} is the occurrence of additional interactions at the interface compared to the internal crystal. This interaction could include hydrogen bonding between the CO group (1700 cm^{-1}) of the 4MBA SAM and the NH_2 group of INA. The peak at 1635 cm^{-1} in the carbonyl region also shows a shift to lower wavenumbers. This shift can be explained by the formation of hydrogen bonding interactions between the carbonyl group of INA (hydrogen bond acceptor) with the hydroxyl group (hydrogen bond acceptor/donor) of the carboxylic acid of the 4MBA SAM.
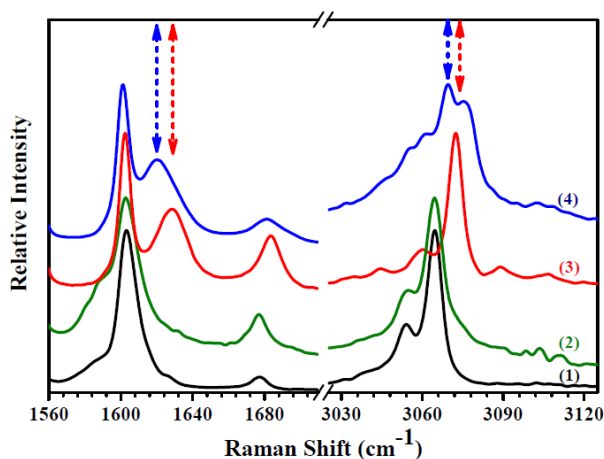

Figure 7.6: Raman spectra of INA crystals showing the NH_2 stretching vibrations (3000-3125 cm^{-1}) and the CO stretching (1550 -1650 cm^{-1}) vibrations. (1) Pure form II, (2) interface region of form II grown from ethanol on the MHDA SAM, (3) pure form I, and (4) interface region of form I grown from ethanol on the 4MBA SAM. The arrows indicates the position of an extra peak at lower wavenumber other than pure form I and a peak shift.

XRPD shows that peculiarly the crystal-SAM interface is the relatively high index face (4 0 -2) of INA form I. **Figure 7.7a** shows the (4 0 -2) face with the

NH_2 and CO groups of two different molecules of INA pointing towards the surface. This suggests a surface interaction involving a CO group (hydrogen bond acceptor) of 4MBA with an NH_2 group of INA (hydrogen bond donor) and an OH group of 4MBA (hydrogen bond acceptor/donor) with a CO group of INA (hydrogen bond acceptor), respectively, which is in accordance with the interpretation of the Raman spectrum.

In case of INA form II crystallized from ethanol on the MHDA SAM, the plate-like crystals grew laterally and flat on the SAM. **Figure 7.6** shows the Raman spectrum of the template-crystal interface, which is similar to that of INA form II. The Raman spectrum of the template-crystal interface for the INA form II crystal formed on the MHDA SAM in ethanol shows that the carbonyl region (1560-1700 cm^{-1}) and NH_2 stretching region (3030-3090 cm^{-1}) has the same peak position as that of INA form II (**Figure 7.6**). As established with XRPD analysis the (1 0 0) and (4 1 0) faces of INA is the interface between the MHDA SAM and the INA form II crystal (**Figure 7.6b**).
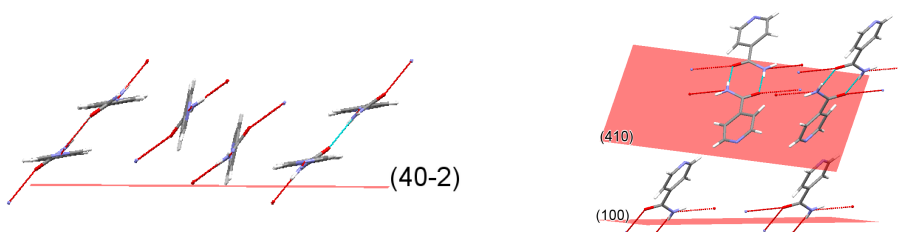
Figure 7.7: a) The (4 0 -2) face is the interface between INA form I grown from ethanol on the 4MBA SAM. The NH_2 and CO groups of some molecules are pointing towards the SAM surface. b) The (1 0 0) and (4 1 0) faces are the interface between INA form II grown from ethanol on the MHDA SAM. The amide group of INA (-$CONH_2$) is pointing towards the template surface.

Figure 7.7b indicates that the amide group and pyridine groups of INA are pointing towards the carboxylic acid group of MHDA. While the results obtained by Raman spectroscopy do not indicate a significant interaction between the amide group of INA with the carboxylic group of MHDA SAM, XRPD suggests a surface interaction involving a pyridine group (hydrogen bond acceptor) of INA with an OH group of 4MBA (hydrogen bond

acceptor/donor) may be present. The lack of a change in Raman spectral features indicates that this may be a relatively weak interaction compared to the results discussed above for INA with the 4MP and 4MBA SAMs.

### 7.2.2.2. 2,6-dihydroxy benzoic acid (DHB)

When DHB is crystallized from chloroform in the presence of 4MP, 4MBA and MHDA SAMs, only form 2 crystals were observed in the vials. Analysis with Raman spectroscopy and XRPD showed that the bulk solution crystals were form 2 (**Table 7.1**).

Upon cooling crystallization of DHB from toluene in the presence of the 4MBA SAM, two different types of crystals were observed in the vials. The first type crystallized on the SAM while the other crystallized in the bulk solution. Analysis with Raman spectroscopy and XRPD showed that the bulk solution crystals were metastable form 1, as expected. However, the crystals formed on the SAM were identified as stable form 2 crystals (**Table 7.1**). Similarly, crystals obtained on the 4MP and MHDA SAM upon cooling crystallization from toluene were form 2, although there were no crystals in the bulk of the same solution.

Figure 7.8 shows the CO stretching region (1650 -1700 cm^{-1}) of the Raman spectra of the crystal-SAM interfaces. In the case of DHB form 2 grown from toluene on the 4MP SAM the Raman spectrum shows shifts in this region (**Figure 7.8**). This shift can be explained by the occurrence of hydrogen bonding between the hydrogen bond accepting pyridine group of the template surface and the hydrogen bond donating OH-group of DHB. The Raman spectra of the crystal-SAM interfaces in the case of DHB form 2 grown from toluene on the 4MBA and MHDA SAMs show no substantial peak shifts. This might indicate that the carboxylic acid groups of DHB and of the template surface interact in a similar way as the carboxylic acid groups in the crystal structure of DHB.
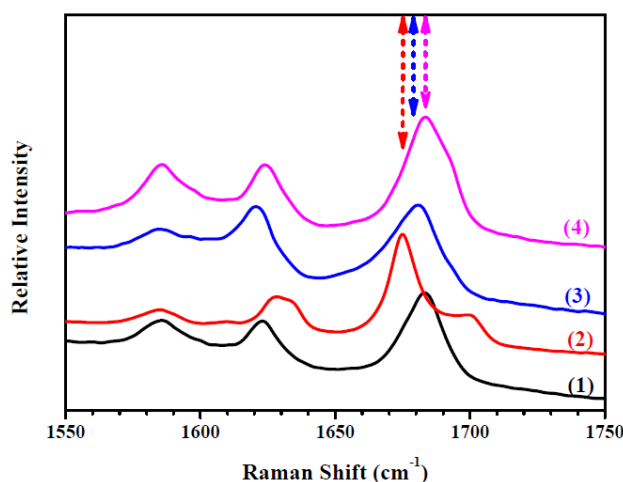
Figure 7.8: Raman spectra of the CO stretching vibration region of DHB. (1) Pure form 2, (2) the interface region of a DHB form 2 crystal grown from toluene on the 4MP SAM, (3) the interface region of a DHB form 2 crystal grown from toluene on the 4MBA surface, and (4) the interface region of a DHB form 2 crystal grown from toluene on the MHDA surface. Arrows are drawn in order to compare the shift of DHB due to surface interactions.
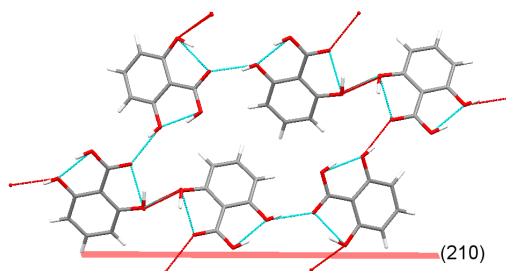

Figure 7.9: The (2 1 0) face of DHB as the interface on the SAM. The OH group of DHB interacts with the 4MP SAM surface while in the case of 4MBA and MHDA SAMs both CO and OH groups are responsible for the formation of catemers of DHB.

XRPD show that peculiarly the crystal-SAM interface in toluene and chloroform are the relatively high index face (2 1 0) of DHB form 2. From the Raman and XRPD results we can conclude that at the interface the OH and CO groups of the DHB molecules point towards the surface and interact with 4MP, 4MBA and MHDA. For instance, the OH of DHB interacts with the pyridine of 4MP while

both the CO and OH of DHB interacts with COOH group of 4MBA and MHDA SAM (**Figure 7.9**).

7.4. Discussion

In this paper we investigate the effect of both solution self-association and templates on polymorph crystallization behaviour. If we assume that the polymorphic outcome is determined in the heterogeneous nucleation stage of the process we can identify a number of factors that may influence this. First, solutes associate to create building units in solution. Second, molecular interactions between associated solute and template can create additional specific pre-arrangement at the template-solution interface of these building units, templating the nucleation of a specific polymorph. This template can stimulate either the already abundantly present associates or associates present in minor amounts into a specific organization leading to polymorphs that are otherwise not able to be obtained.

a)   b)
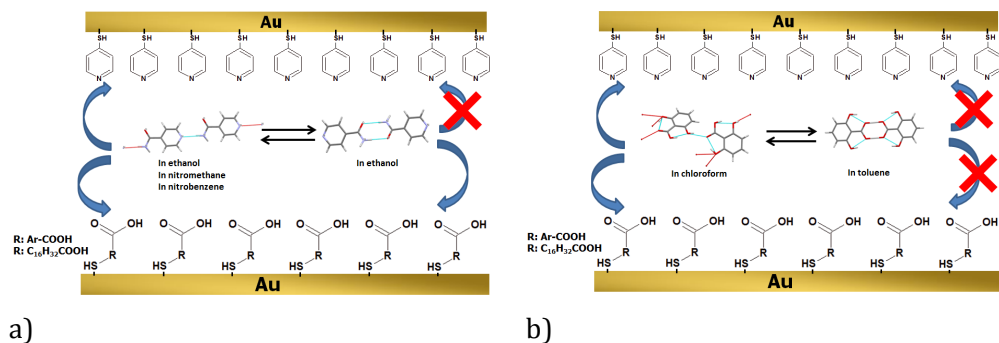
Figure 7.10: Schematic of the interplay between self-association of a) INA and template b) DHB and template. The arrows indicate their relation to the final polymorphic outcome from experiments.

INA in ethanol is an interesting case since in this solvent the dimer and chain building units are both present to form the dimer (form II) and chain polymorphic forms (other forms). In the absence of deliberately added templates polymorph form II is the crystallization outcome. Providing the right template would organize INA chain associates at the template surface and enable the nucleation of an alternative form, for instance form I (**Figure**

7.10a). This is exactly what happens in case of the 4MP and the 4MBA templates.

Interestingly, crystallization of INA from ethanol in the presence of the MHDA template results in form II, the dimer form. Apparently this template does not sufficiently promote the chain arrangement on its surface although it does have the same functional group, the carboxylic acid, as the 4MBA template. In nitrobenzene and nitromethane INA associates as chains and we could not find evidence of the presence of dimers in these solutions. Crystallization of INA from nitromethane in the presence of the 4MP and 4MBA templates results in form I, while in case of nitrobenzene in the presence of 4MP results in form IV (both chain forms). Crystallization of INA from nitromethane and nitrobenzene in the presence of the MHDA and 4MBA template respectively, did not result in crystals on the template. This indicates that the chain associates do not seem to organize on the MHDA and 4MBA template sufficiently to cause template nucleation of a chain form of INA. The crystals formed in the bulk solution were INA form IV and the self-association in nitrobenzene was hard to overcome.

DHB is a similar case. Dimers do not interact with all templates used. Apparently, although catemer associates are undetectable in toluene solutions, they are present in sufficient concentrations or form in the presence of suitable surface interactions enabling their organization on the templates to form the catemer form 2 (**Figure 7.10b**).

The other factor that may influence the heterogeneous nucleation of polymorphic compounds is the balance of the interfacial energies of the crystal-solution (γ_{CS}), crystal-template (γ_{CT}) and solution-template (γ_{ST}) interfaces which might promote the formation of specific crystalline forms as the crystals on the SAM have a very specific orientation. The rather high Miller indices of the faces connected to the SAMs might indicate that the nucleation process is influenced by interfacial energies while molecular interactions might be less important. For example, the (4 0 -2) face of INA form I grows on the 4MBA surface and the (2 1 0) face of DHB form 2 grows on 4MP, 4MBA and MHDA surfaces.

Another possibility is that the template contains stacking faults which provide additional positions on the surface that energetically favor

heterogeneous nucleation of specific polymorphs.[26, 27] However, all of our results appear to show that polymorph nucleation is likely due to molecular interactions or interfacial energies.

7.5. Conclusions

Solvents have a large effect on the kind of associates present in solution. For instance, INA is present as chains in the solvents nitrobenzene and nitromethane. These building units have a significant influence on the polymorphic outcome of crystallization. INA, for instance, crystallizes as a form containing chains from nitrobenzene. Additionally, many of the used template surfaces are effective in promoting crystallization; some even promote the crystallization of a different polymorph.

   Understanding solution self-association offers the ability to develop a more fundamental understanding of the heterogeneous nucleation process in terms of the interplay between association and templates. The interfacial energies as well as the molecular interactions between solute and SAM play an important role during polymorph nucleation of INA. The type of end group of the SAMs as well as the hydrogen bonding capabilities of solvent and self-association of INA are important for polymorph nucleation. If both chain and dimer self-associates of INA are present in the solution, it is possible to provide surfaces that induce crystallization of forms that are related to these self-associates. However, the templates are not able to crystallize polymorphs containing dimer association motifs unless these are present in solution. The crystallized polymorphs in all cases arises from matching the hydrogen bond donor or acceptor sites of INA or DHB with complementary sites on the SAM, suggesting an approach for polymorph control within a given solvent system. Further systematic analysis of the association processes in solutions and the interplay with well-defined templates would be beneficial in the development of polymorph control, discovery and preparation within crystallization processes.

7.6. Acknowledgement

7.7. References

(1) Woo, X. Y.; Tan, R. B. H.; Braatz, R. D., Precise tailoring of the crystal size distribution by controlled growth and continuous seeding from impinging jet crystallizers. CrystEngComm 2011, 13, (6), 2006-2014.

(2) Davey, R. J.; Allen, K.; Blagden, N.; Cross, W. I.; Lieberman, H. F.; Quayle, M. J.; Righini, S.; Seton, L.; Tiddy, G. J. T., Crystal engineering - nucleation, the key step. CrystEngComm 2002, 4, (47), 257-264.

(3) Kramer, H. J. M.; Jansens, P. J., Tools for Design and Control of Industrial Crystallizers – State of Art and Future Needs. Chemical Engineering & Technology 2003, 26, (3), 247-255.

(4) Bernstein, J., Polymorphism in Molecular Crystals. ed.; Oxford University Press: Oxford, 2007; p 424.

(5) Bernstein, J.; Hagler, A. T., Conformational polymorphism. The influence of crystal structure on molecular conformation. Journal of the American Chemical Society 1978, 100, (3), 673-681.

(6) Diao, Y.; Whaley, K. E.; Helgeson, M. E.; Woldeyes, M. A.; Doyle, P. S.; Myerson, A. S.; Hatton, T. A.; Trout, B. L., Gel-Induced Selective Crystallization of Polymorphs. Journal of the American Chemical Society 2011, 134, (1), 673-684.

(7) Herman, C.; Haut, B.; Douieb, S.; Larcy, A.; Vermylen, V.; Leyssens, T., Use of in Situ Raman, FBRM, and ATR-FTIR Probes for the Understanding of the Solvent-Mediated Polymorphic Transformation of II–I Etiracetam in Methanol. Organic Process Research & Development 2011, 16, (1), 49-56.

(8) Davey, R. J.; Schroeder, S. L. M.; ter Horst, J. H., Nucleation of Organic Crystals—A Molecular Perspective. Angewandte Chemie International Edition 2012, 52, (8), 2166-2179.

(9) Kitamura, M., Controlling Factors and Mechanism of Polymorphic Crystallization. Crystal Growth & Design 2004, 4, (6), 1153-1159.

(10) Lee, A. Y.; Erdemir, D.; Myerson, A. S., Crystal polymorphism in chemical process development. Annu Rev Chem Biomol Eng 2011, 2, 259-80.

(11) Parveen, S.; Davey, R. J.; Dent, G.; Pritchard, R. G., Linking solution chemistry to crystal nucleation: the case of tetrolic acid. Chemical Communications 2005, (12), 1531-1533.

(12) Davey, R. J.; Blagden, N.; Righini, S.; Alison, H.; Quayle, M. J.; Fuller, S., Crystal Polymorphism as a Probe for Molecular Self-Assembly during Nucleation from Solutions: The Case of 2,6-Dihydroxybenzoic Acid. Crystal Growth & Design 2000, 1, (1), 59-65.

(13) Kulkarni, S. A.; McGarrity, E. S.; Meekes, H.; ter Horst, J. H., Isonicotinamide self-association: the link between solvent and polymorph nucleation. Chemical Communications 2012, 48, (41), 4983-4985.

(14) Yang, X.; Sarma, B.; Myerson, A. S., Polymorph Control of Micro/Nano-Sized Mefenamic Acid Crystals on Patterned Self-Assembled Monolayer Islands. Crystal Growth & Design 2012, 12, (11), 5521-5528.

(15) Carter, P. W.; Ward, M. D., Directing Polymorph Selectivity During Nucleation of Anthranilic Acid on Molecular Substrates. Journal of the American Chemical Society 1994, 116, (2), 769-770.

(16) Frostman, L. M.; Ward, M. D., Nucleation of Molecular Crystals beneath Guanidinium Alkanesulfonate Monolayers. Langmuir 1997, 13, (2), 330-337.

(17) Chadwick, K.; Myerson, A.; Trout, B., Polymorphic control by heterogeneous nucleation - A new method for selecting crystalline substrates. CrystEngComm 2011, 13, (22), 6625-6627.

(18) Cox, J. R.; Ferris, L. A.; Thalladi, V. R., Selective growth of a stable drug polymorph by suppressing the nucleation of corresponding metastable

polymorphs. Angewandte Chemie (International ed. in English) 2007, 46, (23), 4333-6.

(19) DiBenedetto, S. A.; Facchetti, A.; Ratner, M. A.; Marks, T. J., Molecular Self-Assembled Monolayers and Multilayers for Organic and Unconventional Inorganic Thin-Film Transistor Applications. Advanced Materials 2009, 21, (14-15), 1407-1433.

(20) Canaria, C. A.; So, J.; Maloney, J. R.; Yu, C. J.; Smith, J. O.; Roukes, M. L.; Fraser, S. E.; Lansford, R., Formation and removal of alkylthiolate self-assembled monolayers on gold in aqueous solutions. Lab on a chip 2006, 6, (2), 289-95.

(21) Hiremath, R.; Basile, J. A.; Varney, S. W.; Swift, J. A., Controlling molecular crystal polymorphism with self-assembled monolayer templates. J Am Chem Soc 2005, 127, (51), 18321-7.

(22) Rupa, H.; W, V. S.; A, S. J., Oriented crystal growth of 4-iodo-4'-nitrobiphenyl on polar self-assembled monolayer templates: A case for chemical epitaxy. Chemistry of materials 2004, 16, (24), 4948-4954.

(23) Li, J.; Bourne, S. A.; Caira, M. R., New polymorphs of isonicotinamide and nicotinamide. Chemical Communications 2011, 47, (5), 1530-1532.

(24) Aakeroy, C. B.; Beatty, A. M.; Helfrich, B. A.; Nieuwenhuyzen, M., Do Polymorphic Compounds Make Good Cocrystallizing Agents? A Structural Case Study that Demonstrates the Importance of Synthon Flexibility. Crystal Growth & Design 2003, 3, (2), 159-165.

(25) Davey, R. J.; Blagden, N.; Righini, S.; Alison, H.; Ferrari, E. S., Nucleation Control in Solution Mediated Polymorphic Phase Transformations: The Case of 2,6-Dihydroxybenzoic Acid. The Journal of Physical Chemistry B 2002, 106, (8), 1954-1959.

(26) Caridi, A.; Kulkarni, S. A.; Di Profio, G.; Curcio, E.; ter Horst, J. H., Template-Induced Nucleation of Isonicotinamide Polymorphs. Crystal Growth & Design 2014.

(27) Di Profio, G.; Fontananova, E.; Curcio, E.; Drioli, E., From Tailored Supports to Controlled Nucleation: Exploring Material Chemistry, Surface Nanostructure, and Wetting Regime Effects in Heterogeneous Nucleation of Organic Molecules. Crystal Growth & Design 2012, 12, (7), 3749-3757.

CHAPTER 8

Conclusions and Recommendations

The main objective of this thesis was to increase understanding of crystallization processes by studying the relation between crystal product quality and nucleation and growth. The thesis results in methods for crystallization process optimization for crystal product quality. The thesis also offers the opportunity to not only discover new polymorphs but also to control the nucleation of the most stable polymorphic form. This thesis aims to define the crystallization conditions, like supersaturation, temperature and the choice of substrate for heterogeneous nucleation that leads to the right polymorph with the desired physical properties such as crystal morphology. Industries can improve existing crystal product qualities but also can optimize the quality of new crystalline products by incorporating the new methods in the development process.

8.1. Conclusions

8.1.1. Fast and accurate nucleation rate measurements

The research starts with two newly developed methods to measure nucleation kinetics and I compared these two recently developed methods by determining crystal nucleation rates in stirred solutions. Both the induction time method as well as the MSWZ method results in an estimate of the nucleation rate parameters in stirred solutions. The MSZW method is less labour intensive, the induction time method seems to have higher accuracy and is easier to analyze. The MSZW has less control over temperature in the vials due to a possible temperature difference between cooling coil and crystallization volume while the temperature dependence of the kinetic factor A and the thermodynamic factor B are not accounted for in the model. Thus we conclude that the induction time method probably is more accurate. The values of the kinetic parameter *(A)* obtained in the present paper are low compared to the theoretical values. This could be due to both a lower than expected attachment frequency of building units to the nucleus and a lower than expected concentration of active nucleation sites in the solution. For the crystal nucleation of INA from ethanol the concentration of active nucleation sites in the solution could be reduced by filtering the solution.

8.1.2. Polymorphism Control through a Single Nucleation Event

The single nucleus mechanism, in which all crystals in the suspension originate from the same parent single crystal, might occur more generally than is currently recognized, even in larger volumes. This has important implications for the control of industrial crystallization processes of polymorphic compounds. In chapter 3, polymorphism was used as a tool to validate this single nucleus mechanism. Crystallization of INA from the solvents ethanol, nitromethane and nitrobenzene results in respectively pure form II, pure form I and pure form IV. Because the transformation rate was measured to be relatively slow for INA as well as 4HAP this would not influence the polymorphic outcome from a relatively fast crystallization process. Nucleation experiments combined with polymorph detection could therefore be used to validate the single nucleus mechanism. Crystallization of INA from a 70:30 vol% mixture of EtOH-NM and 90:10 vol% mixture of EtOH-NB always resulted in either pure form I or pure form II. Similar to INA the crystallization of 4HAP at different concentrations in a 3 mL solution of ethyl acetate always resulted in either pure form I or II of 4HAP. At 100 mL scale four experiments resulted in pure form II and two resulted in the mixtures of form I and II. The data generated on polymorphs of INA and 4HAP are highly supportive to the proposed single nucleus mechanism and backing up our visual observations reported earlier.

8.1.3. Liquid-liquid phase separation during crystallization

We have investigated the effect of LLPS on the crystallization of HAP in water and water-ethanol mixtures. In this study, in-situ cameras were used to determine the disappearance and reappearance temperatures of LLPS. The unexpected presence of two liquid phases can be a serious problem during industrial crystallization processes. We have studied the effect of LLPS on crystallization of HAP in water and water-ethanol mixtures. Observation by Crystalline in situ camera of the nucleation of droplets of the supersaturated solution of HAP shows the crystal forming at the edges of the droplets. Crystallization experiments of HAP in water resulted in either hydrate of HAP or mixtures of hydrate and pure I. In case of HAP in water ethanol mixtures the

crystallization outcome was either anhydrous form I and form II or mixtures of both. The data generated on polymorphs of HAP suggest that LLPS hinder the primary and secondary nucleation and the single nucleus mechanism does not hold anymore. The amount of ethanol also dramatically influences the phase distribution of a solute between the liquid phases by changing the solubility of HAP in solvent mixtures. A control favoring either LLPS or crystallization provides a possible method in preparing kinetically trapped morphologies for practical applications.

8.1.4. Self-association in Solution for Polymorph preparation and control

We demonstrated that the structural outcome of the crystallization process of INA, NA, PA, CBZ and DPL are directed by the association and self-association processes in solutions which are largely influenced by the hydrogen bonding capacity of the solvent. Our results thus suggest that a systematic analysis method of the association processes in solutions method would be beneficial in polymorph discovery and preparation. The self-association method offer the ability to develop a more fundamental understanding of the crystallization process, based on knowledge generated from large numbers of experiments on diverse compounds and conditions. In the chapter 5 and 6 the self-association method that we have developed is described. Solvents have a large effect on the kind of associates present in solution. For instance, INA is present as chains in the solvents nitrobenzene and nitromethane. These building units have a significant influence on the polymorphic outcome of crystallization. INA, for instance, crystallizes as a form containing chains from nitrobenzene. Not only the published forms of INA were found, but also new form was identified. We used Raman spectroscopy of solutions as a novel analytical tool in combination with FTIR and NMR to identify the self-association of INA, NA, PA, CBZ, pABA and DPL in different solvents. This new systematic method could also be applied to discover new multicomponent crystals such as salts and co-crystals.

8.1.5. Self-association during heterogeneous nucleation onto well-defined templates

Understanding solution self-association offers the ability to develop a more fundamental understanding of the heterogeneous nucleation process in terms of the interplay between association and templates. The interfacial energies as well as the molecular interactions between solute and SAM play an important role during polymorph nucleation of INA. The type of end group of the SAMs as well as the hydrogen bonding capabilities of solvent and self-association of INA are important for polymorph nucleation. If both chain and dimer self-associates of INA are present in the solution, it is possible to provide surfaces that induce crystallization of forms that are related to these self-associates. However, the templates are not able to crystallize polymorphs containing dimer association motifs unless these are present in solution. The crystallized polymorphs in all cases arises from matching the hydrogen bond donor or acceptor sites of INA or DHB with complementary sites on the SAM, suggesting an approach for polymorph control within a given solvent system. Further systematic analysis of the association processes in solutions and the interplay with well-defined templates would be beneficial in the development of polymorph control, discovery and preparation within crystallization processes.

8.2. Recommendations

1. The values of the kinetic parameter (A) obtained in the present study were very low ($<10^6$) as compared to the postulated values (10^{15}-10^{25}). The kinetic parameter (A) is largely determined by the attachment frequency of molecules to the nucleus and the concentration of the active nucleation sites in the solution. A low concentration of heterogeneous particles (nucleation sites) may explain the low pre-exponential factor, which was measured with the filtered solutions. Nothing is known, however, about the actual concentration and functionality of the heterogeneous particles. The combination of sophisticated experimental nucleation studies in the presence of known heterogeneous particles and computer modelling of the nucleation behaviour applied to the same compounds will lead to a fundamental understanding. Detailed insight in the nucleation behaviour of

specific compounds should subsequently be exploited to improve the crystal product quality. The experiments could be performed in controlled environment where values of the pre-exponential factor can be controlled.

2. We have shown here that the single nucleus mechanism occurs for a number of systems on small and lab scale. Some observations indicate that the single nucleus mechanism might break down at larger scales (>1 L)[3]. However, on industrial scales (>1000 L) at the cooling surface or the vapor-liquid surface at which evaporation takes place high local supersaturation will exist. Those will be the locations where crystal nucleation is most likely to take place. Thus, on industrial scales the occurrence of nucleation is bound to a small part of the industrial crystallizer, which would be advantageous for the single nucleus mechanism as compared to conventional nucleation. It is important to study the occurrence of the single nucleus mechanism on an industrial scale. Seeding approaches using only a single crystal should be tested which lead to the avoidance of primary nucleation and thus control over the polymorph obtained.

3. The combination of well-defined template surfaces and the self-association method can be used as a screening method in the early drug discovery and development phase but also define robust conditions for industrial crystallization of polymorphs. This will not only help to discover and reproducibly prepare polymorphs, but a more comprehensive screening can be performed at reduced cost. Industries can implement the results to improve crystal product qualities and can also discover and optimize the quality of new crystal products by incorporating the methods in the development process. Molecular simulations are still needed to bridge the gap between solution chemistry and crystal nucleation rate analysis to come to a molecular interpretation of crystal nucleation of organic compounds. The new methods are needed for polymorph prediction and in particular for predicting the conditions for polymorph formation.

4. The factor that may influence the heterogeneous nucleation of polymorphic compounds is the balance of the interfacial energies of the crystal-solution (γ_{CS}), crystal-template (γ_{CT}) and solution-template (γ_{ST}) interfaces which might promote the formation of specific crystalline forms as the crystals on the SAM have a very specific orientation. The crystals can grow on template surface due to the molecular interactions between the solute and template surface but can also occur on imperfections of the surface. The lattice matching across the crystalline solid and substrate interface also play an important role in the process of heterogeneous nucleation. The size and shape of the pore of the template can also strongly affect the nucleation rate by confining the nucleus in one or more directions. It is important to study the heterogeneous nucleation by calculating the interfacial energies and studying the other parameters, which influence nucleation process. A strong experimental approach is needed which includes understanding of self-association, molecular interactions, different interfacial energies and other parameters.

List of publications, Curriculum Vitae, Acknowledgements

List of publications

Journal articles:

1. <u>S. A. Kulkarni</u>, E. S. McGarrity, H. Meekes, J. H. ter Horst, 'Isonicotinamide self-association: the link between solvent and polymorph nucleation', Chemical Communications 48 (41), 2012, 4983-4985.

2. S. S. Kadam, <u>S.A. Kulkarni</u>, R. Coloma Ribera, A. I. Stankiewicz, J. H. ter Horst, Herman J. M. Kramer, 'A new view on the metastable zone width during cooling crystallization', Chemical Engineering Science, 72, 2012, 10-19.

3. <u>S. A. Kulkarni</u>, S. S. Kadam, H. Meekes, A. I. Stankiewicz, J. H. ter Horst, 'Crystal Nucleation kinetics from induction times and metastable zone widths', Crystal growth and design, 2013 (6), 2435-2440.

4. <u>S. A. Kulkarni</u>, H. Meekes, J. H. ter Horst, 'Polymorph control through a single nucleation event', Crystal growth and design, 2014 (3), 1493-1499.

5. A. Caridi, <u>S. A. Kulkarni</u>, G. Di Profio, E Curcio, J. H. ter Horst, 'Template-induced nucleation of Isonicotinamide polymorphs', Crystal Growth and Design, 2014 (3), 1135-1141.

6. <u>S. A. Kulkarni,</u> C. C. Weber, A. S. Myerson. J. H. ter Horst, 'Self-association during heterogeneous nucleation onto well-defined templates', Langmuir, Article ASAP, DOI: 10.1021/la5024828

7. <u>S. A. Kulkarni</u>, H. Meekes, J. H. ter Horst, 'Self-association in Solution for Polymorph preparation and control', submitted manuscript.

8. <u>S. A. Kulkarni</u>, H. Meekes, J. H. ter Horst, 'A Liquid-Liquid phase separation during Crystallisation of 4-Hydroxyacetophenone from solution', submitted manuscript.

Book contributions

Kadam S. S., <u>Kulkarni S. A.,</u> ter Horst J. H. (Editors), Proceedings of 18th Industrial Workshop on Industrial Crystallization (BIWIC), ISBN: 978-94-6191-003-5, 2011.

Selected Conference Proceedings

1. Kulkarni S. A.; Weber C. C.; Myerson A. S.; ter Horst, J. H., Polymorph Nucleation: Interplay between self-associates and templates, In proceedings of 19th International Symposium on Industrial Crystallization (ISIC19), page 91-93.
2. Kulkarni S. A.; Meekes, H.; ter Horst, J. H, Polymorph discovery by controlling the self-association in solution, In proceedings of 19th Industrial Workshop on Industrial Crystallization (BIWIC), 2011, 75-80.
3. Kulkarni S. A.; Kadam S. S.; Meekes, H.; ter Horst, J. H., Easy Access to Valuable Industrial Nucleation Kinetics, In proceedings of 18th International Symposium on Industrial Crystallization (ISIC18), 2011, 529-530.
4. Kadam, S. S.; Kulkarni, S. A.; ter Horst, J. H.; Kramer, H. J. M, A New View on Crystal Nucleation in Industrial Crystallization, In proceedings of 18th International Symposium on Industrial Crystallization (ISIC18), 2011, 7-8.
5. Kulkarni S. A.; Kadam S. S.; Stankiewicz, A. I.; Meekes, H.; ter Horst, J. H, Validation of the Single Nucleus Mechanism, In proceedings of 18th Industrial Workshop on Industrial Crystallization (BIWIC), 2011, 75-80.

Selected Oral presentation:

1. Kulkarni S. A.; Weber C. C.; Myerson A. S.; ter Horst, J. H., Polymorph Nucleation: Interplay between self-associates and templates, ISIC conference, 16-19 September 2014, Toulouse, France.

2. Kulkarni S. A.; ter Horst, J. H., Nucleation Kinetics of organic compounds, Group of Users of Technology for Separation in the Netherlands, 3rd December 2013, Geelen, The Netherlands.

3. Kulkarni S. A.; Stankiewicz, A. I.; Meekes, H.; ter Horst, J. H, Polymorph discovery and control based on scientific principles, 9th European congress of chemical engineering, 21-23rd April 2013, The Hague, The Netherlands.

4. Kulkarni S. A.; Meekes, H.; ter Horst, J. H, Discovery and control of pharmaceutical polymorphs through self-association, BACG Conference 2013, 11-16 August 2013, Manchester, United Kingdom.

5. Samir Kulkarni, J. Urbanus, Andrzej Stankiewicz, Joop H. ter Horst, Co-crystallization as a Separation Technology: Separating Co-crystal Components, BACG Conference 2011, 10-12 July 2011, London, United Kingdom.

6. Kulkarni S. A.; Kadam S. S.; Stankiewicz, A. I.; Meekes, H.; ter Horst, J. H, Validation of the Single Nucleus Mechanism, BIWIC conference, 7-9 September 2011, Delft, The Netherlands.

7. Kulkarni S. A.; Weber C. C.; Stankiewicz, A. I.; Myerson A. S.; ter Horst, J. H., Polymorph Nucleation: Interplay between self-associates and templates, YSC conference, 24-05 May 2014, Cracow, Warsaw, Poland.

Selected Poster presentation:

1. Kulkarni S. A.; Kadam S. S.; Meekes, H.; ter Horst, J. H., Easy Access to Valuable Industrial Nucleation Kinetics, In 18th International Symposium on Industrial Crystallization (ISIC18), Zurich, Switzerland.

List of publications

2. Kulkarni S. A.; Meekes, H.; ter Horst, J. H, Polymorph discovery by controlling the self-association in solution, In 19th Industrial Workshop on Industrial Crystallization (BIWIC), 2013 China. (Poster Prize)

Curriculum vitae

Samir Kulkarni was born in Aurangabad, Maharashtra, India on 4th June 1981. He attended secondary and higher secondary school at Kendriya Vidyalaya Aurangabad, India. He received his Bachelor of Technology degree in Pharmaceutical and fine chemical technology from UDCT Aurangabad in 2003. Thereafter, he worked as Chemist with Dai-Ichi Karkaria Limited (Pharmaceutical company) in Hyderabad, India for a rich span of 2 years. He considered himself lucky to be a part of Technology Transfer & Projects Department of the company and he proved to be one of the most successful chemist during the course of project. He worked closely with the R&D department and Process Development Lab. During his tenure, he was involved with various critical scale-up activities in Pilot Plant, which were further successfully implemented on production scale. He was promoted twice a year in Dai-Ichi Karkaria Limited for major contributions towards product development and cost savings.

He completed his Master of Science from Muenster University of Applied Sciences, Germany in 2008, specializing in Applied Chemistry. He worked as a Scientist in the pharmaceutical development team with Avantium Pharma BV, Amsterdam, in the Netherlands for 2.3 years starting from March 2008. He proved to be one of the most successful scientist during the course of project as his work resulted in four patent applications. He was responsible for project planning and execution, focusing on solid-state research of pharmaceutical compounds and also for product improvement and stabilizing the process for reproducibility of results. He joined Delft University of Technology as PhD candidate in June 2010 in the Department of Process and

energy under the supervision of Prof. A. I. Stankiewicz and Dr. Joop H. ter Horst. His PhD topic dealt with high product quality through controlled nucleation and growth. Throughout his PhD education, he has been working on polymorph discovery and control, co-crystals, phase diagrams, chiral crystallization, nucleation kinetics, heterogeneous nucleation and was exposed to advanced research tools like in-situ Raman, ATR-FTIR, FBRM, PVM, XRD which have helped him to shape his career into applied scientific research. During his PhD he went to Massachusetts Institute of Technology in Boston, USA as an exchange student to further gain some more fundamental understanding in heterogeneous nucleation and polymorph control.

At present he is working at Massachusetts Institute of Technology in Boston, USA, as Postdoctoral associate with the group of Prof. Dr. Allan Myerson.

Acknowledgements

One of the joys of completion is to look over the journey past and remember all the colleague's friends and family who have helped and supported me along this long but fulfilling road. My words would hardly do justice to their immense contributions but nevertheless I do not want to miss on this opportunity of thanking them.

I would first like to thank my promotor, Professor Andrzej Stankiewicz, who provided encouraging and constructive feedback. I could not have asked for better role model, he was very inspirational, supportive, and patient. He not only helped me with my research but also helped me with the administrative work for my visa and helped my wife getting a free scholarship for master equivalent courses at TU Delft. I do not have words to express my real appreciation for Professor Andrzej Stankiewicz. He has always been there and gone beyond what I expected from anyone during my PhD tenure.

I would like to express my heartfelt gratitude to my co-promotor and now promotor, Professor Joop H. ter Horst, the real owner of this dissertation. He spent endless hours proofreading my research papers and giving me excellent suggestions that always resulted in improved versions of documents. How come a person can be busy and available at the same time? In fact, he is. I was always walking to his office without prior appointment and was full of motivation whenever I left his office. The joy and enthusiasm he has for his research was contagious and motivational for me. I appreciate all his contributions of time and ideas to make my Ph.D. experience productive and stimulating. He also helped me with the unique opportunity to go to MIT as an exchange student. It was a challenge and an opportunity to explore and identify ways of improving myself. I am also thankful for the excellent example he has provided as a successful supervisor.

I would also like to thank a young Associate Professor Herman Kramer, who provided encouraging and constructive feedback through many discussions. At the age of 60+, he amassed many in the department, and he does all different sports, which I cannot do at the age of 32. I am a big fan of him and that is the reason I call him a young associate professor.

My project committee guided me through all these years. Thank you to Tine Bertrand (STW), Dr. Hugo Meekes (Radboud University Nijmegen), Elias Vlieg (Radboud University Nijmegen), Zjak van Eupen (Synthon), Rob Geertman (DSM), Danny Stam (Avantium) and Roel Ferwerda (Mettler Toledo) for being my advisors. The research was financially supported by the Dutch Technology Foundation (STW), DSM, Synthon B.V., Mettler-Toledo International Inc. and Avantium B.V in The Netherlands.

I am very thankful to Marcel Hoffmann, my ex-boss and Chief Scientific Officer of Crystallics B.V. and a mentor ever since, for all his help, advice, and encouragement. He allowed me to do experiments during my PhD tenure at Crystallics B. V. and also played a crucial role in my decision to join MIT as postdoc researcher. I am also thankful to Dr. Eva Dova for her help with the interpretation of XRPD data.

I am pleased to have the opportunity to work at MIT with Professor Allan Myerson. I'm really honoured to have had this opportunity to discuss my research with someone like Professor Allan Myerson, who is a big name in the field of Crystallization.

I thank all the present and past members and colleagues of the Intensified reaction and separation group as well as process and energy department: Somanth Kadam (helpful, and friendly - best of luck at BASF! Thanks for helping with the fruitful discussions and collaboration), Marloes Reus (has been helpful with translating my summary and propositions to Dutch, Person with full of Joy, good luck with your PhD), Sayee Prasad Balaji and Lalit Gagurde (persons who has been pretty helpful), Wei-Wei Li (life is not

complicated, I am sure you will do a great job in your PhD), Norbert Radasci, Rohit Kacker (Warsaw and Toulouse both are good places for collaborations just go for it), Fatemeh Anisi, Javier Fernandez, Iza Franssen, Daniel Irimia, Maryam Khodadadian, George Krintiras, Guido Sturm, Bernardo Oyarzun Rivera, Albert Stoop, Thijs van Westen and Mahinder Ramdin. In IRS I have received a constant support from Leslie, Helma and Illona. Thank you for that. Also my gratitude towards Michel for his assistance during my experiments in the laboratory. I am also thankful to have the fruitful and valuable collaboration with Dr. K. (Kristina) Djanashvili (TNW-TU Delft), Dr. Cameron Weber (MIT, USA), Antonella Caridi (University of Calabria, Italy), Gérard Coquerel and Clement Brandel (Université de Rouen, France), Professor Roger Davey (Manchester), Peetikamol Kongsamai (Suranaree University of Technology, Thailand) and António O. L. Évora (University of Coimbra, Portugal).

My greatest gratitude goes to my friend and roommate Kedar Deshpande. I would never forget the scientific discussions and chats we had especially on Fridays with his delicious recipes. He supported and helped me from the start of my PhD till the end with final proof reading of my dissertation and many more things. He is like an elder brother than a friend to me. I also like to thank my other best friend Abhay Markande who is the person with a great personality. He has a very good attitude and always treats others kindly, with respect. I learned a lot from him and had very useful discussions especially during a long jogging session we had together. My heartfelt thanks to my friend Amol Chinchole who helped me during my time in the Netherlands. We had a better understanding of each other as friends and he was always there for me when needed. I find myself lucky to have friends like them in my life from the past 8 years through my journey from Germany to the Netherlands till the United States of America.

I would never forget some of my beautiful moments I shared with some of my friends and families. I would like to thank for those wonderful family gatherings we had in the Netherlands together with Kedar-NoK, Abhay-Pallavi,